MECHANISMS OF CYST GROWTH AND FIBROSIS IN CONGENITAL HEPATIC FIBROSIS IN AUTOSOMAL RECESSIVE POLYCYSTIC KIDNEY DISEASE

BY

©2018

Lu Jiang

M.S., Emporia State University, 2013

Submitted to the graduate degree program in Toxicology and the Graduate Faculty of the University of Kansas in partial fulfillment of the requirements for the degree of Doctor of Philosophy.

_____

Co-chair: Michele T. Pritchard, Ph.D.

_____

Co-chair: Udayan Apte, Ph.D.

_____

Yuxia (Lisa) Zhang, Ph.D.

_____

Beth Levant, Ph.D., M.P.A.

_____

Pamela V. Tran, Ph.D.

_____

Darren P. Wallace, Ph.D.

Date defended: 22 May 2018

The Dissertation Committee for Lu Jiang
certifies that this is the approved version of the following dissertation:

MECHANISMS OF CYST GROWTH AND FIBROSIS IN CONGENITAL HEPATIC FIBROSIS IN AUTOSOMAL RECESSIVE POLYCYSTIC KIDNEY DISEASE

_____

Co-chair: Michele T. Pritchard, Ph.D.

_____

Co-chair: Udayan Apte, Ph.D.

Date Approved: 22 May 2018

ABSTRACT

Autosomal recessive polycystic kidney disease (ARPKD) is a rare genetic disorder that occurs in 1:20,000 live births. Patients present with a broad spectrum of symptoms involving the kidneys, liver, and pancreas. Renal manifestations are characterized by the presence of cysts that are derived from dilated collecting ducts. All patients with ARPKD develop some degree of congenital hepatic fibrosis (CHF) at birth. CHF is characterized by bile duct dilation resulting in eventual development of cysts and pericystic fibrosis in the liver. Accompanying cyst growth and fibrosis, recent reports suggest that inflammation is also present, and likely contributes to disease pathogenesis and/or progression. Therefore, three interrelated processes form a 'pathogenic triumvirate' in CHF/ARPKD: cell proliferation (cyst growth), fibrosis, and inflammation. Aside from management of symptoms, and liver and/or kidney transplant, no effective pharmacologic therapies exist for CHF/ARPKD. Therefore, the goal of this research was to explore additional mechanisms of hepatic cyst and pericystic fibrosis progression in CHF/ARPKD to identify new points of therapeutic intervention.

We first characterized the gene expression in CHF/ARPKD by performing RNA-seq in whole liver from Sprague Dawley (SD) and PCK rats at postnatal day (PND) 15, 20, 30, and 90. Upstream regulator and pathway analysis of differentially expressed genes was subsequently conducted using Ingenuity Pathways Analysis (IPA). We found the number of differentially expressed genes was increased in PCK rats over time. Among the top genes upregulated in PCK rats, *Cd44*, the most well-described receptor for the extracellular matrix glycosaminoglycan hyaluronan, and *Tead4*, a transcription factor required for regulation of genes downstream of the Hippo-kinase- yes-associated

protein pathway, were consistently upregulated from PND 15 to PND 90. This led us to investigate the role of hyaluronan and yes associate protein (YAP) in CHD/ARPKD.

Upstream regulator analysis predicted activation of several pro-proliferative and pro-inflammatory transcription factors in PCK rats including *Ctnnb* (catenin beta-1), *Mtpn* (myotrophin), *Tcf7l2* (transcription factor 7 like 2), and several *Stat* (signal transducer and activator of transcription) family members (z score ≥ 2). Further, PCK rat livers exhibited inhibition of *Smad7*, an inhibitory SMAD, which is expected to result in a pro-fibrotic effect by preventing the Smad7-induced negative regulation of TGF-β/SMAD signaling. Additionally, a significant suppression of *Hnf4a*, the master regulator of hepatic differentiation, was also observed in the PCK rat livers.

Mast cells (MCs) are immune cells involved in many liver diseases and release mediators such as histamine from preformed granules found in their cytoplasm. In fact, previously published data demonstrate that histamine induces proliferation of cholangiocytes, which are the precursors of the cyst wall epithelial cells (CWEC) in CHF. We observed MC infiltration in the hepatic periportal areas, but not in the kidneys, in polycystic kidney (PCK) rats. Therefore, we hypothesized that MCs contribute to hepatic cyst growth in PCK rats. To test this hypothesis, we treated PCK rats with one of two different mast cell stabilizers, cromolyn sodium (CS) or ketotifen, or saline from PND 15 to PND 30. We confirmed that CS and ketotifen treatment decreased MC degranulation in liver. Interestingly, we observed an increase in liver/body weight ratio after CS and ketotifen treatment paralleled by a significant increase in cyst size. In contrast, we saw a decreased kidney/body weight ratio paralleled by a significant decrease in individual cyst size after CS treatment. We excluded the direct effect of CS

on cyst growth by treating isolated cyst wall epithelial cells (CWECs) and a mouse model (no MC observed) of ARPKD with CS. Taken together, these data demonstrate that hepatic and renal cysts are differentially regulated by MC granule contents in PCK rats.

RNA-seq analysis suggested that TEA Domain Transcription Factor 4 (*Tead4*), a transcription factor in Hippo signaling pathway, is upregulated in PCK rats. Hippo signaling pathway is a conserved signaling that plays critical roles in liver size control and cell proliferation. Our preliminary data suggested that YAP, the downstream effector of the Hippo signaling pathway, was increased in proliferating CWECs in PCK rats and in human ARPKD patients. Consistently, there was increased expression of YAP target genes, *Ccnd1* (cyclin D1) and *Ctgf* (connective tissue growth factor), in PCK rat livers. Extensive expression of YAP and its target genes was also detected in human CHF/ARPKD liver samples. Therefore, we hypothesized that YAP plays a role in CWEC proliferation in CHF/ARPKD. We inhibited YAP activity pharmacologically using verteporfin and genetically using short hairpin (sh) RNA in primary liver CWECs. We found that CWEC proliferation was significantly reduced. These data indicate that increased YAP activity, possibly through dysregulation of the Hippo signaling pathway, is associated with hepatic cyst growth in CHF/ARPKD.

In RNA-seq analysis, we found that *Cd44* was upregulated in PCK rats from PND 15 to PND 90. Hyaluronan (HA), a CD44 ligand, is a ubiquitous, anionic glycosaminoglycan present in the extracellular matrix (ECM). HA is implicated in liver injury, inflammation, and fibrogenesis. Our study showed an increased HA level in livers from PCK rats and polycystic liver disease patients relative to healthy controls. HA

accumulation could be due to an increased *Has1* (a HA synthase) expression and decreased expression of HA degrading enzymes. Therefore, we hypothesized that HA plays a pathogenic role in progression of CHF/ARPKD. Future studies can be performed to test the role of HA in CHF/ARPKD by genetically deleting *Has* enzymes or the HA receptor, CD44, in PCK rats or in *Pkhd1* mutant mice

Taken together, CHF/ARPKD is a hepatobiliary disease that is regulated by a 'pathogenic triumvirate' (cell proliferation/cyst growth, inflammation, fibrosis). My studies aimed to discover novel mechanisms driving CHF/ARPKD and investigated how MC, and YAP, regulated the 'pathogenic triumvirate' in CHF/ARPKD. Moreover, we identified and upregulation of HA and *Cd44* in PCK rats the significance of which can be explored in future studies. Overall, these studies have uncovered several new avenues for additional research into the mechanisms of cell proliferation/cyst growth, inflammation, and fibrosis, in CHF/ARPKD and from which future therapeutic strategies can be developed.

ACKNOWLEDGEMENTS

First, I want to express my deepest gratitude to my mentors Dr. Michele Pritchard and Dr. Udayan Apte. Dr. Pritchard has mentored me along my Ph. D, study in many aspects. She took me in the lab when I had little experience in animal study, presentation, and scientific writing. She is incredibly patient and supportive, and her wonderful guidance helps me become an independent researcher. I also want to thank my co-mentor, Dr. Udayan Apte. He has been a great mentor throughout my study. He has given me the freedom of my scientific ideas and has guided me to the right direction. He has made me think about what I want for my career and how to achieve it. Without my mentors, I wouldn't be who I am today.

I would like to thank my dissertation committee members: Dr. Lisa Zhang, Dr. Beth Levant, Dr. Pam Tran, and Dr. Darren Wallace. They have provided valuable feedback on my research, advice for my future career goals, and guidance through the process of completing my Ph. D. I also want to thank Dr. Hagenbuch, the graduate committee coordinator for helping me to be on track with my graduation deadlines. Thank you also to the administrative staff, Elizabeth Jamison and Cody Tully, for the help in travel reimbursement and for making sure I have all requirements completed for graduation. Lastly, thank you to Dr. Mary Lynn Bajt and Huina Cai for their help in the histology and cell isolation core.

I want to thank the previous members of the Pritchard lab. Jennifer McCracken has been a great co-worker and big sibling to me for the past four years. She helped me with experimental troubleshooting and course study. I also want to Krutika Desphande and Briana Holt for helping me in the early stage of my project.

Additionally, I would like to thank Dr. Christopher Ward (KUMC) for generously providing us the *Pkhd1*$^{LSL(-)/LSL(-)}$ mice and Dr. Stephan Somlo (Yale University) for providing us the *Pkhd1*$^{del4/del4}$ mice.

The work cannot be done without the support of funding. This dissertation was supported by National Institutes of Health, National Center for Research Resources (P20 RR021940) and National Institute of General Medical Sciences (P20 GM103549, P20 GM103418, P30GM118247). The work is also funded by R01 DK098414, AASLD/ALF Liver Scholar Award (Udayan Apte), University of Alabama at Birmingham (P30DK074038, Michele T. Pritchard), and P30 DK074038 (Michele T. Pritchard). The PKD Biomarkers and Biomaterials Core is supported by a grant from NIH P30 DK106912.

Last but not least, I want to thank my parents, families and friends for the great support and love over the years. My parents have been role models for me and have taught me how to be a responsible person. They support my decisions and give me valuable advice for my education. I would like to thank my friends for the day-to-day support. There are too many people to name but at this moment of my life, I remember them all. I thank each of them for being an incredible source of support.

Table of Contents

List of abbreviations

αSMA	=	α smooth muscle actin
ACE	=	angiotensin converting enzyme
ADPKD	=	autosomal dominant polycystic kidney disease
ARB	=	angiotensin II receptor blockers
ARPKD	=	autosomal recessive polycystic kidney disease
C3a	=	complement 3a fragment
C5a	=	complement 5a fragment
cAMP	=	cyclic adenosine monophosphate
CCl_4	=	carbon tetrachloride
Ccnd1	=	cyclin D1
CD44	=	cluster of differentiation 44
cDNA	=	complementary DNA
Ced1d	=	carboxylesterase 1d
CG	=	chlorhexidine gluconate
CHF	=	congenital hepatic fibrosis
CK	=	cytokeratin
Cma1	=	chymase
Cpk	=	congenital polycystic kidney
CTGF	=	connective tissue growth factor
CWEC	=	cyst wall epithelial cell
CRE	=	causes recombination

CS	=	cromolyn sodium
Ctnnb	=	catenin beta
Da	=	Dalton
DAPI	=	4,6-Diamidino-2-phenylindole
ECM	=	extracellular matrix
EGF	=	epidermal growth factor
ERK	=	extracellular signal-related kinase
ESRD	=	end-stage renal disease
Fcer1a	=	Fcε receptor I alpha
FGF	=	fibroblast growth factor
FSK	=	forskolin
GSK3β	=	glycogen synthase kinase 3β
H&E	=	Hematoxylin and eosin
HA	=	hyaluronan
HABP	=	hyaluronan binding protein
HARE	=	hyaluronan receptor for endocytosis
HAS1	=	hyaluronan synthase 1
HAS2	=	hyaluronan synthase 2
HAS3	=	hyaluronan synthase 3
HC	=	hepatocyte
HCC	=	hepatocellular carcinoma
HDAC	=	histone deacetylase
HMMR	=	hyaluronan mediated motility receptor

HMW	=	high molecular weight
HRP	=	horseradish peroxidase
HSC	=	hepatic stellate cell
HYAL	=	hyaluronidase
IL	=	interleukin
IPA	=	Ingenuity Pathway Analysis
ISZ	=	*in situ* zymography
JNK2	=	c-Jun N-terminal kinase
LMW	=	low molecular weight
LPS	=	lipopolysaccharide
MAB	=	monoclonal antibody
MC	=	mast cell
MCP-1	=	monocyte chemoattractant protein-1
MFB	=	myofibroblast
MiR	=	microRNA
MMP	=	matrix metalloproteinase
Mtpn	=	myotropin
NPC	=	nonparenchymal cells
OCT	=	optimal cutting temperature medium
PAB	=	polyclonal antibody
PC-1	=	polycystin-1
PCNA	=	proliferating cell nuclear antigen
PCK	=	polycystic kidney

PCR	=	polymerase chain reaction
PE	=	pair-ended
PND	=	postnatal
PDGF	=	platelet derived growth factor
PF	=	portal fibroblast
PKD	=	polycystic kidney disease
PLD	=	polycystic liver disease
RAS	=	renin-angiotensin system
qPCR	=	quantitative polymerase chain reaction
ROS	=	reactive oxygen species
SD	=	Sprague-Dawley
TGFβ	=	transforming growth factor β
TIMP	=	tissue inhibitor of matrix metalloproteinase
TLR	=	Toll like receptor
Tmem2	=	transmembrane protein 2
TNFα	=	tumor necrosis factor α
Tpsab	=	tryptase
TSA	=	tyramide signal amplification
UUO	=	unilateral ureteral obstruction
VEGF	=	vascular endothelial growth factor receptor 2
VP	=	verteporfin
YAP	=	yes associated protein

CHAPTER I: INTRODUCTION

Portions of this chapter are adapted from Jiang, L., P. P. Fang, J. L. Weemhoff, U. Apte and M. T. Pritchard. "Evidence for a 'pathogenic triumvirate' in Congenital Hepatic Fibrosis in Autosomal Recessive Polycystic Kidney Disease," BioMed Research International, vol. 2016, Article ID 4918798, 10 pages, 2016. doi:10.1155/2016/4918798; licensed under Creative Commons Attribution License.

1.1 AUTOSOMAL DOMINANT POLYCYSTIC KIDNEY DISEASE (ADPKD) AND AUTOSOMAL RECESSIVE POLYCYSTIC KIDNEY DISEASE (ARPKD)

Polycystic kidney disease is a genetic disorder that is inherited as either autosomal dominant (ADPKD) or autosomal recessive (ARPKD). In Table 1.1.1, we summarize the features of ADPKD and ARPKD from different aspects. ADPKD is more common compared to ARPKD with an occurrence of 1:400 – 1:1000 (Torres et al. 2007). It is caused by mutations in gene *PKD1* (~78% pedigrees), *PKD2* (~15% pedigrees), or no mutation detected (~9% pedigrees) (Harris et al. 2014). ADPKD is characterized by progressive development of cysts during the lifetime of the patient, resulting in bilateral renal enlargement and often end-stage renal disease (ESRD) (Torres et al. 2007). Extrarenal manifestations include intracranial aneurysms, polycystic liver disease, and vascular abnormalities (Pirson et al. 2002, Torres 2007, Nowak et al. 2017).

Autosomal recessive polycystic kidney disease (ARPKD) is a rare genetic disorder that occurs in 1:20,000 live births. It develops *in utero* and is mainly diagnosed in pregnancy or in the immediate neonatal period. Among affected patients, approximately 30% die shortly after birth, primarily of pulmonary insufficiency (Zerres et al. 1998). Patients who survive the neonatal period present with a broad spectrum of symptoms involving the kidneys, liver, and pancreas. Renal manifestations are characterized by the presence of cysts that are derived from dilated collecting ducts and distal tubules (Osathanondh et al. 1964, Blyth et al. 1971). A significant portion of patients will progress to end stage renal disease either during the first decade or during

adolescence (Bergmann et al. 2005). A minority of patients develop pancreatic abnormalities consisting of cysts and fibrosis (Bernstein et al. 1987, Williams et al. 2008). All patients with ARPKD develop some degree of congenital hepatic fibrosis (CHF), which, as the name would suggest, is present at birth. CHF is characterized by bile duct dilation resulting in eventual development of cysts and pericystic fibrosis in the liver (Shneider et al. 2005, Turkbey et al. 2009). Accompanying cyst growth and fibrosis, recent reports suggest that inflammation is also present, and likely contributes to disease pathogenesis and/or progression (Tracy et al. 1996, Flores et al. 2008, Nakanuma et al. 2010, Locatelli et al. 2016). Aside from management of symptoms, and liver and/or kidney transplant, no effective pharmacologic therapies exist for CHF/ARPKD (Masyuk et al. 2015).

Table 1.1.1. Comparison between ADPKD and ARPKD.

Type	Occurrence	Mutated gene	Symptoms
ADPKD	1:400 - 1:1000 (Adulthood)	*PKD1/PKD2* (polycystin1/2)	Cystic kidney Renal failure Intracranial aneurysms Polycystic liver disease Vascular abnormalities
ARPKD	1:20,000 (Neonates)	*PKHD1* (fibrocystin)	Cystic kidney, liver Pulmonary hypoplasia Portal hypertension Congenital hepatic fibrosis

1.2 GENETIC DEFECTS AND CURRENT THERAPIES IN CHF/ARPKD

CHF/ARPKD is caused by mutations in the *PKHD1* gene on chromosome 6p12. *PKHD1* extends over 470 kb, includes a minimum of 86 exons and encodes a 4,074-amino-acid protein called fibrocystin/polyductin. Fibrocystin is predicted to be a receptor-like protein that consists of a large glycosylated extracellular region, a single transmembrane domain, and a short cytoplasmic tail (Onuchic et al. 2002, Ward et al. 2002). Fibrocystin is expressed in the primary cilia of epithelial cells. Immunohistochemistry studies suggest that fibrocystin is located in renal collecting ducts and loops of Henle, pancreatic epithelial ducts, and hepatic biliary ducts (Menezes et al. 2004). Different mutations in *PKHD1* have been described in human ARPKD patients, including missense mutations, deletion/insertion mutations, and splicing mutations. Among all types of mutations found in *PKHD1,* about 45% of them are predicted to truncate fibrocystin (Bergmann et al. 2003). Disease in patients carrying two truncating mutations is usually more severe, whereas patients bearing missense mutations exhibit a milder phenotype (Harris et al. 2004).

There is no pharmacologic cure for CHF/ARPKD. Treatment mainly focuses on management of symptoms and includes therapies for cardiac hypertension, chronic liver/kidney disease, cholangitis, and portal hypertension (Guay-Woodford et al. 2003). Hypertension associated with chronic kidney disease occurs at the early stage of disease and is regulated by the renin-angiotensin system (RAS) (Goto et al. 2010). Hypertension in ARPKD is treated empirically. Angiotensin converting enzyme (ACE) inhibitors and angiotensin II receptor blockers (ARBs) are considered the main treatment options in ARPKD patients (Gunay-Aygun et al. 2006, Turkbey et al. 2009). If

kidney failure occurs, patients undergo dialysis or kidney transplantation. Treatment for CHF/ARPKD is more challenging since patients have recurrent cholangitis and an increased risk of malignant cholangiocarcinoma after liver transplantation (Gunay-Aygun et al. 2006). Other therapeutic strategies include targeting components of the cAMP signaling pathway since cAMP levels are increased in cyst wall epithelial cells (CWEC) and drive CWEC proliferation. Octreotide and pasireotide, two somatostatin analogs, decrease CWEC proliferation in PCK rats *in vitro* and inhibit hepatorenal cyst growth in PCK rats *in vivo* by reducing cAMP levels. Consistently, clinical trials in patients with polycystic liver disease (PLD) and ADPKD showed that octreotide or lanreotide are well tolerated, and decrease total liver volume by 4% - 6% (Masyuk et al. 2015), suggesting that somatostatin analogs could be effective as therapeutic drugs for CHF/ARPKD patients.

1.3 ANIMAL MODELS OF ARPKD

Several rodent models of human ARPKD are available to study the mechanisms of disease and to test therapeutic strategies (Table 1.1.2). One of the best-characterized models is the polycystic kidney (PCK) rat, derived from Sprague-Dawley (SD) rats at Charles River, Inc. (Katsuyama et al. 2000). The PCK rat carries a spontaneous splicing mutation, IVS35–2A→T, in the rat *Pkhd1* gene (Ward et al. 2002). PCK rats bear hepatic and renal cysts, and associated fibrosis, similar to human ARPKD (Lager et al. 2001). The lifespan of a PCK rat is about 1.5 years, and they develop numerous cysts in kidneys and liver by one year of age (Nagao et al. 2012).

In mice, the congenital polycystic kidney (*cpk*) mouse mimics human ARPKD. This mouse harbors a spontaneous mutation in *cpk* gene, the gene that encodes a 145-amino acid protein termed cystin. Cystin is mainly located in the axoneme of the primary cilia found in the kidney proximal tubules and collecting ducts and in the cholangiocytes found in the liver (Avner et al. 1987, Hou et al. 2002). *Cpk* mice, on the BALB/c background, exhibit both renal and extrarenal manifestations associated with cystin mutations (Ricker et al. 2000). When on a C57Bl/6J background, *cpk* mice do not have extrarenal pathology (Preminger et al. 1982), limiting the utility of this model for those interested in studying CHF/ARPKD. In addition, a *Pkhd1*$^{del2/del2}$ mouse model, which lacks exon 2 of the mouse *Pkhd1* gene, also reproduces the human ARPKD liver pathology. Both genders develop hepatic cysts and fibrosis by 3 months as a result of biliary ductal plate malformation (Woollard et al. 2007). Another widely accepted murine model with *Pkhd1* mutation was generated by Christopher Ward and colleagues. In this model, the *Pkhd1* gene was transcriptionally silenced by inserting a loxP flanked STOP (LSL) cassette into intron–2. The *Pkhd1*$^{LSL(-)/LSL(-)}$ mice, both male and female, develop liver cysts and fibrosis at 3 months of age (Bakeberg et al. 2011). Among all rodent models for ARPKD, the PCK rat is one of the most well-accepted models because the phenotypic resemblance to human ARPKD.

Table 1.1.2. Current rodent models of ARPKD.

Model	Species	Liver phenotype	Kidney phenotype	Others	Reference
PCK	Rat	Cysts and fibrosis	Cysts	Pancreatic cysts	(Lager et al. 2001)
BALB/c-*cpk/cpk*	Mouse	Cysts and fibrosis	Cysts	Pancreatic cysts and fibrosis	(Ricker et al. 2000)
C57BL/6J-*cpk/cpk*	Mouse	No liver disease	Cysts	None	(Gattone et al. 1988)
Pkhd1$^{del2/del2}$	Mouse	Cysts and fibrosis	Cysts in female	Pancreatic cysts	(Woollard et al. 2007)
Pkhd1$^{LSL(-)/LSL(-)}$	Mouse	Cysts and fibrosis	Cysts in female	Unknown	(Bakeberg et al. 2011)
Pkhd1ex40	Mouse	Cysts and fibrosis	No kidney disease	Portal hypertension	(Moser et al. 2005)
Pkhd1$^{lacZ/lacZ}$	Mouse	Cysts and fibrosis	Cysts	Pancreatic and gall bladder cysts	(Mortazavi et al. 2008)
Pkhd1$^{del4/del4}$	Mouse	Cysts and fibrosis	No kidney disease	Pancreatic cysts, splenomegaly	(Gallagher et al. 2008)

1.4 MECHANISMS OF CYSTOGENESIS IN ARPKD

Although the mechanisms of cystogenesis are not well characterized in human ARPKD, a study using PCK rats suggested a possible link between cystogenesis and ciliary dysfunction (Masyuk et al. 2004). Primary cilia, microtubule-based organelles, extend from the surface of eukaryotic cells. Primary cilia are non-motile cilia containing a “9+0” axoneme, and function as mechano-, osmo-, and chemosensors that deliver signals from the extracellular environment into the cell (Masyuk et al. 2008). The abnormal primary cilia in PCK rat cholangiocytes may compromise their sensory organelle function in response to fluid secretion or fluid flow. Recent research suggests that primary cilia are also important components of multiple signaling pathways such as

the hedgehog and PDGF-A signaling pathways, and mutation of *PKHD1* gene may disrupt these pathways contributing to cyst formation (Huangfu et al. 2003, Schneider et al. 2005).

Hepatic cystogenesis in human ARPKD patients is characterized by abnormal remodeling of the ductal plate from the double cell layer during embryonic liver development. Clinical manifestations include dilated bile ducts, an increased number of bile ducts, and abnormal branching (Turkbey et al. 2009). It remains to be determined if hepatic cysts in ARPKD become disconnected from the biliary tree as is the case for ADPKD. (Patterson et al. 1982). Cyst development in PCK rat liver has been well-described by Dr. Nicholas LaRusso's group (Perugorria et al. 2014, Wills et al. 2014, Masyuk et al. 2015). They found that (1) hepatic cysts are derived from bile duct segments due to ductal plate malformation during development and (2) most cysts become isolated from biliary tree by 6 months of age (Masyuk et al. 2004).

Along with cyst formation, the mechanisms of cyst expansion are proposed to be the result of: (1) cholangiocyte hyperproliferation, (2) cell-matrix interactions, and (3) fluid secretion (Figure 1.4.1, (Gradilone et al. 2010)). Many factors can regulate these processes through different signaling pathways and are briefly described below: (1) Intracellular cyclic adenosine monophosphate (cAMP) is likely the major driver of hepatic cyst growth (Masyuk et al. 2015). In addition, cAMP levels are elevated in PCK rat cholangiocytes as compared to cholangiocytes from control rats. Octreotide, a somatostatin analog, reduces hepatic and renal cyst expansion in PCK rats by decreasing cAMP levels (Masyuk et al. 2007). Another factor that contributes to CWEC proliferation is low intracellular [Ca^{2+}], and is observed in CWECs from PCK rat livers

(Banales Jú et al. 2009). Activation of Trpv4, a calcium-permeable cation channel expressed in normal cholangiocytes, increases intracellular calcium levels and suppresses proliferation of cholangiocytes isolated from PCK rats *in vitro* (Gradilone et al. 2010). (2) Remodeling of extracellular matrix includes alteration of extracellular matrix composition, basement membrane thickness, and the activities of matrix metalloproteases (MMP) and their inhibitors, all of which can lead to cyst expansion (Wilson 2004). (3) In ARPKD, little is known about how fluid secretion impacts hepatic cyst expansion (Figure 1.4.1). Previous data suggest that cystic epithelia can respond to secretin and secrete fluid through activating a cAMP-dependent signaling pathway (Everson et al. 1990, Qian 2010).

In addition, there are other factors that regulate CWEC proliferation. Recent studies have shown that deregulation of the Hippo signaling pathway results in increased expression and activity of its downstream effector Yes-associated protein (YAP), which is involved in a number of fibro-proliferative hepatic disorders including hepatic fibrosis, hepatocellular carcinoma and cholangiocarcinoma (Camargo et al. 2007, Pan 2010, Li et al. 2012, Septer et al. 2012). When the Hippo signaling pathway is ‘on’, activation of LATS1/2 kinases directly phosphorylate YAP, which inhibits YAP nuclear translocation. When the Hippo signaling pathway is ‘off ’, YAP is translocated to the nucleus and binds to different transcription factors to regulate target genes involved in cell proliferation, cell survival, and apoptosis (Di Cara et al. 2015, Yu et al. 2015). A previous study showed increased YAP activation in kidney cyst epithelial cells from ADPKD and ARPKD patients (Happe et al. 2011); however, the role of YAP in hepatic cyst development in CHF/ARPKD is not known. It is known that primary cilia in cystic

cholangiocytes are malformed and dysfunctional, it is plausible to propose that YAP is activated as the result failing to function properly as a sensory organ.

Renal cysts in ARPKD are commonly described as dilated collecting ducts (Kern et al. 2000). Compared to what is observed in ADPKD, dilated collecting ducts and distal tubules lined with cuboidal or columnar epithelial cells which remain connected to the urinary system (Bergmann 2015). It remains unclear in ARPKD whether or not cysts with squamous epithelial cells detach from the tubular segment from which they are derived (Calvet et al. 2001). Cyst formation and expansion are associated with increased proliferation of renal epithelial cells (Nadasdy et al. 1995) and altered fluid secretion (Veizis et al. 2004). Recent data suggest that cAMP induces renal epithelial cell proliferation and promotes cyst growth by activating PKA/B-Raf/MAPK pathways in CWECs from ARPKD patients (Yamaguchi et al. 2006). Similarly, renal epithelial cells also exhibit a lower level of intracellular [Ca^{2+}], and sustained reduction of intracellular [Ca^{2+}] in normal cells induces a cAMP-growth stimulated phenotype (Yamaguchi et al. 2006). In addition, an increased level of epidermal growth factor (EGF) is demonstrated in renal cyst fluid, which is consistent with an overexpression of EGF receptor (EGFR) mRNA and protein in renal epithelia in cpk mice (Horikoshi et al. 1991). However, the administration of EGFR tyrosine kinase inhibitor does not protect PCK rats from developing renal cysts and liver cysts, possibly due to an increased level of cAMP after treatment (Torres et al. 2004). In addition, arginine vasopressin (AVP) V2 receptor antagonists have shown beneficial effects on slowing renal disease progression in PCK rats (Torres 2008). Administration of the AVP receptor antagonist OPC-31260 to PCK rats reduced the renal accumulation of cAMP and renal cyst progression by the

inhibition of Ras/B-Raf/ERK pathway (Gattone et al. 2003, Wang et al. 2005). Tolvaptan, a V2R antagonist, slowed the increase in total kidney volume and the decline in kidney function in patients with ADPKD over a 3-year preclinical study (Torres et al. 2012). In 2018, Tolvaptan was approved by the Food and Drug Administration for the treatment of ADPKD (Ostrowski et al. 1993). Considering the fact that V2R is not expressed in liver, CHF/ARPKD patients may not benefit from Tolvaptan. This emphasizes the persistence of a critical need for a pharmacological agent specific, and more effective than octreotide/pasireotide, for PKD patients with liver diseases.

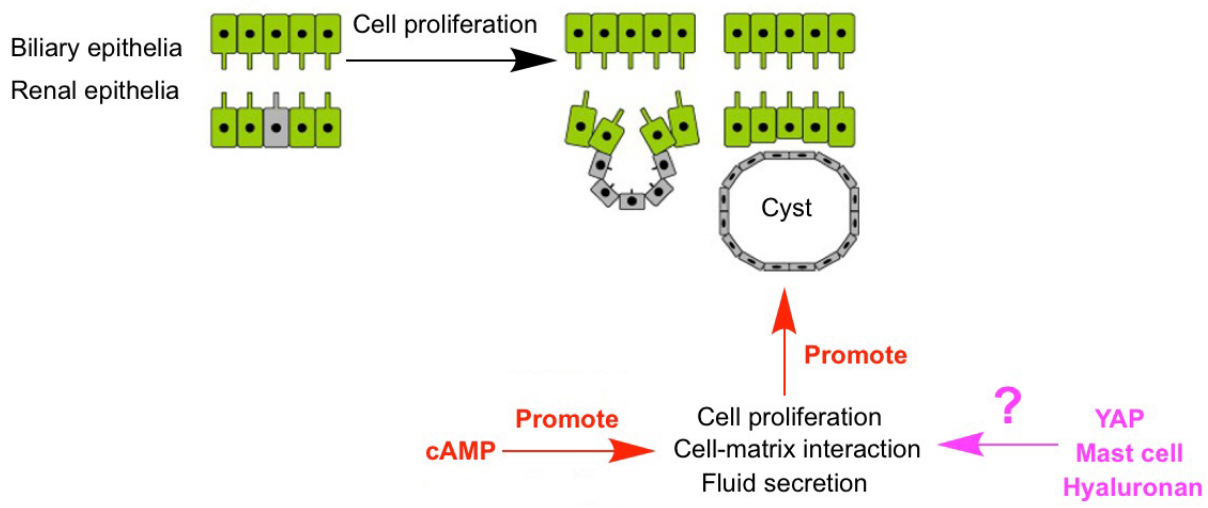

Fig.1.4.1. Schematic representation of cystogenesis in ARPKD. Cystogenesis is initiated with mutations in gene *PKHD1,* encoding for fibrocystin. Biliary/renal epithelial cells with mutations proliferate and become an isolated cyst. Cyst growth can be promoted by cell proliferation, cell-matrix interactions, and fluid secretion. cAMP promotes cyst growth cyst growth. Other factors such as Yes-associated protein (YAP), mast cells, and hyaluronan will be examined in this dissertation as other potential mediators.

1.5 MECHANISMS OF FIBROSIS IN ARPKD

Liver fibrosis typically results from chronic liver injury in conjunction with the accumulation of extracellular matrix (ECM) proteins synthesized by myofibroblasts (MFB). In the liver, the major cell types that contribute to MFB formation are hepatic stellate cells (HSC) and portal fibroblasts (PF). Residing in the space of Disse, HSCs are the principle cell type responsible for collagen synthesis in response to liver injury or changes in ECM stiffness (Gabele et al. 2003). HSCs are also activated by various mediators released from Kupffer cells, the liver-resident macrophage population, and include transforming growth factor-beta (TGF-β) and tumor necrosis factor-alpha (TNF-α) (Matsuoka et al. 1990). In addition, connective tissue growth factor (CTGF) is produced by multiple cells types in liver, and it promotes the activation of HSCs (Huang et al. 2012). When HSCs are activated, they convert from quiescent cells to proliferative, fibrogenic, and contractile MFB, and release a variety of inflammatory chemoattractants such as monocyte chemoattractant protein-1 (MCP-1) to recruit monocytes to the liver (Marra et al. 1998). PFs are found in the portal tract area, and play a predominant role in biliary fibrosis (Dranoff et al. 2010). Although both cell types express alpha smooth muscle actin (αSMA) upon activation, research suggests that the MFB population that contributes to CHF/ARPKD is likely derived from PFs (Wen 2011). Similar to HSCs, TGF-β and CTGF are involved in the activation of PFs (Sedlaczek et al. 2001, Li et al. 2007, Borkham-Kamphorst et al. 2014). By contrast, TNF-α does not seem important for PF activation or fibrogenic potential (Dranoff et al. 2010). In addition to their role in biliary fibrosis, activated portal MFB regulate cholangiocyte proliferation through activating P2Y receptors on bile duct epithelium (Jhandier et al. 2005).

Following the activation of HSCs or PFs to MFB, two major events occur which promote fibrogenesis. First, activated MFB directly increase the synthesis and deposition of ECM proteins. Second, the MFB proliferate and amplify the fibrotic response (Parsons et al. 2007).

Matrix degradation is an important mechanism to reverse fibrosis or cirrhosis and can restore normal liver architecture. Two kinds of matrix degradation mechanisms exist: “pathologic matrix degradation” that disrupts low density matrix and “restorative matrix degradation” that degrades excess scar (Friedman 2003). Matrix remodeling is carried out through a fine balance between activities of MMPs and their inhibitors. MMPs are a family of enzymes secreted as proenzymes and are activated by proteolytic cleavage. They play a pivotal role in the regression of liver fibrosis by degrading ECM and inducing MFB apoptosis. Expression of tissue inhibitors of metalloproteinase 1 (TIMP-1) promotes fibrosis, first, by inhibiting MMP activity, and second, by inhibiting MFB apoptosis (Murphy et al. 2002). Figure 1.5.1. summarizes the mechanisms of liver fibrosis in CHF/ARPKD.

The connection between cyst growth and fibrosis in CHF/ARPKD is thus far unclear. Unlike some of the liver diseases, liver injury due to ARPKD may not be the initial event that causes HSC activation and fibrosis. Instead, cystogenesis may disrupt normal ECM remodeling and induces fibrogenesis. This hypothesis is supported by the fact that HSCs and PFs are activated and differentiate into MFB when microenvironmental stiffness increases (Li et al. 2007, Olsen et al. 2011); enlarging cysts may promote this increase in mechanical stiffness and facilitate PF and HSC activation. Recent evidence suggests that bile duct epithelia directly regulate PF

proliferation and PF transdifferentiation to MFB via release of MCP-1 (Kruglov et al. 2006). These data indicate that release of MCP-1 released by cystic epithelia is likely an additional link between cyst growth and fibrosis by recruiting macrophages, and inhibition of which could have therapeutic effects in CHF/ARPKD.

A polysaccharide called hyaluronan (HA) regulates both cholangiocyte proliferation and liver fibrosis (Guechot et al. 1995, He et al. 2008). HA is composed of repeating disaccharides of D-glucuronic acid and N-acetylglycosamine, and It can be found in association with the collagen of our skin, joint synovial, and eye vitreous fluid. Increased serum HA level has been detected in patients with liver diseases, such as non-alcoholic fatty liver disease (Suzuki et al. 2005), alcoholic liver diseases (Stickel et al. 2003, Gudowska et al. 2016), hepatitis C (Guechot et al. 1995, Gudowska et al. 2016), primary biliary cirrhosis (Nyberg et al. 1988), and hepatocellular carcinoma (Li et al. 2016). HA has been used as a biomarker for liver disease severity (Gudowska et al. 2016). The production of HA increases as a critical component of collagen deposition under various inflammatory conditions (Engstrom-Laurent et al. 1985, Levesque et al. 1988, Bachem et al. 1989, Savani et al. 2000). In addition, a decreased number of HA uptake receptor CD44 on injured sinusoidal endothelial cells might also cause an increased level of HA in serum (Tamaki et al. 1996). Recently, a study using bile duct ligated-rats to mimic cholestasis suggests that biliary epithelial cells are the source of CD44, and HA-CD44 interaction promotes biliary epithelium proliferation (He et al. 2008). However, the role of HA in CHF/ARPKD is unknown.

Compared to what has been established regarding development of hepatic fibrosis, little is known about renal fibrosis in regarding the mechanisms and

consequences in ARPKD. Although patients exhibit very different renal symptoms, they always develop some degree of interstitial fibrosis around renal cysts (Avni et al. 2002). In PCK rats, renal interstitial fibrosis is not evident until 70 days of age, and renal disease is more severe in males than in females (Lager et al. 2001). Interestingly, administration of a B-type natriuretic peptide, a guanylyl cyclase A agonist, in PCK rats can effectively reduce renal cyst size and fibrosis through regulating Ca^{2+} level. This suggests that guanylyl cyclase A-cGMP axis may provide a new insight to ARPKD therapy (Holditch et al. 2017). Glycogen synthase kinase-3β (GSK3β), a serine/threonine protein kinase, is increased in renal cyst-lining epithelia from a mouse model of ARPKD, and inhibition of its activity reduces renal cyst expansion (Tao et al. 2015). GSK3β also promotes renal fibrosis by activating TGF-β signaling in a mouse model of renal fibrosis induced by ischemia-reperfusion injury (Singh et al. 2015). Therefore, GSK3β is a key pathogenic determinant in ARPKD, and pharmacological inhibition of which could suppress renal cyst expansion and fibrosis.

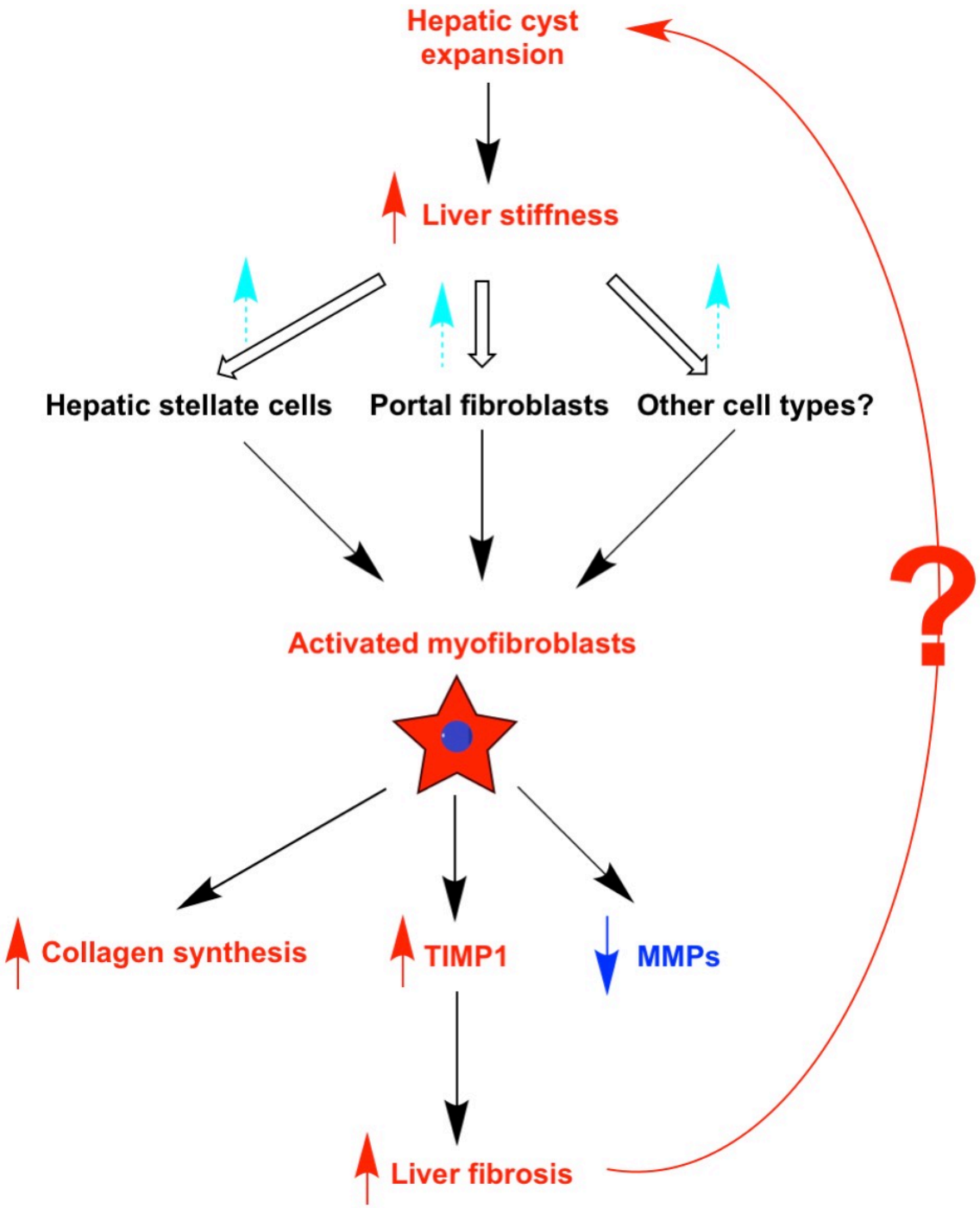

Fig.1.5.1. Schematic representation of fibrogenesis in CHF/ARPKD. Although not yet explored in CHR/ARPKD, hepatic cyst expansion may increase liver stiffness and induce the activation of myofibroblasts from hepatic stellate cells, portal fibroblasts, and perhaps other cell types. Activated myofibroblasts will synthesize collagen, decrease expression of matrix metalloproteases (MMPs), and increase expression of their inhibitor metalloproteinase 1 (TIMP-1). All of these contribute to liver fibrosis development and may in turn affect hepatic cyst growth.

1.6 MECHANISMS OF INFLAMMATION IN ARPKD

In addition to cyst growth and fibrosis, inflammation is another pathological feature of CHF/ARPKD. Although inflammation in the liver has not been well studied as that in the kidney, immune cells such as mast cells (MC) accumulate in the pericystic areas in livers of human CHF/ARPKD patients (Ozaki et al. 2005). Consistently, we have observed pericystic MC infiltration in PCK rats (see chapter III). Tryptase, a MC granule component, was increased in serum from PCK rats compared to its level in SD rats. Histamine level didn't differ between PCK rats and SD rats. Inhibition of MC degranulation and histamine release with cromolyn sodium, a MC stabilizer, decreases cholangiocyte proliferation in bile duct ligation-induced cholestasis (Kennedy et al. 2014), suggesting MC may also contribute to cholangiocyte-derived, CWEC proliferation. In addition to MCs, other immune cells are also found in patients with PKD. For example, $CD45^+$, a molecule found on all leukocytes, and $CD4^+$ lymphocytes were identified in the interstitium of rodent models of PKD and ADPKD patients (Kaspareit-Rittinghausen et al. 1989, Takahashi et al. 1991, Zeier et al. 1992, Vogler et al. 1999). The significance of lymphocytes has not been addressed in PKD, which requires additional study. Further, an increased amount of complement protein 3 (C3a), a potent pro-inflammatory molecule and chemotactic agent, is detected in kidneys from *cpk*, BALB/c-*bpk,* and FVB-*orpk* mice, all of which are mouse models of ARPKD (Mrug et al. 2008). Taken together, these data suggest that activation of innate and adaptive immune effector cells and associated proteins contribute to progression of PKD.

Although PKD is not primarily considered an inflammatory disorder, accumulating evidence suggests that inflammation occurs in the early stage of the disease and may

also drive disease progression. For example, macrophage infiltration is found in the renal interstitium in human ADPKD patients with kidney failure (Zeier et al. 1992). Activated macrophages stimulate vascular endothelial cell proliferation *in vitro* (Polverini et al. 1977). Further, TNF-α, an inflammatory cytokine, is present in renal cyst fluid of human ADPKD, and induces renal cyst formation through regulating polycystin-2 (Li et al. 2008). In ARPKD, M2-like macrophages are present in kidneys from ARPKD patients and *cpk* mice, and depletion of macrophages in *cpk* mice restrains pathological enlargement of kidneys (Swenson-Fields et al. 2013). In *PKHD1*$^{del4/del4}$ mice, cystic cholangiocytes secrete a range of chemokines, such as chemokine (C-X-C motif) ligands 1, 10, and 12, which stimulate M1- and M2- macrophage recruitment to portal regions of the liver. Recruited macrophages release pro-inflammatory cytokines such as TNFα (M1) and TGFβ1 (M2), both of which up-regulates αvβ6 integrin on cystic cholangiocytes. In *PKHD1*$^{del4/del4}$ mice, the proportion of M1 macrophages is high initially, but the contribution of M2 macrophages increases progressively at 9 months. αvβ6 is an activator of latent local TGFβ1, and activation of which promotes liver fibrosis (Figure 1.6.1, (Locatelli et al. 2016)). Depletion of macrophages by clodronate in *PKHD1*$^{del4/del4}$ mice treated from 3 to 6 months could reduce macrophage infiltration, myofibroblast activation, and halt liver fibrosis progression (Locatelli et al. 2016). This supports a role of macrophages in the progression of ARPKD. Work from others has found increased MCP-1 in kidneys from PCK rats (Zoja et al. 2015). Consistent with a role for MCP-1 and macrophage infiltration in progression in PKD, inhibition of MCP-1 synthesis with bindarit reduces renal inflammation and renal dysfunction, but did not

attenuate cyst growth (Zoja et al. 2015). Whether or not MCP-1 depletion affected hepatic inflammation, cyst growth or fibrosis was not evaluated in this study.

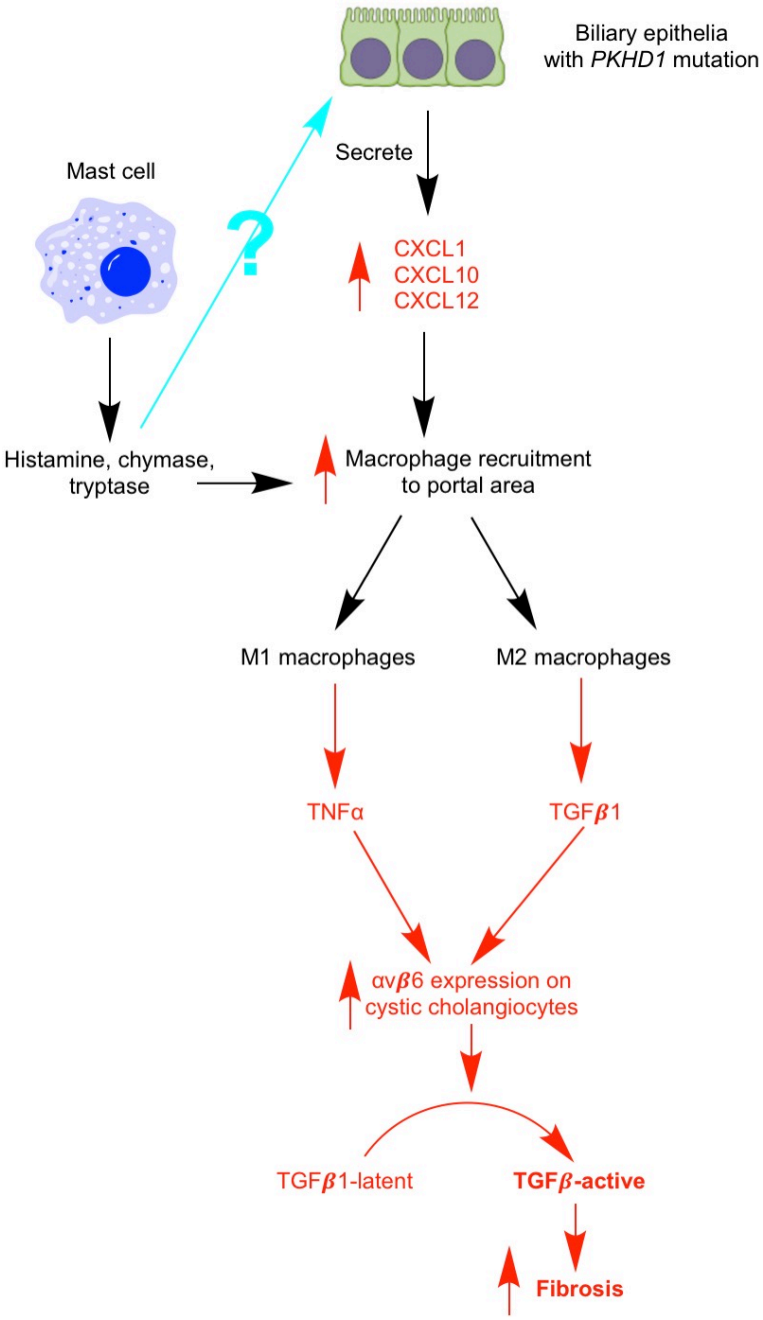

Fig.1.6.1. Schematic representation of inflammation in CHF/ARPKD. Biliary epithelia with *PKHD1* mutation secrete chemokines such as CXCL1. CXCL10, and CXCL12, which recruit M1- and M2- macrophages to the portal area. M1- and M2-macrophages produce TNFα and TGFβ that further cause αvβ6-induced activation of TGFβ. TGFβ activation eventually promotes liver fibrosis progression (Locatelli et al. 2016). Mast cells release histamine, tryptase, and chymase. They directly and indirectly act as chemoattractants for inflammatory cells (Zoja et al. 2015).

1.7 THE 'PATHOGENIC TRIUMVIRATE' IN CHF/ARPKD: INSIGHTS INTO THE DEVELOPMENT OF NEW THERAPIES

Although mutations in the human *PKHD1* gene, or mutations in *PKHD1* orthologs in rats and mice, are required for development of CHF/ARPKD, other factors are also involved in disease progression. It is from a review of the published literature and summarized in this chapter that we propose a 'pathogenic triumvirate' in CHF/ARPKD which includes three factors, cyst growth, fibrosis, and inflammation, as mediators contributing to disease progression (Figure 1.7.1). Despite recent advances in our understanding of what contributes to the initial pathology of CHF/ARPKD, less is known about the molecular mechanisms regulating continued cyst growth, progression of fibrosis, and how inflammation contributes to these interrelated processes. Furthermore, whether or not a common mechanism drives all members of the 'pathogenic triumvirate' is also not known. We propose that leveraging what we do know about the CHF/ARPKD pathogenesis in the context of the pathogenic triumvirate will lead the way to new research and possibly, new therapies for this disease. For example, finding a central mechanism that regulates all three components would be an attractive target for the development of new pharmacologic approaches to manage CHF/ARPKD. Alternatively, if a common mechanism does not exist, therapeutically targeting each member of the triumvirate concurrently may provide an advantage over any monotherapy used in isolation.

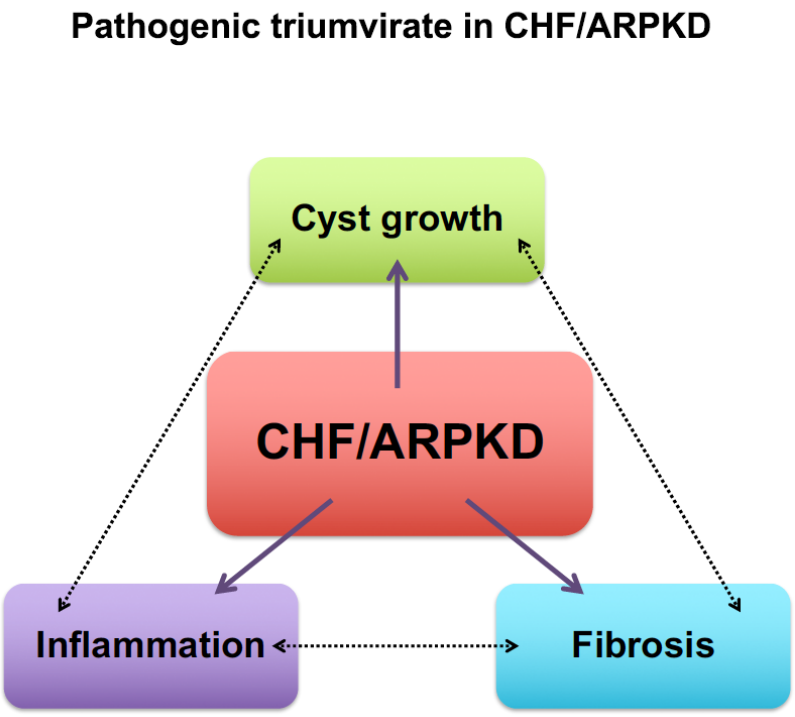

Figure 1.7.1: A 'pathogenic triumvirate' in congenital hepatic fibrosis (CHF) in autosomal recessive polycystic kidney disease (ARPKD).
Published data suggest that cyst growth, fibrosis, and inflammation drive CHF/ARPKD (solid purple arrows). We propose that relationships exist between cyst growth, fibrosis, and inflammation which drive progression of CHF/ARPKD (black, double-headed arrows with broken lines). Targeting a single pathway which drives each of the triumvirate members, or targeting multiple members concurrently, may provide better therapeutic strategies than if targeting any one member in isolation.

1.8 STATEMENT OF PURPOSE

ARPKD is a severe monogenic disorder that can affect both liver and kidney. Among all affected patients, approximately 30% die shortly after birth due to pulmonary insufficiency (Zerres et al. 1998). There is no cure besides liver/kidney transplantation. CHF is present as bile duct dilation resulting in eventual development of cysts and pericystic fibrosis in the liver (Shneider et al. 2005, Turkbey et al. 2009). The mechanisms behind hepatic cystogenesis and fibrogenesis are still unknown. Due to these reasons, my dissertation research aims to understand the mechanisms of cyst and fibrosis development in ARPKD, and to identify new targets for therapeutic purposes. To achieve this objective, we used mouse and rat models of CHF/ARPKD to study the mechanisms of disease development, identify potential therapeutic targets, and test novel interventional strategies to attenuate or halt disease progression, if not reverse disease pathogenesis entirely.

RNA-seq is a high-throughput sequencing assay that can be used for discovering differentially expressed genes (Mortazavi et al. 2008, Trapnell et al. 2010). Recent studies suggest that RNA-seq is more accurate than microarray in a large dynamic range of gene expression (Marioni et al. 2008). RNA-Seq is also more sensitive in detecting genes with very low expression and more accurate in detecting expression of extremely abundant genes (Zhao et al. 2014). To uncover changes of gene expression in CHF/ARPKD at the transcriptional level, we performed RNA-seq in SD as control and PCK rats at different time points. Our sequencing data provided us a better understanding of the disease and potential targets for future study.

Our RNA-seq analysis suggested that the Hippo signaling pathway was activated in PCK rats. Previous studies show that YAP and TAZ (a related transcriptional coactivator) are key activators of fibroblasts, and they sustain fibrosis by activating fibroblasts (Liu et al. 2015). As an oncoprotein, YAP activation is found in several human cancers (Zhao et al. 2007), and it plays a key role in the Hippo signaling pathway to control cell proliferation in response to cell contact (Zhao et al. 2007). Finally, YAP activation promotes endothelial cell proliferation and inflammatory response in atherosclerosis (Wang et al. 2016). Therefore, it is logical to predict that the Hippo signaling pathway could be the central pathway regulating each member of the pathogenic triumvirate in CHF/ARPKD. Our preliminary data suggest that YAP activity was increased in PCK rats and in ARPKD patients (Jiang et al. 2017). We hypothesized that YAP drives cyst progression in CHF/ARPKD.

In addition to cyst growth and fibrosis, inflammation is another pathological feature of CHF/ARPKD. In CHF/ARPKD patients, immune cells such as mast cells (MC) accumulate in hepatic pericystic areas (Ozaki et al. 2005). MCs are innate immune cells with a broad range of effector activity (Urb et al. 2012). They synthesize and store many molecules including chymase, tryptase and histamine in large cytoplasmic granules which they release during tissue injury and in response to other stimuli (Metcalfe et al. 1997). Inhibition of MC degranulation and histamine release with cromolyn sodium, a MC stabilizer, decreases cholangiocyte proliferation in bile duct ligation-induced cholestasis (Kennedy et al. 2014), suggesting MC may also contribute to cholangiocyte-derived, CWEC proliferation. Therefore, we hypothesized that MC plays a role in CHF/ARPKD progression.

HA-CD44 interaction is shown to enhance cholangiocyte proliferation and liver fibrosis in cholestasis (He et al. 2008). We found that *Cd44* expression was upregulated in PCK rats by real-time PCR and RNA-seq. Increased HA accumulation was also detected in liver samples from PCK rats and human ARPKD patient. Therefore, we hypothesized that HA-CD44 interaction may drive pathogenesis of CHF/ARPKD.

CHF/ARPKD is a hepatobiliary disease with no cure available. We hypothesized that there is a 'pathogenic triumvirate' that regulates disease progression. The objective of this dissertation is to expand our understanding of this disease at the molecular level and to identify central molecular mediators of the 'pathogenic triumvirate'. By testing multiple hypotheses in animal models of CHF/ARPKD, we expected to identify novel points of intervention and apply that information to benefit CHF/ARPKD patients in the clinic.

CHAPTER II: DISCOVERING MOLECULAR MEDIATORS OF CHF/ARPKD USING RNA-SEQ

2.1 ABSTRACT

Congenital hepatic fibrosis (CHF) is a neonatal hepatic inherited disease characterized by the presence of hepatic cysts derived from dilated bile ducts and a robust, pericystic fibrosis. To characterize early disease progression at the molecular level, we performed an RNA-seq analysis on liver samples from PCK rats, a model of CHF, over a time course of postnatal day (PND) 15 to 90. Sprague-Dawley (SD) rats were used as controls. The number of differentially expressed genes increased in PCK rats over time. Upstream regulator analysis using the Ingenuity Pathway Analysis (IPA) predicted activation of several pro-proliferative and pro-inflammatory regulators in PCK rats including *Ctnnb* (catenin beta 1), *Mtpn* (myotrophin), *Rb1* (RB transcriptional corepressor 1) and several *Stat* (Signal transducer and activator of transcription) family members (z score ≥ 2). Further, PCK rat livers contained gene signatures consistent with decreased activation of *Smad7*, which inhibits fibrosis. Finally, PCK rat livers exhibited significant suppression of *Hnf4a*, the master regulator of hepatic differentiation. Overall, our RNA-seq data suggest that cystogenesis and fibrosis in PCK rats is driven by an imbalance between anti and pro-proliferative and anti and pro-fibrotic factors on the background of significant ongoing inflammation.

2.2 INTRODUCTION

Autosomal recessive polycystic kidney disease (ARPKD) is a hereditary disorder caused by mutations in *PKHD1* (Onuchic et al. 2002). The clinical spectrum is widely variable with multiple organs affected, primarily kidneys and liver. Kidney disease is characterized by tubule dilation and focal cyst development from collecting ducts (Blyth et al. 1971, Ward et al. 2003). Liver disease in ARPKD is called congenital hepatic fibrosis (CHF), which involves development of segmental dilations of bile ducts accompanied by periportal fibrosis (Desmet 1992). CHF causes a significant proportion of morbidity and mortality in ARPKD patients who develop portal hypertension (Shneider et al. 2005). Although the mechanisms of hepatic cyst expansion are not well characterized in human ARPKD, different factors, such as cholangiocyte hyperproliferation and fluid secretion, have been proposed that contribute to the progression of cysts (Gradilone et al. 2010). To study ARPKD, one of the best-characterized animal models for human ARPKD is the PCK rat, derived from a colony of Sprague-Dawley (SD) rats at Charles River, Inc (Katsuyama et al. 2000). As a spontaneously occurring inherited model of ARPKD, they bear a striking resemblance with human ARPKD pathobiology including hepatorenal cysts and fibrosis (Lager et al. 2001).

The mechanisms underlying gene expression involved in CHF/ARPKD pathogenesis are not known. We applied RNA-seq technology to analyze liver samples from SD rats and PCK rats at different time points after birth. Our data provide a significant amount of new information on gene expression changes, upstream

regulators changes, and their associated pathways at the transcriptional level in CHF/ARPKD.

We previously proposed a ‘pathogenic triumvirate’ to describe the three pathogenic components in CHF/ARPKD, which includes cyst growth, inflammation, and fibrosis (Jiang et al. 2016). Using RNA-seq analysis, we found that differentially expressed genes, transcription factors, and canonical pathways in PCK can be categorized into one of the three components. In addition, we identified several genes and transcription factors related to liver development and metabolism in PCK rats that may contribute to the pathogenesis of CHF/ARPKD. Overall, our study provides a comprehensive characterization of gene expression profile in CHF/ARPKD. By identifying potential regulators of the ‘pathogenic triumvirate’ and other possible contributors of CHF/ARPKD, we propose several molecular targets of the disease that can be informative for therapy in future studies.

2.3 MATERIALS AND METHODS

Animals

Male and female polycystic kidney (PCK) rats and Sprague-Dawley (SD) rats (control strain for PCK) were purchased from Charles River and housed in an AAALAC-approved vivarium at the University of Kansas Medical Center (KUMC). All animal studies were approved by the KUMC Institutional Animal Care and Use Committee (IACUC) and were performed in accordance with IACUC guidelines.

Sample preparation and RNA isolation

Liver samples were collected from SD and PCK rats at postnatal day (PND) 15, 20, 30, and 90 (n = 3 each time point each genotype). Both male and female rats were included. Liver pieces (20 – 30 mg) for RNA isolation were transferred to 1.5 mL of RNAlater-ICE (Ambion Inc., Austin, TX, USA) and stored at −80 °C overnight before use. Total RNA was isolated with an RNeasy Mini Kit (Qiagen, Valencia, CA, USA) after homogenization using a MP Biomedicals Fast Prep 24 bead homogenizer with lysing matrix D homogenization tubes (Solon, OH, USA). The total RNA concentration and purity were determined by a NanoDrop apparatus.

RNA library preparation and data collection

Total RNA (500 ng) was used to construct the Stranded mRNA-Seq library. Briefly, the total RNA fraction was fragmented, reverse transcribed into cDNA, and ligated with the appropriate indexed adaptors using the TruSeq Stranded mRNA LT Sample Preparation Kit (Illumina, San Diego, CA, USA). The quality of library was validated by an Agilent Bioanalyzer. Library quantification was measured using the Roche Lightcycler96 with FastStart Essential DNA Green Master. Library concentrations were adjusted to 4 nM and pooled for multiplexed sequencing. Libraries were denatured and diluted to the appropriate pM concentration followed by clonal clustering onto the sequencing flow cell using the TruSeq Paired-End (PE) Cluster Kit v3-cBot-HS. The clonal clustering procedure is automated using the Illumina cBOT Cluster Station. The clustered flow cell was sequenced on the Illumina HiSeq 2500 Sequencing System

using the TruSeq SBS Kit v3-HS. Sequence data is converted to Fastq format from Bcl files and de-multiplexed into individual sequences for further downstream analysis.

Bioinformatic analysis for RNA-Seq

100 bp reads were mapped to the Rnor_5.0 genome using STAR (Dobin et al. 2013). Transcript assembly was performed with Cufflinks and Cuffmerge (Trapnell et al. 2012). A counts table was generated using HTSeq-count (Anders et al. 2015) and imported into EdgeR (Robinson et al. 2010, McCarthy et al. 2012) to evaluate differential gene expression. Volcano plots are created with EdgeR to visualize differentially expressed gene pattern. The heatmap and hierarchical clustering were analyzed using GenePattern platform at BROAD Institute (http://software.broadinstitute.org/cancer/software/genepattern/). Pathway analysis was performed using Ingenuity Pathway Analysis (IPA, Ingenuity Systems, www.ingenuity.com). Differential expression was determined by absolute fold change > 1.5 and a q-value (the p-value adjusted for multiple hypothesis correction using the Benjamini-Hochberg procedure) less than or equal to 0.05. The IPA upstream analysis was performed to predict the activated and inhibited upstream regulators using activation of z-score algorithm. The activation Z-score is applied to quantify the significance of the concordance between the direction of change of genes (up-/down-regulated) in a gene dataset and the established direction of change (derived from literature) of genes associated with a transcriptional regulator. A z-score ≥ 2 or ≤ -2 is considered significantly activated or inhibited. P value of overlap reflects that the

overlap between the experimental dataset and a given transcriptional regulator is due to a random chance. An overlap p-value≤0.05 was considered significant.

2.4 RESULTS

Identification of differentially expressed genes in PCK rats over progression of CHF/ARPKD.

The PCK rat liver showed a total of 3163 genes upregulated and 2285 genes down regulated over the four time points (Figure 2.4.1A). With increase in time after birth, the number of the differentially expressed genes also increased. Figure 2.4.1B shows volcano plots of differentially expressed genes in PCK rats from PND 15 to PND 90. We selected top 100 upregulated genes and top 100 downregulated genes at in PCK rats at PND 15, 20, 30, and 90. We found 24 genes were in common. A heatmap representation of the transcript levels coupled to a hierarchical clustering of the time point was obtained to show the gene pattern in PCK rats (Figure 2.4.1C). Among the analyzed time points, *Adgrg1, Cdh6, Clec2l, Krt7, Reg3b*, and *Sncg* expression peaked at PND 30. *Ctgf*, *Cyp2b2,* and *RGD1560242* expression decreased from PND 15 to PND 90. *Ddx39b, Fam111a, Krt20, Lamc2, Lilrb31, Loc10091107, Lyc2, Lypd8*, *Ms4a18, Msln, Nfkbi*, and *Tead4* expression increased from PND 15 to PND 90 in PCK rats (Figure 2.4.1C). At PND 15, the top 10 upregulated and downregulated genes ranked according to fold change are described in Table 2.4.1. Similarly, the top upregulated and downregulated genes in PCK rats at PND 20, 30, and 90 are summarized in Tables 2.4.2 – 2.4.4.

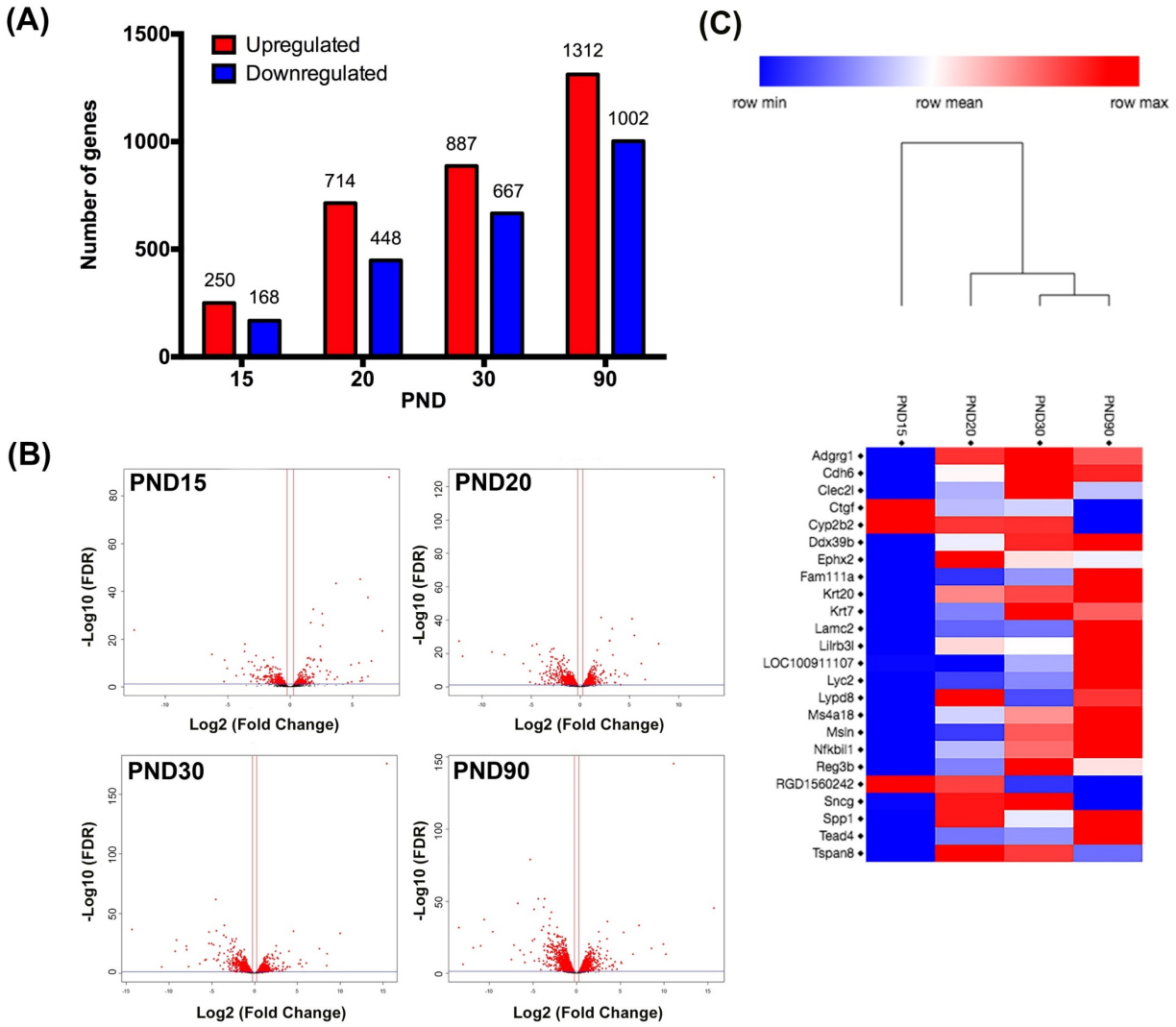

Figure 2.4.1. Differentially expressed genes in PCK rats at postnatal (PND) 15, 20, 30, and 90. (A) Number of genes up- or down- regulated in PCK rats at postnatal (PND) 15, 20, 30, and 90. n = 3 per genotype per time point. Cut off fold change is ± 1.5 compared to Sprague Dawley (SD) rats at each individual time point, $q < 0.05$. (B) Volcano plots for differentially expressed genes in PCK rats from at PND 15, 20, 30, and 90. The horizontal axis is the log2 (fold change) between SD and PCK rats. The -log10 (FDR) is plotted on the vertical axis. Each gene is represented by one point on the graph. (C) Heatmap and hierarchical clustering of four time points (PND 15, 20, 30, and 90) by similar expression profiles. The fold change of each gene in PCK rats are converted to heatmap color using the mean and maximum values for each gene. The intensity scale of the standardized expression values ranges from dark blue (low expression) to dark red (high expression).

Table 2.4.1. Top 10 up- and down-regulated genes In PCK rats at PND 15.

Gene Name	Gene Symbol	Fold Change	q-value
Up-regulated Genes			
Leukocyte elastase inhibitor A-like	*LOC100911107*	76.62	2.08E-14
Protease, serine, 32	*Prss32*	39.19	0.004261265
TEA domain transcription factor 4	*Tead4*	38.07	4.70E-12
Regenerating islet-derived protein 3-beta	*Reg3b*	32.74	1.67E-08
LY6/PLAUR domain containing 8	*Lypd8*	20.06	1.98E-05
Membrane spanning 4-domains A18	*Ms4a18*	13.18	5.42E-06
Family with sequence similarity 111	*Fam111a*	12.31	1.00E-18
Connective tissue growth factor	*Ctgf*	10.10	2.49E-11
Cadherin 17	*Cdh17*	8.93	5.46E-06
Otogelin-like	*Otogl*	8.85	0.005534415
Down-regulated Genes			
DExD-box helicase 39B	*Ddx39b*	-74.90	3.15E-38
Hepcidin antimicrobial peptide	*Hamp*	-74.79	3.38E-05
Similar to RIKEN cDNA 1700028P14	*RGD1560242*	-54.49	0.001730345
Urinary protein 3-like	*AABR07069676.1*	-48.67	0.003629237
NFKB inhibitor like 1	*Nfkbil1*	-12.71	4.03E-44
Complement factor H	*Cfh*	-11.89	0.000542193
Epoxide hydrolase 2	*Ephx2*	-8.24	7.72E-06
17-beta-hydroxysteroid dehydrogenase type 6	*LOC100362350*	-3.77	5.84E-06
DNA ligase 4	*Lig4*	-3.63	2.40E-33
Regulator of G-protein signaling 16	*Rgs16*	-3.62	0.02294837

Table 2.4.2. Top 10 up- and down-regulated genes In PCK rats at PND 20.

Gene Name	Gene Symbol	Fold Change	q-value
Up-regulated Genes			
Regenerating family member 3 beta	*Reg3b*	5203.98	3.70E-28
LY6/PLAUR domain containing 8(Lypd8)	*Lypd8*	4059.76	3.58E-19
TEA domain transcription factor 4	*Tead4*	210.19	4.46E-20
Leukocyte elastase inhibitor A-like	*LOC100911107*	56.05	1.01E-14
Membrane spanning 4-domains A18	*Ms4a18*	34.88	1.96E-10
Tetraspanin 8	*Tspan8*	30.07	1.53E-25
Family with sequence similarity 111	*Fam111a*	21.52	2.13E-26
Lipocalin2	*Lcn2*	17.13	1.23E-08
Gamma-aminobutyric acid type A receptor pi subunit	*Gabrp*	15.06	1.29E-06
Keratin7	*Krt7*	14.71	7.25E-16
Down-regulated Genes			
Similar to RIKEN cDNA	*RGD1560242*	-74.79	3.38E-05
DExD-box helicase 39B	*Ddx39b*	-54.49	0.001730345
Achaete-scute family bHLH transcription factor 1	*Ascl1*	-11.89	0.000542193
Adenylate cyclase 1	*Adcy1*	-8.24	7.72E-06
Similar to RalA binding protein 1	*LOC304239*	-3.77	5.84E-06
NFKB inhibitor like 1	*Nfkbil1*	-9.48	1.39E-35
Insulin-like growth factor 2	*Igf2*	-8.40	1.37E-07
Angiomotin-like 1	*Amotl1*	-7.84	1.39E-28
Adenylate cyclase 10	*Adcy10*	-6.00	3.07E-06
Alpha-fetoprotein	*Afp*	-5.23	7.25E-10

Table 2.4.3. Top 10 up- and down-regulated genes In PCK rats at PND 30.

Gene Name	Gene Symbol	Fold Change	q-value
Up-regulated Genes			
Regenerating family member 3 beta	*Reg3b*	20353.43	2.48E-37
Interferon-inducible GTPase 1-like	*LOC100910934*	1837.83	4.52E-06
LY6/PLAUR domain containing 8	*Lypd8*	623.59	2.35E-19
Leukocyte elastase inhibitor A-like	*LOC100911107*	565.93	1.11E-28
Membrane spanning 4-domains A18	*Tead4*	253.25	1.51E-23
Ubiquitin D	*Ubd*	210.70	2.52E-06
Similar to interferon-inducible GTPase	*RGD1309362*	84.26	6.98E-09
Gamma-aminobutyric acid type A receptor pi subunit	*Gabrp*	55.37	1.03E-11
Membrane spanning 4-domains A18	*Ms4a18*	50.83	2.53E-12
Family with sequence similarity 111, member A	*Fam111a*	39.95	2.89E-35
Down-regulated Genes			
Similar to RIKEN cDNA	*RGD1560242*	-349.90	4.36E-17
Major urinary protein 4	*Mup4*	-338.82	3.06E-07
Urinary protein 1-like1	*Rup4*	-186.77	2.19E-21
3 beta- and steroid delta-isomerase 2	*Hsd3b2*	-64.83	2.72E-09
Urinary protein 3-like	*LOC100912405*	-39.71	7.61E-09
DExD-box helicase 39B	*Ddx39b*	-16.06	3.31E-19
Cytochrome P450, subfamily 2, polypeptide 11	*Cyp2c11*	-14.47	2.52E-06
SH3 and cysteine rich domain 3	*Stac3*	-13.71	6.50E-06
Tectorin beta	*Tectb*	-12.29	0.00025377
Ras homolog family member U	*Rhou*	-10.34	7.66E-10

Table 2.4.4. Top 10 up- and down-regulated genes In PCK rats at PND 90.

Gene Name	Gene Symbol	Fold Change	q-value
Up-regulated Genes			
Regenerating family member 3 beta	*Reg3b*	11396.22	1.37E-32
Interferon-inducible GTPase 1-like	*LOC100910934*	8275.89	4.22E-07
LY6/PLAUR domain containing 8	*Lypd8*	3642.45	1.26E-18
Serine peptidase inhibitor, Kazal type 1	*Spink3*	2016.91	5.84E-20
Leukocyte elastase inhibitor A-like	*LOC100911107*	1557.14	6.02E-38
TEA domain transcription factor 4	*Tead4*	781.09	1.21E-29
Lipocalin 2	*Lcn2*	146.66	2.79E-20
Family with sequence similarity 111	*Fam111a*	106.52	2.26E-49
Membrane spanning 4-domains A18	*Ms4a18*	65.89	1.07E-13
Similar to interferon-inducible GTPase	*RGD1309362*	60.81	2.09E-08
Down-regulated Genes			
SH3 and cysteine rich domain 3	*Stac3*	-982.80	6.32E-21
Similar to RIKEN cDNA 1700028P14	*RGD1560242*	-382.83	4.97E-18
ATP binding cassette subfamily G member 8	*Abcg8*	-139.79	4.07E-34
ATP binding cassette subfamily G member 5	*Abcg5*	-41.83	3.17E-29
Hydroxy-delta-5-steroid dehydrogenase	*LOC100911154*	-34.57	1.24E-07
Carbonic anhydrase 3	*Car3*	-34.39	1.50E-08
Major urinary protein 4	*Mup4*	-24.26	0.000915635
Small nucleolar RNA SNORD113/SNORD114 family	*SNORD113*	-16.77	0.003332349
Carboxypeptidase A1	*Cpa1*	-15.28	5.27E-11
Urinary protein 3-like	*LOC100912405*	-13.54	1.06E-05

Identification of upstream regulators and canonical pathways in PCK rats.

To further investigate the global gene expression data to identify key players, we performed an upstream regulator analysis using the Ingenuity Pathway Analysis (IPA) software. The upstream regulators were predicted based on the IPA database. Predicted upstream regulators at PND 15 are shown in Table 2.4.5. CTNNB1, MTPN, TCF7L2 and STAT5B were significantly activated ($z \geq 2$) in PCK rats, and CBX5 was significantly inhibited ($z \leq -2$) in PCK rats. Interestingly, IPA analysis predicted activation of various members of STAT family of proteins from PND 20 to PND 90 (Table 2.4.6 – 2.4.8). Our data suggest that STAT3 was the most significantly activated upstream regulator at PND 90 (Table 2.4.8). Similarly, IPA predicted activation of myotrophin (MTPN), a protein involved in regulation of NF-κB activity at all time points studied. The analysis showed predicted inhibition of HNF4α at PND 30 and 90 in PCK rats.

IPA analysis was used to identify changes in canonical pathways (Figure 2.4.2). The top canonical pathways changed included LPS/IL-1 signaling at PND 20, 30 and 90 where it was significantly upregulated at PND30 and 90 indicating ongoing inflammatory signaling in PCK rat livers. Consistent with this increased IL-8 signaling was also observed at PND 90.

Table 2.4.5. Upstream regulators at PND 15 in PCK rats.

Upstream Regulator	Function	Predicted Activation State	Activation z-score	p-value of overlap
CTNNB1	β-catenin, role in liver development, regeneration, and cancer	Activated	2.782	2.91E-05
MTPN	Regulates cardiac hypertrophy, cell growth, and NFκB activity	Activated	2.433	1.03E-03
TCF7L2	Role in Wnt signaling, blood glucose homeostasis	Activated	2.167	2.27E-04
STAT5B	Activated by IL2, IL4, CSF1; involved in TCR signaling, apoptosis	Activated	2.000	8.28E-02
CBX5	Involved in the production of kinetochores	Inhibited	-2.236	2.45E-02

Table 2.4.6. Upstream regulators at PND 20 in PCK rats.

Upstream Regulator	Function	Predicted Activation State	Activation z-score	p-value of overlap
RB1	Negative regulator of cell cycle, tumor suppressor	Activated	3.359	2.13E-01
STAT4	Activated by IL12, regulates T cell differentiation	Activated	3.174	7.72E-03
SMARCA4	Binds to BRCA1, regulates CD44 expression	Activated	3.022	4.79E-08
MTPN	Regulates cardiac hypertrophy, cell growth, and NFκB activity	Activated	2.728	7.06E-04
ARNT	Role in xenobiotic metabolism	Activated	2.513	4.18E-05
KDMSA	Demethylates histone H3	Inhibited	-2.530	5.17E-02
CBX5	Involved in the production of kinetochores	Inhibited	-2.309	1.37E-04

Table 2.4.7. Upstream regulators at PND 30 in PCK rats.

Upstream Regulator	Function	Predicted Activation State	Activation z-score	p-value of overlap
MTPN	Regulates cardiac hypertrophy, cell growth, and NFκB activity	Activated	3.44	0.00154
IRF7	Expressed in lymphoid tissue	Activated	3.01	0.0171
SMARCA4	Binds to BRCA1, regulates CD44 expression	Activated	2.847	3.24E-10
STAT3	Role in cell growth, apoptosis, inflammation, PKD development	Activated	2.641	3.68E-08
STAT1	Activated by IFNα, EGF, PDGF, IL6	Activated	2.629	0.0263
HNF4A	Regulates expression of hepatic genes, liver development	Inhibited	-3.029	2.71E-09
ATF4	Interacts with Nrf2, CREB	Inhibited	-2.94	5.57E-08
CBX5	Involved in the production of kinetochores	Inhibited	-2.84	0.000195
NFE2L2	Regulates genes with ARE, role in inflammation and injury	Inhibited	-2.775	0.000000158
SMAD7	Antagonist of TGFβ signaling	Inhibited	-2.691	0.00000789

Table 2.4.8. Upstream regulators at PND 90 in PCK rats.

Upstream Regulator	Function	Predicted Activation State	Activation z-score	p-value of overlap
STAT3	Role in cell growth, apoptosis, inflammation, PKD development.	Activated	4.599	1.2E-12
FOXO1	Involved in gluconeogenesis	Activated	4.186	2.32E-06
STAT4	Activated by IL12, regulates T cell differentiation	Activated	4.016	0.00127
MTPN	Regulates cardiac hypertrophy, cell growth, and NFκB activity	Activated	3.501	8.04E-07
HNF4A	Regulates expression of hepatic genes, liver development.	Inhibited	-2.821	1.3E-15
SMAD7	Antagonist of TGF$\boldsymbol{\beta}$ signaling	Inhibited	-2.668	0.00062
ZFP36	Role in metabolic processes, autoimmune diseases	Inhibited	-2.559	0.00995
SNAI1	Role in mesoderm formation	Inhibited	-2.509	0.00554
HDAC5	Represses MEF2, controls cell cycle, and cancer cell survival	Inhibited	-2.236	0.00576

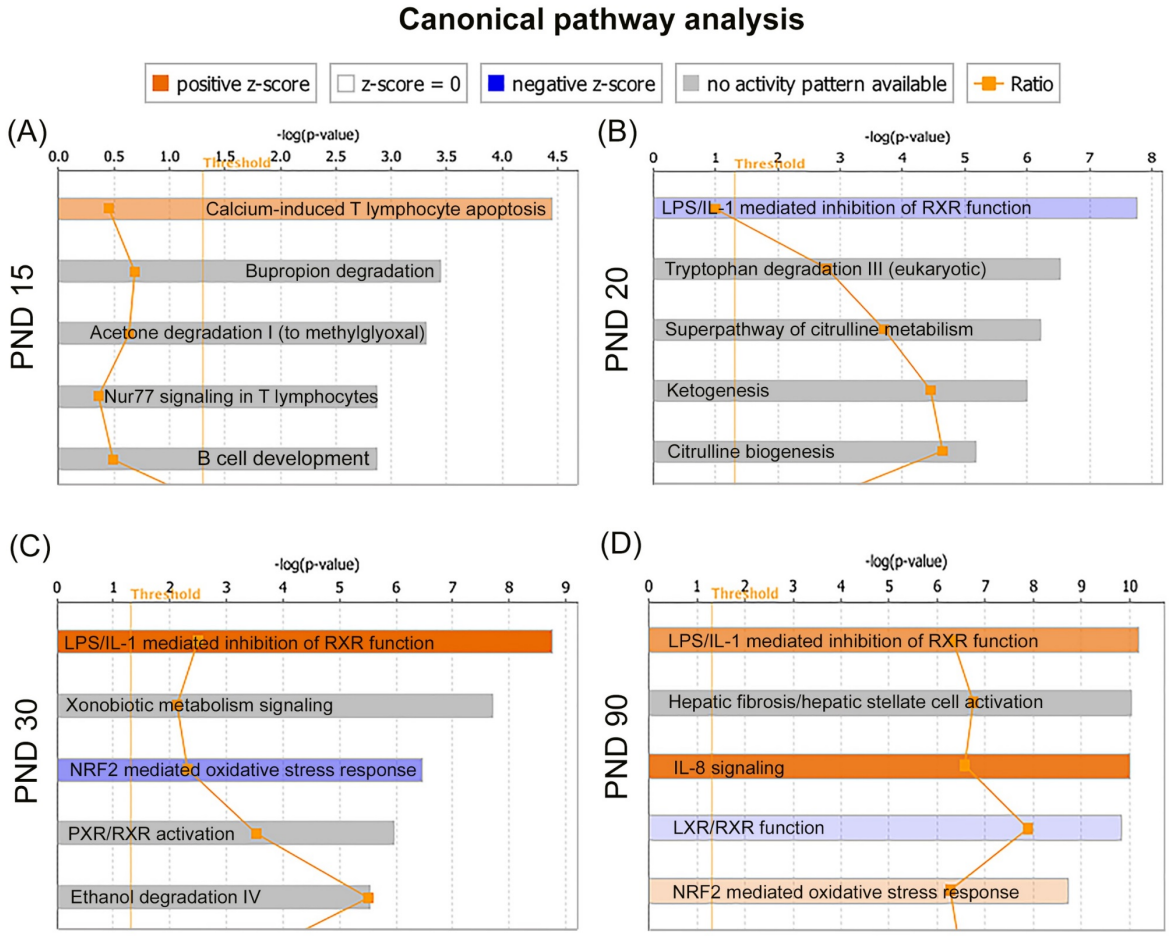

Figure 2.4.2. Top five impacted pathways in PCK rats from at PND 15, 20, 30, and 90. Blue bars indicate negative z score**.** Orange bars indicate positive z score. The orange line indicates ratio of genes in the network to total number of genes in the canonical pathway. Threshold is –log(p-value) = 1.3.

Functional analysis of transcriptomic data from PND 30 to PND 90 in SD and PCK rats.

As we found the number of differentially expressed genes was highest at PND 90, we compared the gene changes from PND 30 to PND 90 in SD and PCK rats. In each genotype, we identified the differentially expressed genes from PND 30 to PND 90, and we used IPA to compare the activation/inhibition status of different canonical pathways (Figure 2.4.3A) and diseases and functions (Figure 2.4.3B) in PCK rats compared to SD rats. This analysis revealed significantly higher activation of genes associated with inflammation including NF-κB activation, B and T lymphocyte-associated pathways, increased oxidative signaling via iNOS, and acute phase response (Figure 2.4.3A, indicated by the red box). Similarly, Nrf-2 signaling was reduced in SD rats from PND 30 to 90 but was significantly increased in PCK rats (Figure 2.4.3A, indicated by red asterisk). The disease and function analysis revealed overall decrease in expression of genes associated with tumor growth and cell proliferation in SD rats from PND 30 to 90, and an increased activation of immune-associated functions in PCK rats from PND 30 to PND 90 (Figure 2.4.3B, indicated by the red box). Interestingly, the genes associated with fibrosis were further inhibited in PCK rats compared to SD rats from PND 30 to PND 90 (Figure 2.4.3B, indicated by red asterisk).

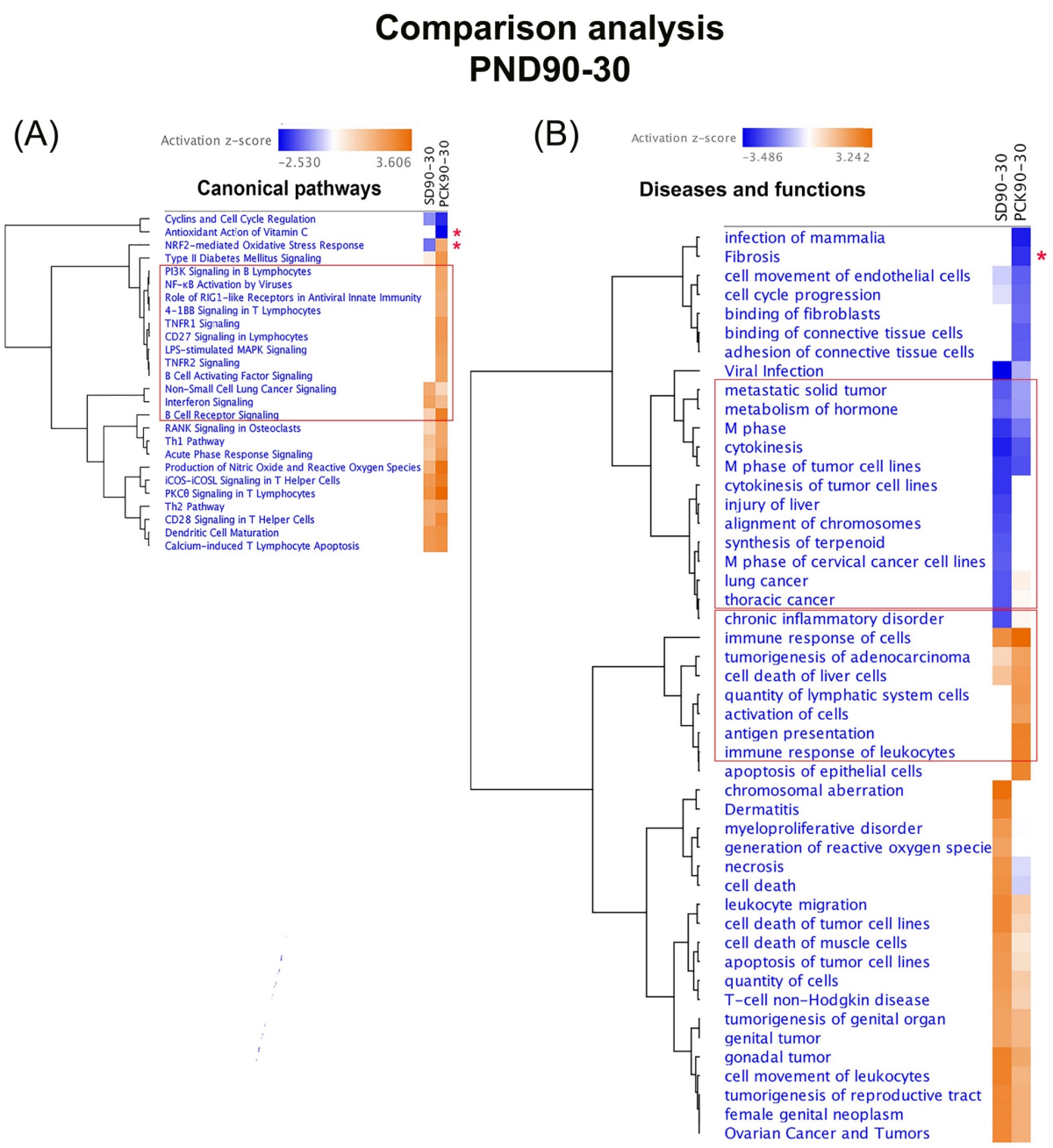

Figure 2.4.3. Comparison analysis between Sprague Dawley (SD) and PCK rats from PND 30 to PND 90. Hierarchical clustering analysis for pathways and disease and function. A dendrogram (tree graph) shows the grouping of the canonical pathways (A) and diseases and function (B) based on the similarity between them. Absolute z score cutoff is 2.

Identification of transcriptional regulators of the 'pathogenic triumvirate'.

We proposed that a 'pathogenic triumvirate' consisting of cyst growth, inflammation, and fibrosis is the central regulator of CHF/ARPKD (Jiang et al. 2016). Therefore, we categorized the IPA-predicted transcriptional regulators based on their potential roles in each component of the 'pathogenic triumvirate' (Figure 2.4.4). In addition, we found several transcriptional regulators related to liver development, such as HNF4α, inhibition of which may cause an impaired liver development (Figure 2.4.4). Taken together, our data suggest that in addition to the components of the 'pathogenic triumvirate' that contribute to the progression of CHF/ARPKD, liver development and metabolism dysfunction may also contribute to the disease progression.

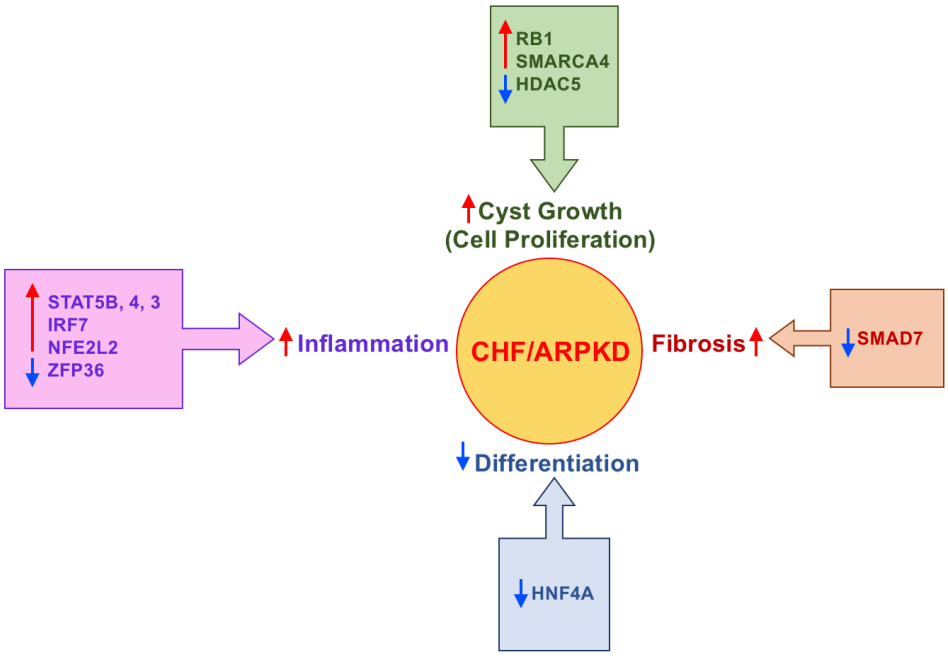

Figure 2.4.4. Schematic diagram showing molecular factors regulating pathogenesis of CHF/ARPKD. Based on the Ingenuity Pathway Analysis (IPA) knowledge base, transcription factors predicted by IPA are categorized into: cyst growth (cell proliferation), inflammation, and fibrosis. Transcription factor HNF4A not originally considered in the context of the 'pathogenic triumvirate' is now included to acknowledge the potential contribution of reduced liver differentiation to CHF/ARPKD pathogenesis.

2.5 DISCUSSION

CHF/ARPKD is a life-threatening genetic disease with distinct clinical features. Although the phenotypes of CHF/ARPKD are well-characterized, the mechanisms driving these phenotypes in CHF/ARPKD are still unknown. To define these mechanisms, we performed RNA-Seq analysis in SD and PCK rats at various time points to compare the gene expression alterations associated with mutation in gene *PKHD1.* Our data suggest that as the disease develops, there is an increased divergence from the normal phenotype. We also identified several canonical pathways and upstream regulators impacted by the disease.

Among the top upregulated genes in PCK rats, *Tead4* is consistently upregulated from PND 15 to PND 90. TEADs are important transcription factors of the Hippo signaling pathway. By partnering with Yes-associated protein (YAP), they activate the downstream targets of the pathway involved in cell proliferation, cell growth, planar cell polarity, and cell death (Vassilev et al. 2001, Zhao et al. 2007, Happe et al. 2011, Wu et al. 2013). Our previous study suggests that YAP is activated in cystic cholangiocytes from PCK rats and ARPKD patients. Inhibition of YAP activity with verteporfin, a YAP-TEAD inhibitor, decreased cystic cholangiocyte proliferation *in vitro* (Jiang et al. 2017). Consistently, *Ctgf,* the YAP-TEAD target gene, is one of the top ten upregulated genes in PCK rats at PND 15, and its transcription level is still increased from PND 20 to PND 90 (data not shown). Connective tissue growth factor (CTGF) is a matricellular protein that plays a central role in tissue remodeling (Lipson et al. 2012). CTGF expression can be induced in pathophysiological conditions, and it induces formation of myofibroblasts from different cell types, such as stellate cells (Paradis et al. 2002), epithelial cells

(Gore-Hyer et al. 2002), resident fibroblasts (Grotendorst et al. 2004), or recruited fibrocytes (Lee et al. 2015). CTGF expression is generally very low in normal liver, and its expression increases in liver fibrogenesis (Paradis et al. 1999). Inhibition of CTGF has been used as a therapeutic option in liver fibrosis (Li et al. 2006, Raghu et al. 2016, Sakai et al. 2017). These data indicate that the Yap-TEAD-CTGF axis could be a therapeutic target in CHF/ARPKD.

Among the upstream regulators predicted by IPA, we found several STAT family members, including *Stat3, Stat4*, and *Stat5b*. Previous studies have shown strong activation of STAT3 regulated by polycystin-1 (PC-1), the gene product of PKD1 (mutated in ADPKD) in cyst-lining epithelial cells in mouse and human ADPKD (Talbot et al. 2011). Further, treatment with STAT3 inhibitors decreased cell proliferation in human ADPKD cells, blocked renal cyst formation in a PKD mouse models and reduced cyst formation and growth in a neonatal PKD mouse model (Takakura et al. 2011). STAT6, another member of STAT family, has an increased activity in two murine PKD models, mediated by interleukins IL4 and IL13 (Olsan et al. 2011). Deletion of STAT6 in bpk/bpk, a model for PKD, resulted in less severe kidney disease and an improvement of kidney function. Pharmacological inhibition of STAT6 led to suppression of renal cystic growth, lower kidney weight and cystic index. (Olsan et al. 2011). Our observations indicate that other members of STAT family including STAT4 and 5B could also be involved in CHF/ARPDK pathogenesis.

The IPA analysis predicted inhibition of *Smad7*, a negative regulator of transforming growth factor β (TGF-β) signaling, in PCK rats at PND 30 and PND 90. Inhibition of SMAD7 suggests an increased activation of the TGF-β signaling pathway,

which may further contribute to myofibroblast activation and fibrosis. The anti-fibrotic role of SMAD7 has been shown in multiple models of liver fibrosis including the CCl_4-induced liver fibrosis (Hamzavi et al. 2008), bile duct ligation, isolated primary hepatic stellate cells, (Dooley et al. 2003) and also in the unilateral ureteral obstruction (UUO)-induced renal fibrosis (Terada et al. 2002). All of these studies suggest that inhibiting TGF- β signaling through activating Smad7 can be a potential therapeutic tool in ARPKD.

In addition to the upstream regulators that were already established in ADPKD, such as STATs and SMAD-TGFβ signaling, we also found some upstream regulators unique in ARPKD. *Mtpn* (myotrophin) is a novel target predicted by IPA in ARPKD. Upstream analysis revealed that *Mtpn* was activated from PND 15 to PND 90, suggesting its role is critical in ARPKD pathogenesis. Interestingly, MTPN stimulates insulin exocytosis, and its function can be suppressed by microRNA-375 (miR-375) (Poy et al. 2004), which is critical in maintenance of normal glucose homeostasis, regulation of insulin secretion and pancreatic α- and β-cell turnover in response to increasing insulin demand in insulin resistance (Poy et al. 2004, Poy et al. 2009). Interestingly, enhanced glycolysis, defective glucose metabolism, insulin resistance, and hyperinsulinemia have been reported in ADPKD patients (Vareesangthip et al. 1997, Rowe 2013). Our studies have identified *Mtpn* as a novel therapeutic target in CHF/ARPKD, which may correct the metabolic disorder inherent in the pathogenesis.

We also found that *Hdac5*, a histone deacetylase, was inhibited in PCK rats at PND 90. HDAC5, a class II HDAC, is generally associated with closed chromatin and represses gene expression through deacetylation of histones (Taunton et al. 1996,

Kadosh et al. 1997, Rundlett et al. 1998). HDAC5 is a negative regulator of angiogenesis, and silencing of HDAC5 increases the expression of fibroblast growth factor 2 (FGF2) and angiogenic guidance factors, including Slit2 (Urbich et al. 2009). Slit2 promotes angiogenesis by upregulating Robo1 and activating the vascular endothelial growth factor receptor 2 (VEGFR2)- extracellular signal-related kinase 1/2 (ERK1/2) pathway (Li et al. 2015). Therefore, inhibited activity of HDAC5 indicates that angiogenesis may be increased in PCK rats, and its increase is possibly related to pathogenesis of CHF/ARPKD. This is consistent with a role for 'pathologic' angiogenesis associated with liver fibrosis and cirrhosis in response to increasing portal hypertension; this is a common feature associated with CHF/ARPKD(Medina et al. 2003, Ni et al. 2017).

Finally, our studies revealed inhibition of *Hnf4a*, the master regulator of hepatic differentiation in CHF/ARPKD. HNF4A plays a critical role in liver development and hepatocyte differentiation. In fact, HNF4A is absolutely essential in differentiation of hepatocytes from hepatoblasts and its downregulation results in increased cell proliferation and cancer in the liver (Walesky et al. 2013, Walesky et al. 2015). A detailed analysis of *Hnf4a* target genes showed decline in several cytochrome P450 family members (*Cyp3a5*, *Cyp2c9*, and *Cyp2b6*), transporters (*Abcc2*, *Abcg5*, *Abcg8*, *Aqp8*, and *Slco1a1*), and lipid metabolism (*Acox2, Acsl1, Lipa, Pla2g4a*, and *Srebf1*). These data, for the first time reveal that CHF/ARPDK is not only associated with increased cystogenesis, fibrosis, and inflammation but also with significant dysregulation in hepatocyte differentiation, which may further increase disease-

associated morbidity. Further studies are needed to investigate the role of HNF4A in the disease and how it regulates the pathogenesis of CHF/ARPKD.

In conclusion, gene expression changes in CHF/ARPKD determined by RNA-Seq analysis provide a detailed map of significantly altered genes, signaling pathways, and upstream regulators that are dysregulated in CHF/ARPKD. Our findings provide insight into the molecular drivers of CHF/ARPKD, and shed light on potential therapeutic targets, such as *Tead4*, *Smad7*, *Mtpn*, *Stats*, *Hdac5*, and *Hnf4a* for this disease.

CHAPTER III: THE ROLE OF MAST CELLS IN CONGENITAL HEPATIC FIBROSIS IN AUTOSOMAL RECESSIVE POLYCYSTIC KIDNEY DISEASE

This chapter is adapted from Jiang L, P. P. Fang, S. Septer, U. Apte and M. T. Pritchard, “Inhibition of mast cell degranulation with cromolyn sodium exhibits organ-specific effects in polycystic kidney (PCK) rats,” Int. J. Toxicol, 2018, Manuscript accepted for publication.

3.1 ABSTRACT

Autosomal recessive polycystic kidney disease (ARPKD) is a monogenic disease characterized by development of hepatorenal cysts, pericystic fibrosis, and inflammation. Previous studies show that mast cell (MC) mediators such as histamine, induce proliferation of cholangiocytes. We observed robust MC accumulation around liver cysts, but not kidney cysts, in polycystic kidney (PCK) rats (an animal model of ARPKD). Therefore, we hypothesized that MCs contribute to hepatic cyst growth in ARPKD. To test this hypothesis, we treated PCK rats with one of two different mast cell stabilizers, cromolyn sodium (CS) or ketotifen. CS treatment decreased MC degranulation in liver and reduced serum tryptase (a MC granule component). Interestingly, we observed an increase in liver/body weight ratio after CS treatment paralleled by a significant increase in individual cyst size. Hepatic fibrosis was not affected by CS treatment. CS treatment increased hepatic cyst wall epithelial cell (CWEC) proliferation and decreased cell death. Ketotifen treatment also increased hepatic cyst size. *In vitro*, CS treatment did not affect proliferation of isolated hepatic CWECs from PCK rats. In contrast, CS decreased the kidney/body weight ratio paralleled by a significant decrease in individual cyst size. The percentage of kidney/body weight ratio was strongly correlated with serum renin (a MC granule component). Ketotifen did not affect kidney cyst growth. Collectively, these data suggest that CS treatment affects hepatic and renal cyst growth differently in PCK rats. Moreover, CS may be beneficial to renal cystic disease, but it may exacerbate hepatic cyst growth in ARPKD.

3.2 INTRODUCTION

Congenital hepatic fibrosis (CHF) associated with autosomal recessive polycystic kidney disease (ARPKD) is a serious hepatobiliary disease for which no curative pharmacologic treatments exist (Dell 2011). Dysfunctional cholangiocyte cilia, due to mutations in *PKHD1* and production of aberrant fibrocystin protein, are found in PCK rats, suggesting a possible role for disease pathogenesis (Onuchic et al. 2002, Ward et al. 2002). Thirty percent of neonatal CHF/ARPKD patients succumb to disease due to pulmonary hypoplasia secondary to grossly enlarged, cystic kidneys (Zerres et al. 1998); those that survive the perinatal period may be plagued by recurrent episodes of acute cholangitis, severe portal hypertension and development of esophageal varices due to the progression of pericystic fibrosis. Adult CHF/ARPKD patients' conditions are often further complicated due to development of biliary malignancies (Roy et al. 1997, Zerres et al. 1998).

Previous research has identified several pathways which contribute to cyst wall epithelial cell (CWEC) proliferation and pericystic fibrosis in CHF/ARPKD. In CWECs, these mechanisms include reduced intracellular calcium, increased cAMP production and cAMP-mediated signaling, and increased production of pro-proliferative cytokines including IL6, EGF, VEGF and IGF-1 (Nichols et al. 2004, Masyuk et al. 2006, Masyuk et al. 2015). Therapeutic interventions targeting these pathways attenuate disease progression (Masyuk et al. 2015). In addition, pericystic fibrosis was reduced in polycystic kidney (PCK) rats after treatment with pioglitazone, a PPARγ agonist (Blazer-Yost et al. 2010). Increased activation of the renin and angiotensin-converting enzyme system in PKD, consistent with severe portal hypertension which occurs in CHF/ARPKD

patients, is attenuated after treatment with telmisartan, an angiotensin receptor blocker (Yoshihara et al. 2013). However, even with these advances in our understanding of disease pathogenesis, pharmacologic interventions for CHF/ARPKD patients have not lead to significant improvements in patient outcome. Indeed, transplant remains the only cure for this disease.

Mast cells (MCs) are components of the innate immune system with a broad range of effector activity (Urb et al. 2012). They synthesize and store many molecules including chymase, tryptase, and histamine, and renin in large cytoplasmic granules which they release during tissue injury and in response to other stimuli (Metcalfe et al. 1997). MC produce a diverse array of cytokines, chemokines and growth factors including IL6 and VEGF (Kruger-Krasagakes et al. 1996, Boesiger et al. 1998). In addition to their well-known roles in allergy (Borish et al. 1992), MCs also exhibit profibrotic activity (Overed-Sayer et al. 2013) as well as growth-promoting activity for cholangiocytes after bile duct ligation in rats and mice (Hargrove et al. 2016, Hargrove et al. 2017). MCs are also associated with human liver disease (Francis et al. 2010). They are increased in the portal area of cirrhotic patients (Armbrust et al. 1997) and are considered pathogenic in human cholangiocarcinoma (Terada et al. 2000). An abundant literature suggests that MCs are associated with inflammatory and fibrotic disease (Overed-Sayer et al. 2013). Further, MCs are found surrounding the human biliary tree and the number of MCs increases in the liver in ARPKD patients (Ozaki et al. 2005). MCs also participate in the pathogenesis and progression of biliary disease in other animal models (Farrell et al. 1995, Ishii et al. 2005). However, no studies have explored the role of MCs in CHF/ARPKD. Here, we sought to test the hypothesis that MCs are

involved in the progression of CHF/ARPKD and are the common link between a triumvirate of pathogenic mechanisms (inflammation, proliferation and fibrosis (Jiang et al. 2016) involved in this disease.

3.3 MATERIALS AND METHODS

Animals

Polycystic kidney (PCK, an orthologous model of human ARPKD) rats and normal Sprague-Dawley (SD) rats were obtained from Charles River Laboratories (Kingston, NY). *Pkhd1*$^{LSL(-)/LSL(-)}$ mice (an orthologous mouse model of human ARPKD) were a kind gift from Dr. Christopher J. Ward (University of Kansas Medical Center, KUMC) (Bakeberg et al. 2011).Animal treatment was approved by and performed in accordance with the Institutional Animal Care and Use Committee at KUMC.

Treatments and Tissue Collection

PCK rats were injected i.p. with saline or cromolyn sodium (CS, 50 mg/kg/day (Hei et al. 2007)) or ketotifen fumarate (1mg/kg/day) from postnatal day (PND) 15 to PND 30. CS and ketotifen were purchased from Sigma-Aldrich (St. Louis, MO). The treatment period was chosen based on the starting time point of MC infiltration in PCK rats (PND 15, Figure 1B) and the observed development of cysts and fibrosis from our earlier work (Jiang et al. 2017). Rats were euthanized at PND 31. *Pkhd1*$^{LSL(-)/LSL(-)}$ mice were injected with saline or CS from PND 30 to PND 45. The treatment period was chosen based on the initiation of observable cysts and fibrosis in the liver. Liver, kidney,

and plasma were collected for further analysis as previously described (Deshpande et al. 2016).

Histological Analysis

Liver and kidneys were preserved in 10% buffered formalin, embedded in paraffin, and stained with hematoxylin and eosin (H&E). Average cyst size per liver section was calculated as the ratio of cystic area to the number of cysts. Cell death was assessed by terminal deoxynucleotidyl transferase dUTP nick end labeling (TUNEL) staining using the *In Situ* Cell Death Detection Kit, TMR red (Roche Applied Science, Indianapolis, IN). Ki67 staining was performed on frozen sections (5 μm thick) as described before (Deshpande et al. 2016). ImageJ was used to quantify TUNEL staining and Ki67 staining by a blinded individual. For TUNEL staining, data were expressed as percentage of TUNEL positive cyst wall epithelial cells (CWECs) over total number of CWECs. For Ki67 staining, data were expressed as percentage of Ki67 positive CWECs for the liver, or non-CWECs for the kidney over total number of cells counted.

Sirius red staining

Formalin-fixed, paraffin-embedded (5 μM) liver sections were stained with 0.1% Sirius red solution as previously described (McCracken et al. 2016). All images were taken at 100x magnification with an Olympus BX51 microscope with an Olympus BH2RFLT3 burner and Olympus DP71 camera operated by DP Controller software (Olympus, Waltham, MA). Five non-overlapping images were acquired per liver section. One liver section per rat in each experimental group was photographed (n = 4-6 rats per

group). ImageJ was used to quantify the area of positive staining and intensity of that staining above an arbitrary threshold which remained constant for all images.

Toluidine blue staining

Toluidine blue staining was performed on formalin-fixed, paraffin-embedded (5 μM) liver sections as described by Kennedy *et al*. (Kennedy et al. 2014). Briefly, liver sections were deparaffinized, rehydrated, and stained with toluidine blue working solution (pH 2.0-2.5). After staining, 200X images were taken using an Olympus DP71 camera and later quantified by ImageJ using a constant threshold to differentiate "non-degranulated" MCs from "degranulated" MCs, based on intensity of purple staining. A "degranulated" MC can be identified by loss of granule staining and visible release of granules. A "non-degranulated" MC maintains intact cell structure and retains intense granule staining. Total MC number was counted manually using the "Cell Counter" function from ImageJ. MCs above threshold were counted as "non-degranulated". The number of "degranulated MC" was calculated by subtracting "non-degranulated" MC number from total MC number. All images were coded and analyzed by a blinded observer.

RNA isolation, cDNA synthesis and real-time PCR

Total RNA was isolated from RNAlater-stabilized tissue using an RNeasy Mini Kit (Qiagen, Valencia, CA). Four micrograms of RNA were reverse transcribed into complementary DNA (cDNA) using a Retroscript kit (Life Technologies/Ambion, Grand Island, NY). SYBR green (Universal Super Mix, BioRad, Hercules, CA) was used for

real-time PCR. Results were calculated using $2^{-\Delta\Delta Ct}$ method. The data were expressed as fold change over saline-treated animals. 18S was used as the housekeeping gene and did not differ between treatment groups or genotypes. Primers utilized in this study are found in Table 3.3.1.

Table 3.3.1. Primers used for real-time PCR transcript analysis

Gene name	Sequence Source	Forward primer	Reverse primer
Cma1	NCBI	CACTGTGCAGGACGGTCTAT	TTGAAGTTGGCCGAGAGTGG
Tpsab	(Nakano et al. 2012)	ACATCTGAGTGTTGCGCTGAAGCA	CCCAACAGGTTGTGGTGTGCAGAAT
Fcer1l	NCBI	GCTACCACTGCACAGGCTAT	AACCCAGTGTCCACAGCAAA
Acta2	(Vickers et al. 2004)	AGCTCTGGTGTGTGACAATGG	GGAGCATCATCACCAGCAAAG
Col1a1	(Pritchard et al. 2010)	TGAGCCAGCAGATTGAGAAC	TGATGGCATCCAGGTTGCAG
Hrh1	NCBI	CAGACCTGATTGTAGGGGCAG	CATAGAGAGCCAAAAGAGGCAG
Hrh2	NCBI	CCCAATGGCACGGTTCATTC	GCCGACGATTCAAGCTGACA
F2rl1	NCBI	AGTCCGTCATGGCTTTGTCA	CTCGCCTCTGCGGTTCTGTG

Serum histamine and tryptase measurement

Histamine release was measured in serum by histamine enzyme-linked immunosorbent assay (EIA) kits following the manufacturer's instruction (Cayman Chemical, Ann Arbor, MI). Tryptase release was measured in serum by rat tryptase

(TPS) ELISA kit (Neo Scientific, Cambridge, MA). Renin release was measure in serum by rat renin-1 ELISA kit (RayBiotech, Norcross, GA).

Total collagen calculation by hydroxyproline assay

Hydroxyproline level was measured in liver as described by Reddy and Enwemka (Reddy et al. 1996). Brielfly, 10 mg liver tissue was weighed and subjected to digestion in 12 N hydrochloric acid (100 μl) and water (100 μl) at 120 °C for 3h. The samples were vortexed every 30 – 40 min during digestion to achieve complete homogenization. The supernatant was collected following centrifugation at 10,000 x g for 10 min. Samples were incubated with chloramine T (100 μl) at room temperature for 25 min. Ehrlich's reagent (100 μl) was added and the samples were incubated at 60°C for 35 min. Absorbance was measured at 550 nm. Hydroxyproline concentration was calculated using a standard curve. The amount of collagen was estimated by dividing the hydroxyproline concentration by 12.5 % as previously shown (Reddy et al. 1996).

CWEC isolation and cell proliferation assay

CWECs from PCK rats were isolated as described by LaRusso *et al*. and Jiang *et al* (Muff et al. 2006, Jiang et al. 2017). Briefly, the biliary tree was isolated following liver perfusion at 37^{o}C. The biliary tree was then cut into small pieces and digested with Modified Eagle's Medium containing 25 mM HEPES (Sigma-Aldrich), 10 mg hyaluronidase (Sigma-Aldrich), 8 mg collagenase P (Roche, Indianapolis, IN), and 6 mg DNase (Sigma-Aldrich) for 45 min in a 42°C water bath. The tissue pieces were then washed and cultured in collagen-coated plates. After 2-3 days of culture, proliferating

cysts were digested and CWEC plated as a monolayer. A cell proliferation assay was performed as described by Yamaguchi *et al.* (Yamaguchi et al. 2006). In brief, cells were treated with CS (10, 25, 50, and 100 μM) for 48h. Cell proliferation was determined based on the production of formazan using CellTiter 96 Aqueous One Solution Cell Proliferation Assay (Promega). The amount of formazan is directly proportional to the living cell number in culture.

Statistics

Results are represented as mean ± standard error of mean. Student's t-test was used to calculate differences between two groups. One-way ANOVA was used for data in Figure 3.4.9A to determine statistical differences. Two-way ANOVA was used for data in Figure 3.4.1 B-E and Figure 3.4.2B-C to determine statistical differences. Post-hoc pairwise comparisons with multiple testing adjustments were completed using Tukey's method for all data analyzed by ANOVA. A Pearson's correlation was done to determine the relationship between two independent variables (Figure 3.4.12B). In each case, statistical significance was defined as $p < 0.05$.

3.4 RESULTS

Mast cells (MC) infiltrate the pericystic area of PCK rats.

To determine if MC infiltration was increased in PCK rats, we stained liver sections from SD and PCK rats at PND 15, 20, 30 and 90 using toluidine blue, a histological stain which stains MC granules dark purple (Leclere et al. 2006) (Figure 3.4.1A). The number of MCs was low in both SD and PCK rats at PND 15 and PND 20.

MC infiltration in PCK rats was increased at PND 30, and the number was significantly greater than that in SD rats. MC number did not increase further in either strain at PND 90 (Figure 3.4.1B). To confirm the presence of MCs at the transcript level, we performed real time PCR to measure MC-specific target gene expression. Chymase (*Cma1)* and tryptase (*Tpsab)*, two MC serine proteases, and Fcε receptor I alpha (*Fcer1a)*, the receptor which binds IgE on MCs (Kinet 1999), were all increased in livers from PCK rats when compared to SD rats from PND 15 – 90 (Figure 3.4.1C, D, and E). By PND 90, the transcripts for *Cma1* declined relative to their levels at PND 30 in PCK rats (Figure 3.4.1C). Transcripts for *Tpsab* and *Fcer1a* remained elevated even at PND 90 (Figure 3.4.1D and E).

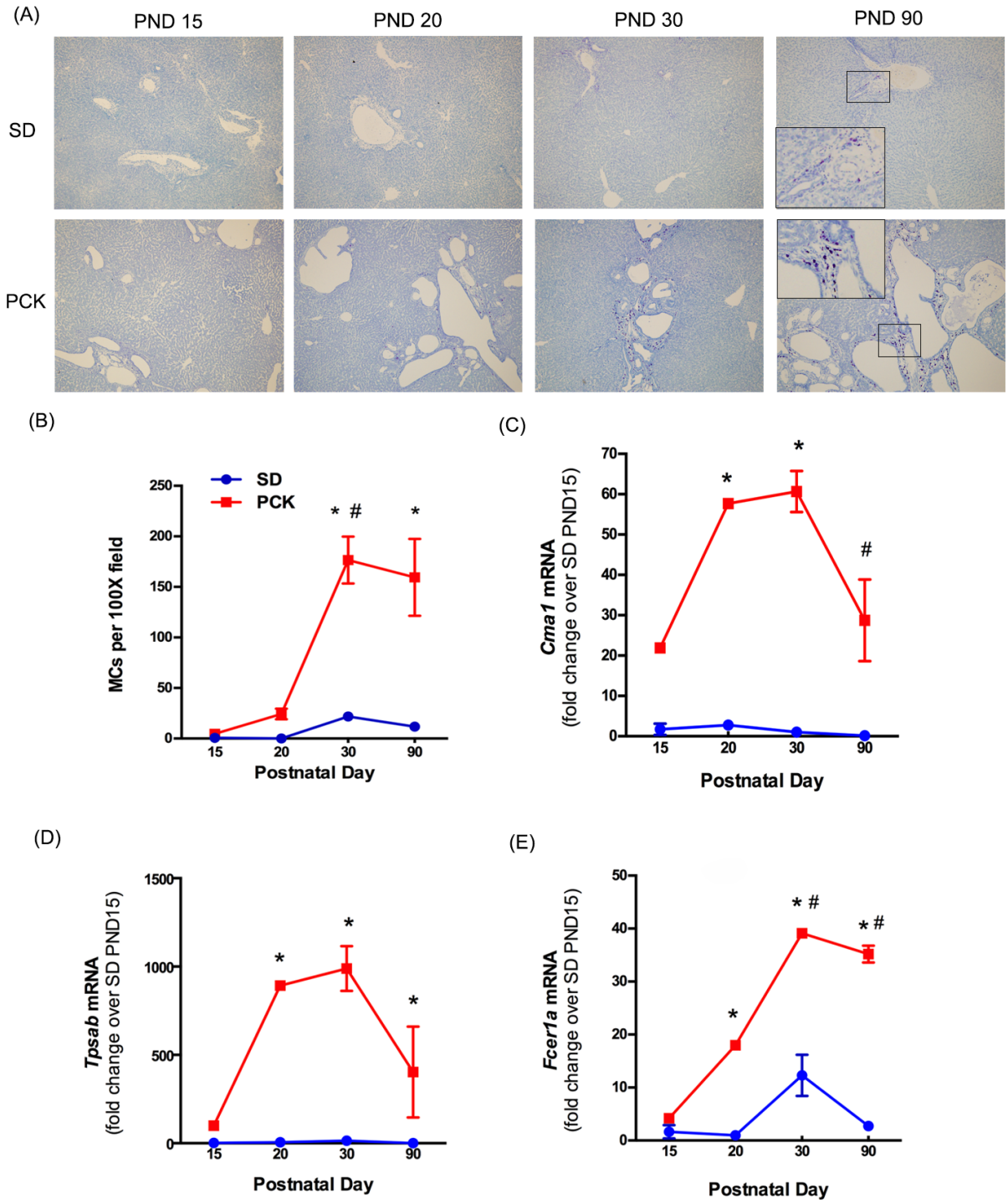

Figure 3.4.1. Mast cell infiltration in SD and PCK rat livers. (A) Representative images of toluidine blue stained livers from SD and PCK rats from postnatal day (PND) 0 to PND 90. Images were taken at 100X magnification. (B) Quantification of mast cell (MC) number over time. (C-E) MC-associated gene expression, *Cma1*(C), *Tpsab* (D), and *Fcer1a* (E)were measured by real-time PCR in SD and PCK rat livers from PND 0 to PND 90. N=3-4 rats per group. *, P<0.05 between genotypes at the indicated time point. #, P<0.05 compared to previous time point within a genotype.

Evaluation of MC degranulation and granule-associated receptors in PCK rats.

Degranulation is one mechanism by which MC can promote cell proliferation, inflammation, and fibrosis (Kondo et al. 2001, Amin 2012, Kennedy et al. 2014). Therefore, we next sought to determine whether or not the MCs found in livers from PCK rats were degranulated. First, we used toluidine blue to assess granule content in hepatic mast cells. A threshold differentiating a “non-degranulated” MC from a “degranulated” MC was set based on morphological differences described in the “method section”. Using this objective approach, the number and percent of non-degranulated vs degranulated MCs was determined in livers from PCK rats. We found that the number and percent of degranulated MCs was greater at PND 30 than PND 20. The number of degranulated MCs did not change from PND 30 to PND 90, and the percent of degranulated MCs at PND 90 was not different than that found at PND 20 (Figure 3.4.2B, C). We further evaluated the expression of two histamine receptors, H1R (*Hrh1)* and H2R (*Hrh2)*, using biliary tree samples from SD and PCK rats. Our data suggest that histamine receptor expression (*Hrh1* and *Hrh2*) did not differ between SD and PCK rats (Figure 3.4.2D, E). Interestingly, protease-activated receptor 2 (PAR2, *F2rl1*), a tryptase receptor, was expressed significantly higher in PCK rat biliary trees compared to biliary trees from SD rats (Figure 3.4.2F).

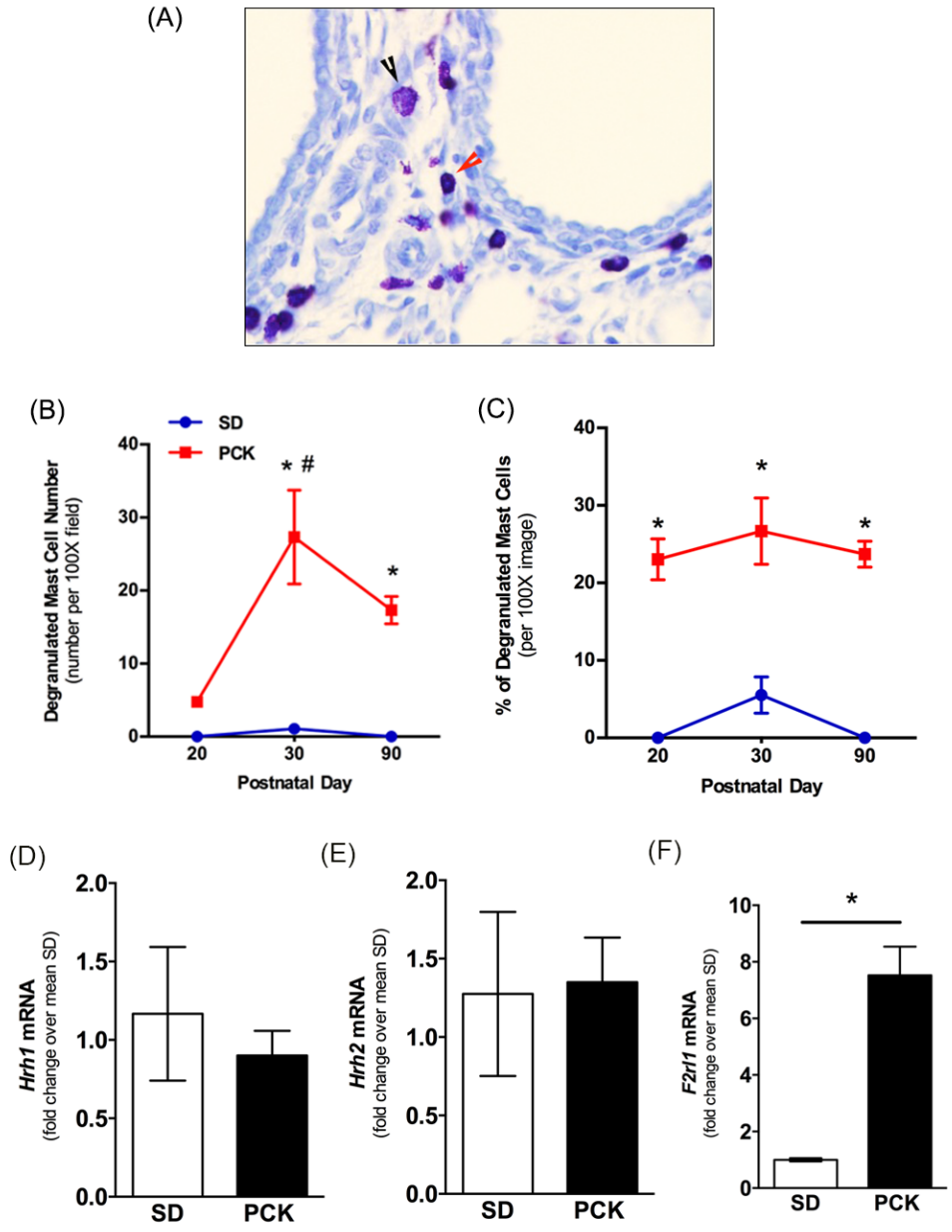

Figure 3.4.2. Evaluation of mast cell (MC) degranulation and granule-associated receptors in PCK rat livers. (A) Examples of a non-degranulated MC (red arrow head) and a degranulated MC (black arrow head). Image was taken at 200X magnification. (B) Number of degranulated MCs in PCK rat livers at postnatal day (PND) 20, PND 30, and PND 90. (C) Percentage of degranulated MC in PCK rat livers at PND 20, PND 30, and PND 90. N=3-4 rats per group. (D-E) Gene expression of histamine receptors, *Hrh1* (D) and *Hrh2* (E), in biliary tree samples from SD and PCK rats. (F) Gene expression of tryptase receptor, protease-activated receptor 2 (PAR2, *F2rl1*), in biliary tree samples from SD and PCK rats. *, P<0.05 between groups.

Inhibition of MC degranulation, *in vivo*, using cromolyn sodium and its impact on hepatic cyst growth and pericystic fibrosis.

Cromolyn sodium (CS) is a MC stabilizer used to treat asthma (Herzig et al. 1975, Murphy et al. 1987). It has also been used to prevent MC degranulation in rats after bile duct ligation (Kennedy et al. 2014), an experimental model of cholestasis in which histamine promotes the proliferation of cholangiocytes. Therefore, we treated PCK rats with CS (50 mg/kg /day) from PND 15 to PND 30 to determine if we could prevent MC degranulation and prevent growth of hepatic cysts. After 15 days of CS treatment, MC degranulation was attenuated relative to saline-treated controls (Figure 3.4.3A). Quantification of the number of non-degranulated cells and degranulated cells indicated a 40% decrease in degranulated cells after CS exposure (Figure 3.4.3B). To further support these observations, we measured histamine and tryptase, two mast cell granule contents, in serum from rats treated with CS. While histamine levels, measured using a histamine EIA, did not differ between saline and CS-treated rats (Figure 3.4.3C), levels of tryptase, as measured using a tryptase ELISA, were reduced (Figure 3.4.3D).

Next, we evaluated the impact of CS exposure on hepatic cysts in PCK rats. Surprisingly, CS exposure increased cyst size determined by histological assessment of H&E staining (Figure 3.4.4A). This was reflected in an ~5% increase in the liver to body weight ratio in saline vs CS-treated rats (Figure 3.4.4B), as well as by a morphological analysis of individual cyst size which was also increased after CS exposure (Figure 3.4.4C). Next, we wanted to elucidate the mechanism responsible for the increase in cyst size found in CS-treated PCK rat livers. In other words, an increase in cyst size could be due to an increased cyst wall epithelial cell (CWEC) proliferation and a

decrease in CWEC death. To determine if the increase in cyst size was due to an increase in CWEC proliferation, we performed Ki67 staining of liver sections from PCK rats. Ki67 staining indicated a 90% increase in CWEC proliferation after CS treatment compared to proliferation found in saline-treated PCK rats (Figure 3.4.5A, C). Next, we used TUNEL staining to determine whether CS exposure altered CWEC cell death. We found a trend to a greater number of TUNEL-positive nuclei in livers from saline-treated PCK rats when compared to CS-treated rats (Figure 3.4.5B, D).

Given that both cyst size and number increase in PCK rats from PND 0 to PND 90 and that fibrosis increases in parallel with cyst expansion (Jiang et al. 2017), we predicted that the increased cyst size observed in CS-treated PCK rats would be associated with increased pericystic fibrosis. To evaluate fibrosis, we used Sirius red staining and a biochemical assay to estimate the amount of collagen found in livers from control and CS-treated PCK rats. Morphometric analysis of Sirius red-positive staining indicated that CS treatment did not increase liver fibrosis when compared to saline-treated PCK rats (Figure 3.4.6A, B, and C). Consistently, hydroxyproline analysis revealed that collagen content was the same in PCK rats, regardless of treatment (Figure 3.4.6D). Levels of α-smooth muscle actin (αSMA/*Acta2*), a marker for myofibroblasts (Frangogiannis et al. 2000), and type I collagen (*Col1a1*) were not different between treatment groups (Figure 3.4.6E, F).

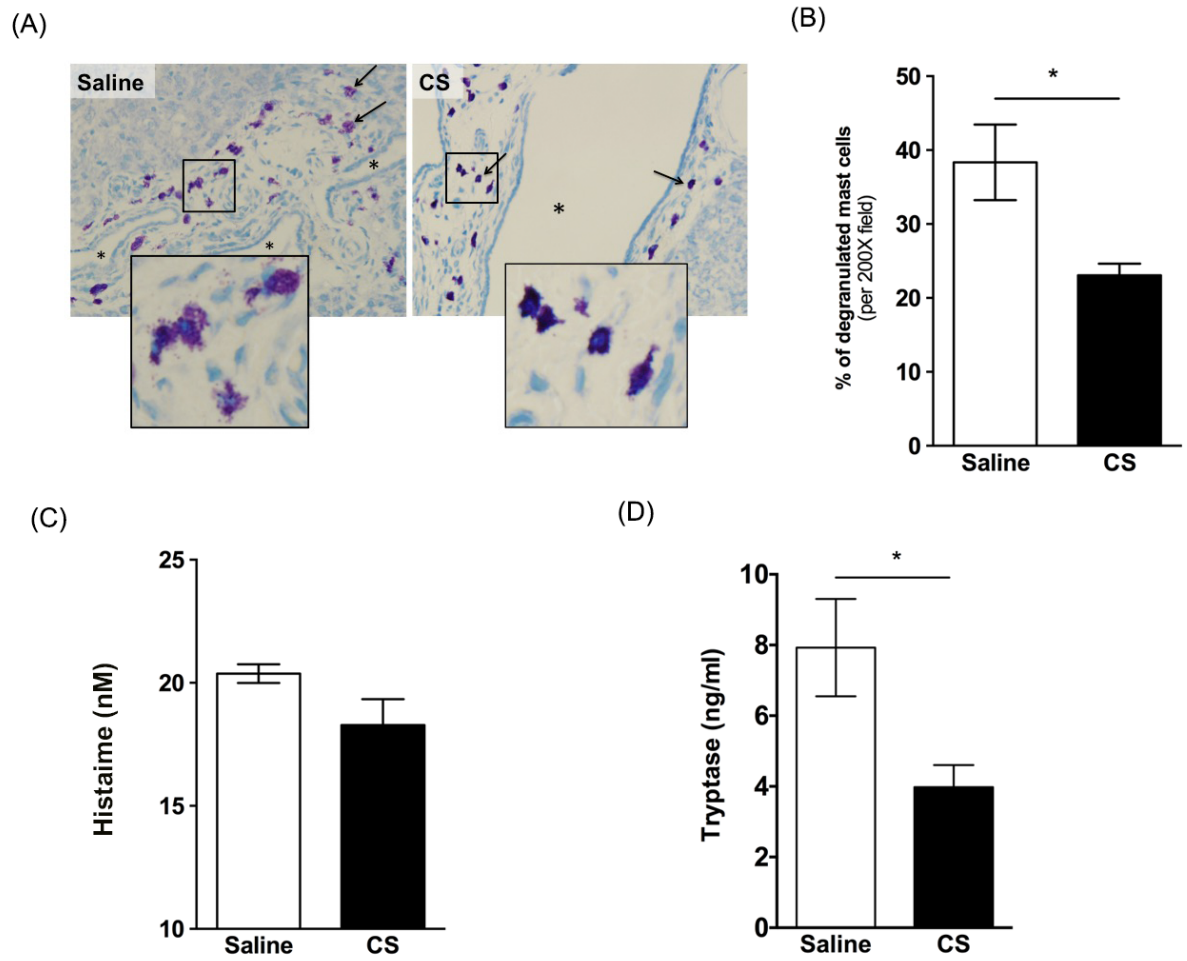

Figure 3.4.3. Effect of cromolyn sodium (CS) on mast cell (MC) degranulation in PCK rat livers. (A) Representative images of toluidine blue stained liver sections from a saline treated PCK rat and a CS treated PCK rat. Images were taken at 200X magnification. (B) Percentage of degranulation of MC in saline and CS treatment group. (C-D) Serum level of histamine (C) and tryptase (D) in saline and CS treatment group. N=4-5 rats per group. *, $P<0.05$ between groups.

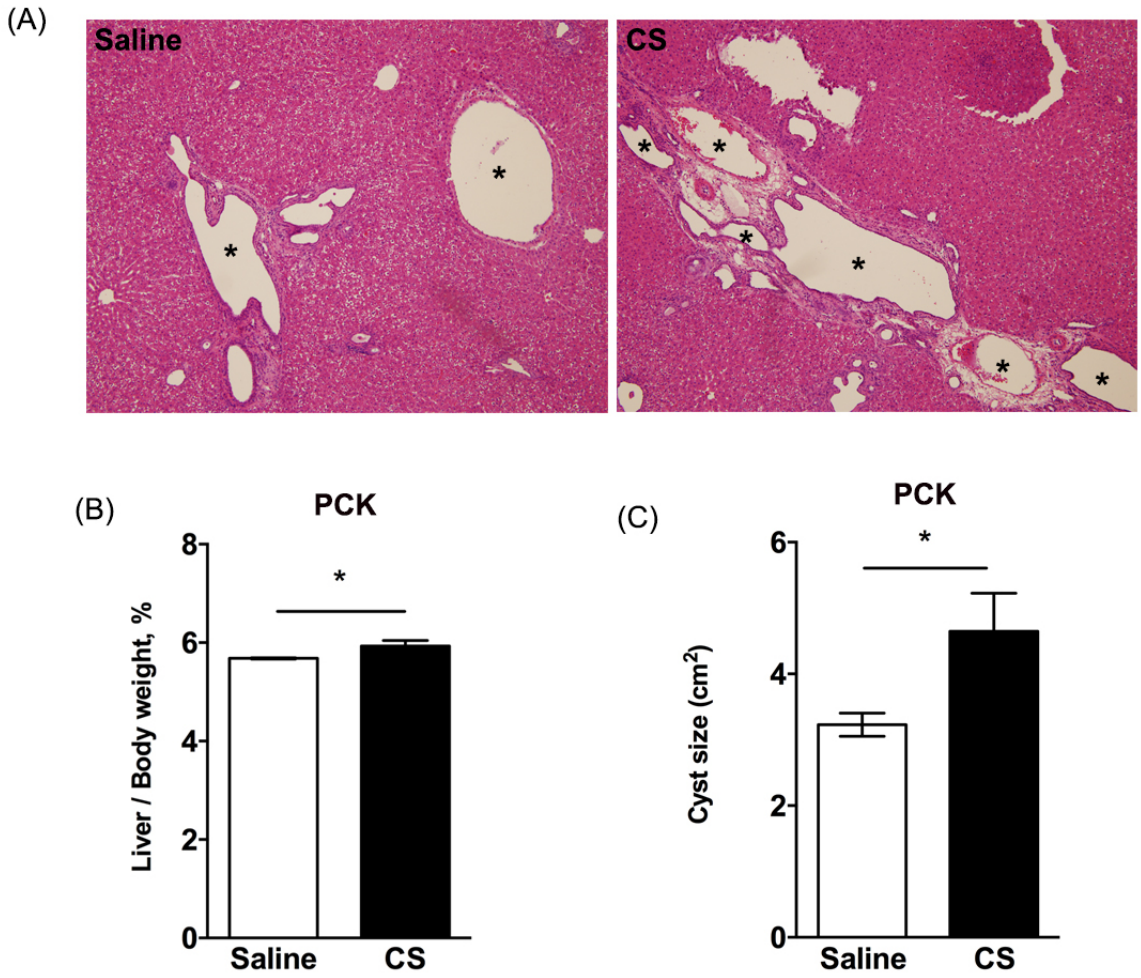

Figure 3.4.4. Effect of cromolyn sodium (CS) on livers from PCK rats. (A) Representative histology of hematoxylin and eosin (H&E) stained liver slides from saline and CS treated PCK rats. Asterisks (*) indicate cysts. Images were taken at 100X magnification. (B-C) Ratio of liver to body weight expressed as a percent of body weight (B) and average cyst (C) in saline and CS treated PCK rats. *, $P<0.05$ between groups.

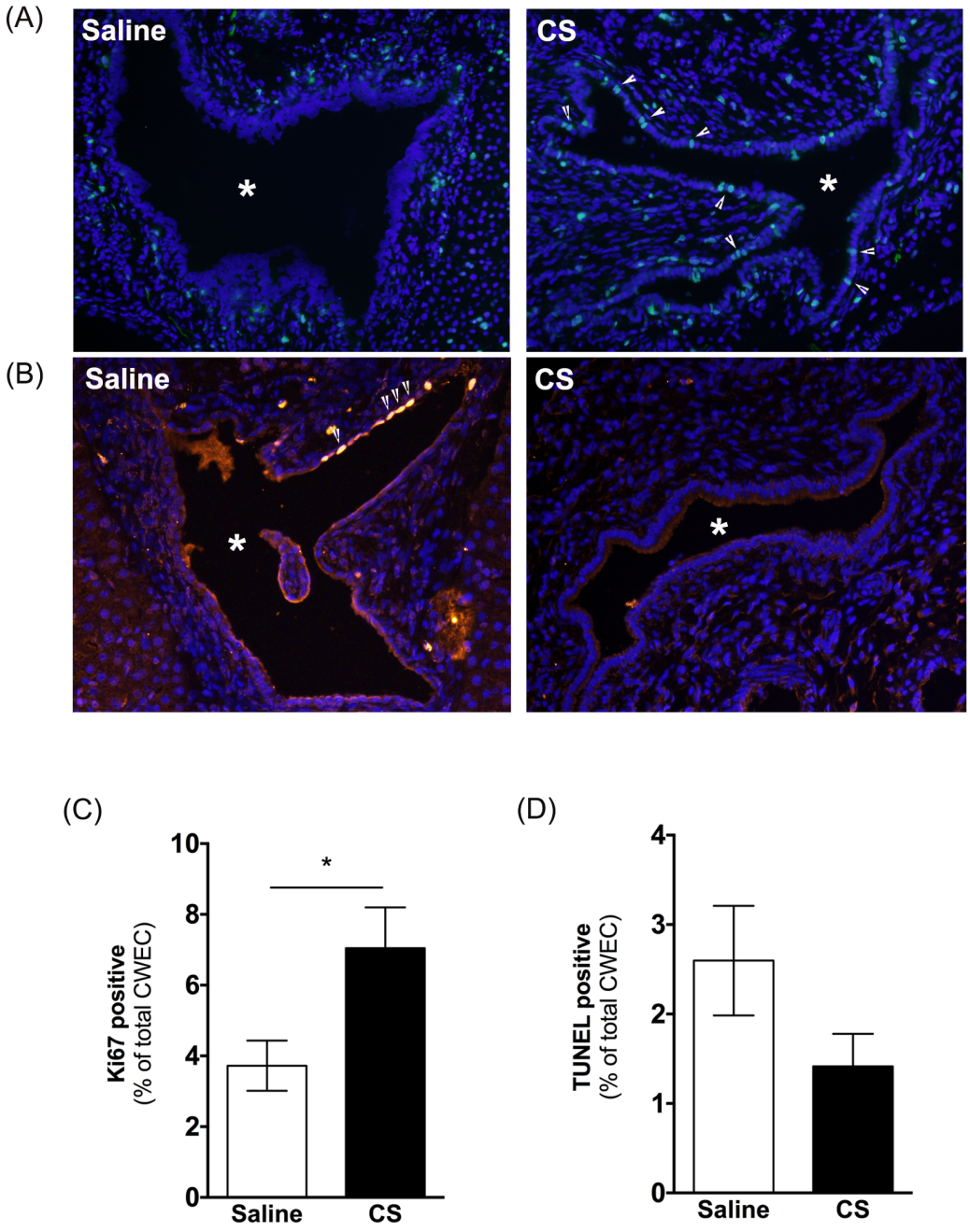

Figure 3.4.5. Evaluation of cell proliferation and cell death following cromolyn sodium (CS) treatment. (A-B) Representative images of Ki67 (A) and TUNEL (B) stained liver sections from saline and CS treated PCK rats. DAPI was used to visualize nuclei. Images were taken at 200X magnification. Asterisks (*) indicate cysts. Arrow heads indicate Ki67 (A) or TUNEL (B) positive cells. (C-D) Percentage of Ki67 (C) and TUNEL (D) positive cyst wall epithelial cells (CWECs) over total CWECs. N=4 rats per group. *, P<0.05 between groups.

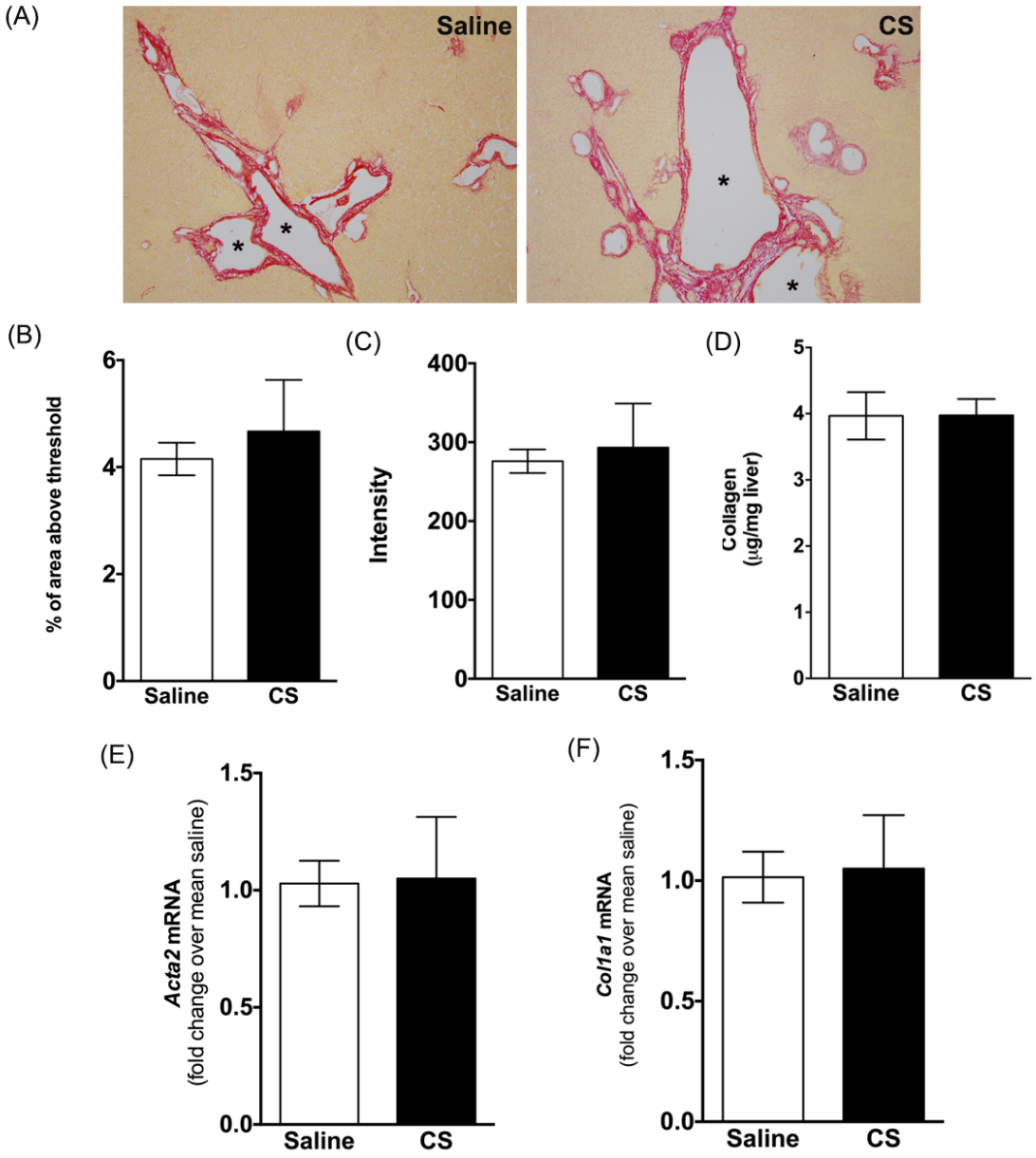

Figure 3.4.6. Evaluation of liver fibrosis following cromolyn sodium (CS) treatment in PCK rats. (A) Representative images of Sirius red stained liver sections from saline and CS treated PCK rats. Images were taken at 100X magnification. Asterisks (*) indicate cysts. (B-C) Quantification of Sirius red staining by measuring percentage of Sirius red positive area (B) and intensity (C) in saline and CS treated PCK rats. (D) Hepatic hydroxyproline concentration was determined using a biochemical assay from which approximate collagen content was calculated. (E-F) Hepatic fibrotic marker transcript *Acta2* (E) and *Col1a1* (F) were measured using real-time PCR. The data are expressed as fold change over saline. N=3-7 rats per group. *P < 0.05 between groups.

Impact of CS exposure on renal cyst growth and fibrosis indices.

Because PCK rats exhibit both hepatic and renal cysts, we sought to determine if CS exposure increases renal cyst growth and fibrosis. First, we evaluated MC numbers in kidneys from PCK rats and found that MC number was limited in the kidney compared to the increased MC accumulation in liver (Figure 3.4.7A). CS treatment caused a reduction in kidney to body weight ratio (Figure 3.4.7B), and morphological analysis of cysts revealed that cystic area was reduced in kidneys from PCK rats treated with CS (Figure 3.4.7C). As expected, CS treatment of SD rats did not affect kidney to body weight ratio compared to saline treatment (Figure 3.4.7D).

Evaluation of renal epithelial cell proliferation by Ki67 staining revealed that CS exposure suppressed proliferation only of non-cystic epithelial cells (i.e. cystic epithelium was Ki67 negative, p=0.0599, Figure 3.4.8A, C). TUNEL staining revealed a decrease in cyst epithelial cell death in kidneys from CS-treated PCK rats (Figure 3.4.8B, D). Renal interstitial fibrosis in PCK rats is not evident until PND 70 (Lager et al. 2001). Therefore, we analyzed *Acta2* and *Col1a1* transcripts as markers of early fibrogenic changes in the kidney. We found that these transcripts were reduced in kidneys from CS-treated PCK rats compared to kidneys from saline-treated PCK rats (Figure 3.4.8E, F).

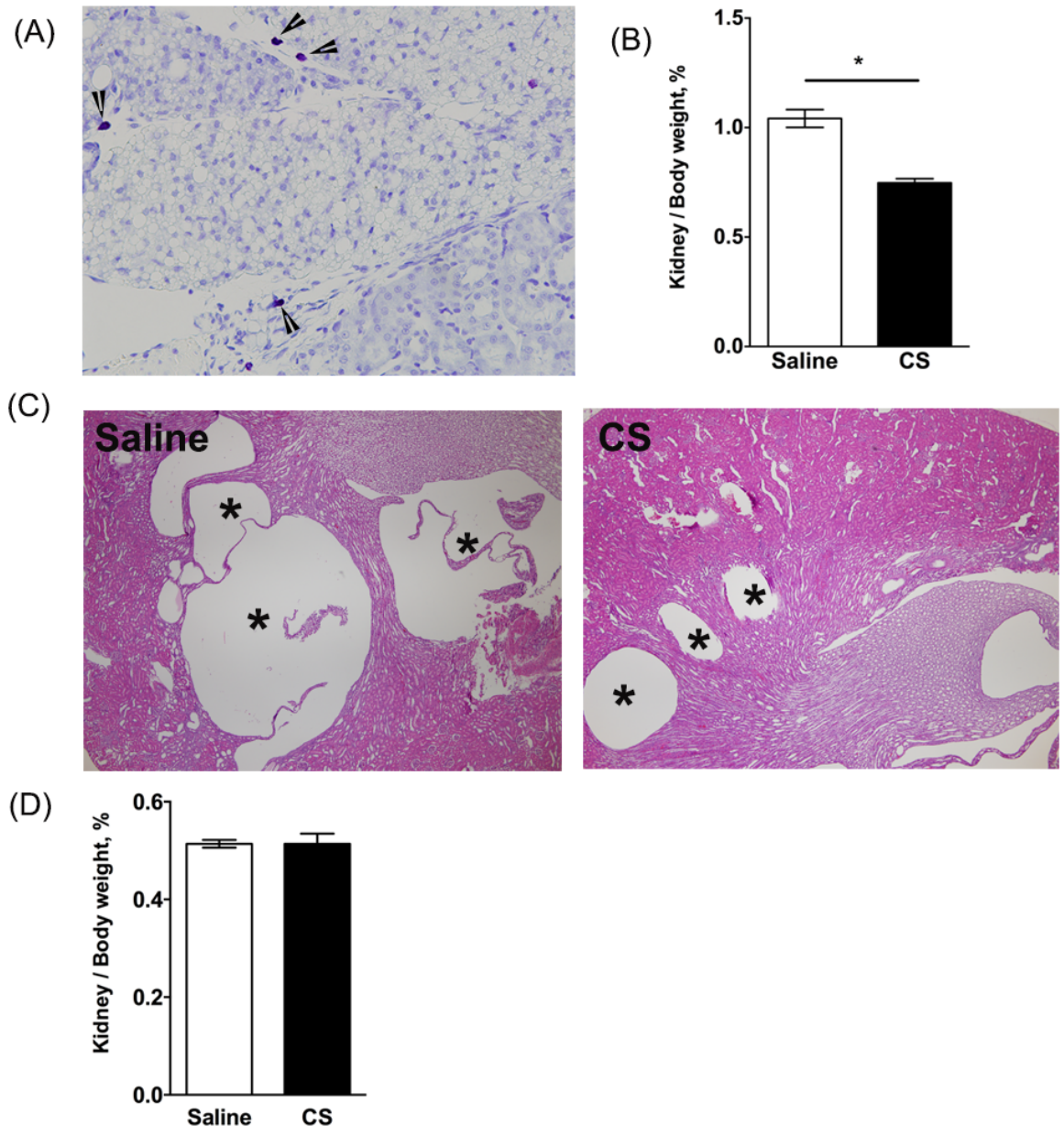

Figure 3.4.7. Effect of cromolyn sodium (CS) on kidney cyst growth in PCK rats and *Pkhd1*$^{LSL(-)/LSL(-)}$ mice. (A) Toluidine blue stained kidney section from a PCK rat. Image was taken at 400X magnification. Arrow heads indicate mast cells. (B) Ratio of kidney to body weight in PCK rats following saline or CS treatment expressed as a percent of body weight. *P < 0.05 between groups. (C) Representative images of hematoxylin and eosin (H&E) stained kidney sections from saline and CS treated PCK rats. Asterisks (*) indicate cysts. N=4-6 rats per group. (D) Ratio of kidney to body weight in SD rats following saline or CS treatment expressed as a percent of body weight. N=6-7 mice per group.

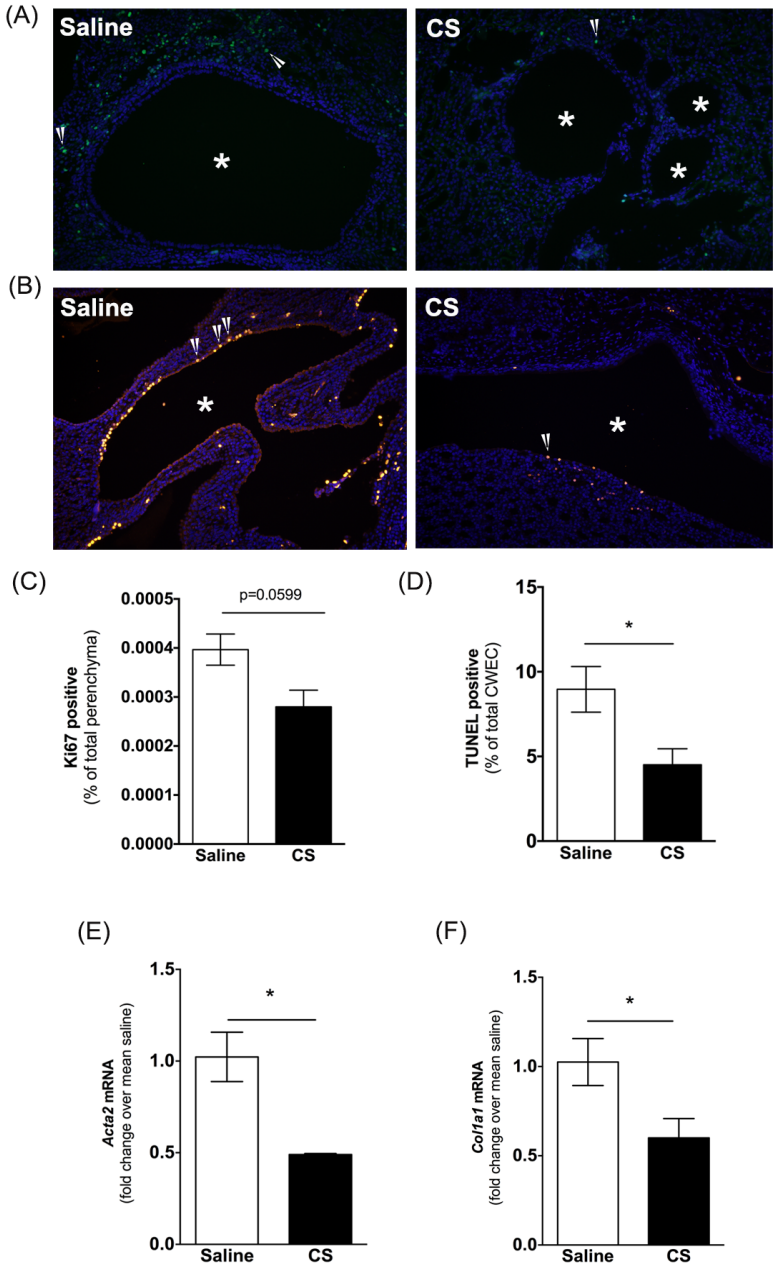

Figure 3.4.8. Evaluation of renal cell proliferation and cell death following cromolyn sodium (CS) treatment. (A-B) Representative images of Ki67 (A) and TUNEL (B) stained kidney sections from saline and CS treated PCK rats. DAPI was used to visualize nuclei. Images were taken at 200X magnification. Asterisks (*) indicate cysts. Arrow heads indicate Ki67 or TUNEL positive cells. (C-D) Percentage of Ki67 positive non-cystic epithelial cells (C) and TUNEL-positive cyst wall epithelial cells over total number of cells counted. (E-F) Fibrotic marker transcript (E) *Acta2* and (F) *Col1a1* were measured in PCK rat kidneys using real-time PCR. Data are expressed as fold change over saline. N=4 rats per group. *P < 0.05 between groups.

Evaluation of an off-target effect of CS on cyst growth.

We performed three additional experiments to determine if CS had a direct effect on cyst growth, independent of its MC stabilization activity. First, in a previous study (Jiang et al. 2017), we optimized the isolation and culture of CWEC from PCK rats and found that they formed cytokeratin (CK) 19-postive colonies consistent with their cholangiocyte origin. Next, we exposed CWECs to increasing concentrations of CS, *in vitro*. We found that at CS did not increase CWEC proliferation (Figure 3.4.9A). Forskolin, a cAMP agonist, stimulates renal cystic epithelial cell proliferation in autosomal dominant polycystic kidney disease (ADPKD) through activating the B-Raf-MEK-ERK pathway (Tesmer et al. 1997, Yamaguchi et al. 2000). In our study, forskolin treatment increased hepatic CWEC proliferation by 50% demonstrating that our CWEC were capable of proliferation, *in vitro*.

To unequivocally prove that MCs have a direct effect on hepatic cyst growth in ARPKD, and that CS did not have an off-target effect on CWECs, we capitalized on an observation we made in mouse models of ARPKD since the mouse model of ARPKD did not show increased MC infiltration (Figure 3.4.9B). Therefore, in our second experiment, we exposed *Pkhd1*$^{LSL(-)/LSL(-)}$ mice to CS and evaluated hepatic cystic indices. Similar to PCK rats, *Pkhd1*$^{LSL(-)/LSL(-)}$ mice exhibited aggressive development of hepatic cysts and pericystic fibrosis by PND 30. However, toluidine blue staining demonstrated that MCs were not present in livers from *Pkhd1*$^{LSL(-)/LSL(-)}$ mice (Figure 3.4.9B). Confident that these mice were effectively liver MC-deficient, we then exposed *Pkhd1* mutant mice to CS and evaluated cyst growth and fibrosis using the same methods as performed for PCK rats. We found that CS treatment did not affect liver to

body weight ratios (Figure 3.4.9C), cyst size (Figure 3.4.9D), or fibrosis (Figure 3.4.9E, F).

As a third approach to investigate if CS directly impacts cyst growth and fibrosis in ARPKD, we treated PCK rats with another MC stabilizer, ketotifen, from PND 15 to PND 30. Similar to what we found in CS-treated PCK rats, ketotifen treatment effectively inhibited MC degranulation compared to the saline-treated group (Figure 3.4.10A, B). We also measured tryptase level in serum, but we did not detect a significant difference between saline- and ketotifen-treated groups (Figure 3.4.10C). We evaluated hepatic cyst burden and fibrosis after ketotifen treatment and found that hepatic cyst size was significantly increased with no change in hepatic fibrosis (Figure 3.4.11A-D); renal cyst size did not change after ketotifen treatment (Figure 3.4.11E).

Increased activity of renin-angiotensin-aldosterone system (RAAS) has been implicated in the pathogenesis of renal cysts in ADPKD and ARPKD (Graham et al. 1988, Torres et al. 1992, Goto et al. 2010). To investigate if renin, a MC granule component, was responsible for the change of renal cyst size. We measured renin level in serum samples from SD rats and PCK rats treated with saline, CS, or ketotifen. We found that renin level in saline-treated PCK rats was significantly higher compared to SD rats (Figure 3.4.12A). Compared to saline treated PCK rats, CS treatment trended to decrease renin, but the decrease was not statistically significant. Ketotifen treatment had no impact on renin level compared to saline treated PCK rats (Figure 3.4.12A). Interestingly, the percentage of kidney/body weight ratio was strongly correlated with renin level in PCK rats, suggesting a role of renin in renal cyst progression (Figure 3.4.12B).

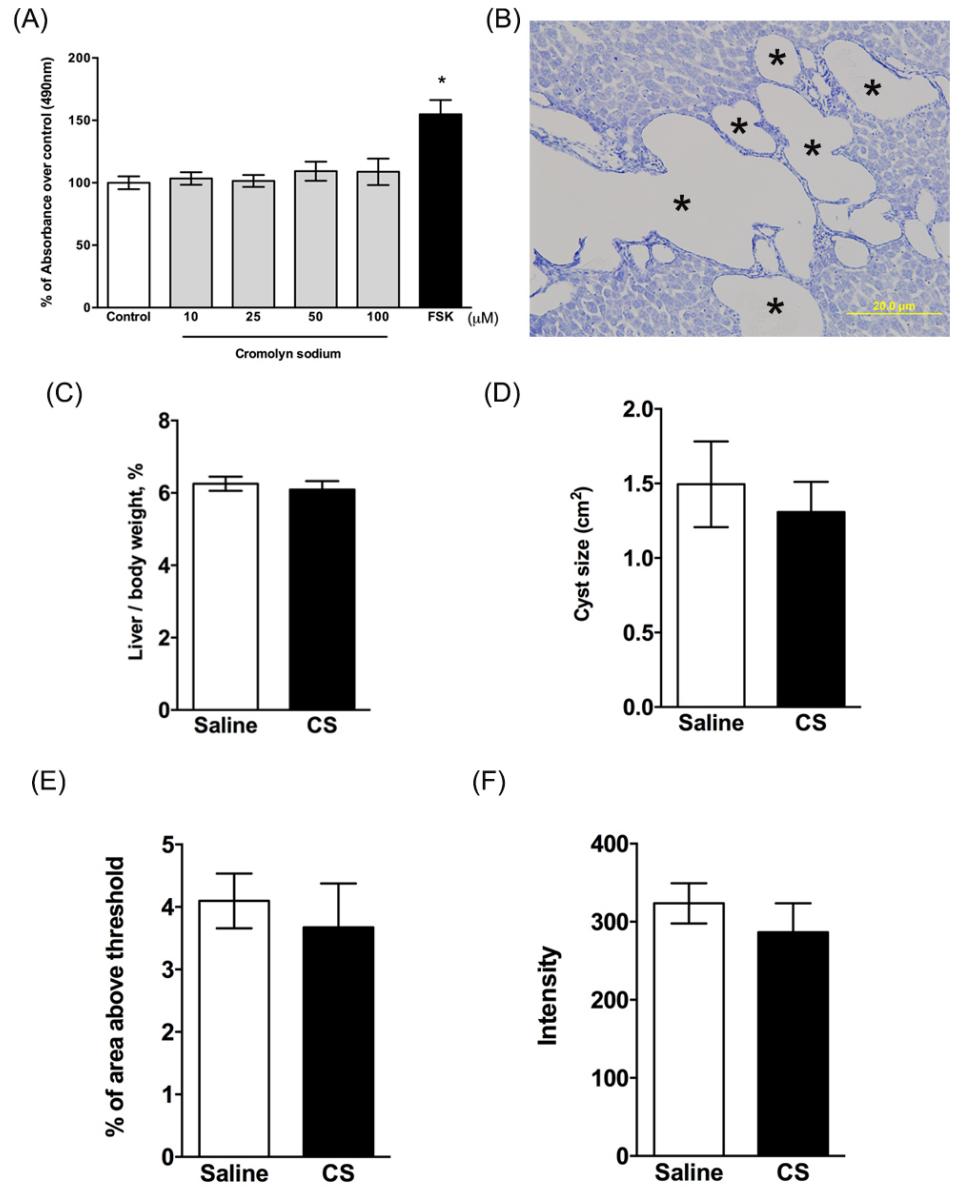

Figure 3.4.9. Effect of cromolyn sodium (CS) on isolated hepatic cyst wall epithelial cells (CWECs) and *Pkhd1*$^{LSL(-)/LSL(-)}$ mice. (A) Effects of different CS concentrations on CWEC proliferation. CWECs were treated with the indicated CS concentrations, vehicle, or forskolin (FSK, 5 μM). Each experiment was repeated three times (CWECs from 3 separate biliary trees from 3 separate rats isolated on 3 separate days). (B) toluidine blue stained liver section from a *Pkhd1*$^{LSL(-)/LSL(-)}$ mouse. Image was taken at 200X magnification. Asterisks (*) indicate cysts. *P < 0.05 compared to control. (C-D) Ratio of liver to body weight expressed as a percent of body weight (C) and average cyst size (D) in *Pkhd1*$^{LSL(-)/LSL(-)}$ mice treated with saline and CS. (E-F) Quantification of Sirius red stained liver sections by calculating percentage of Sirius red positive area (E) and measuring intensity of staining (F) per 100X magnification field. N=6-7 mice per group.

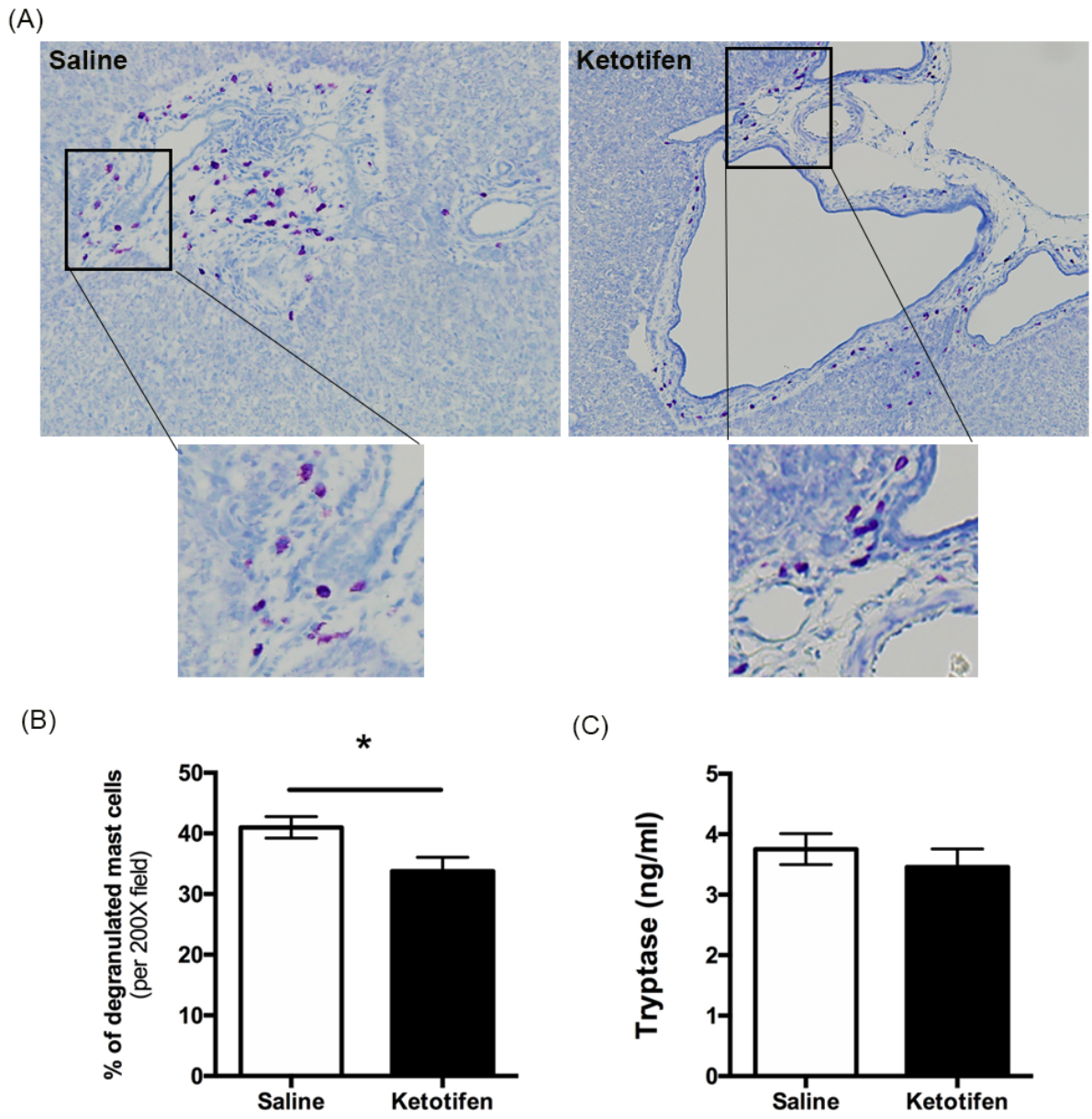

Figure 3.4.10. Effect of ketotifen on mast cell (MC) degranulation in PCK rats. (A) Representative images of toluidine blue-stained liver sections from a saline-treated PCK rat and a ketotifen-treated PCK rat. Images were taken at 200X magnification. (B) Percent degranulated MC after saline or ketotifen treatment. (C) Serum level of tryptase in saline and ketotifen treatment groups. N=8 rats per group. *, $P<0.05$ between groups.

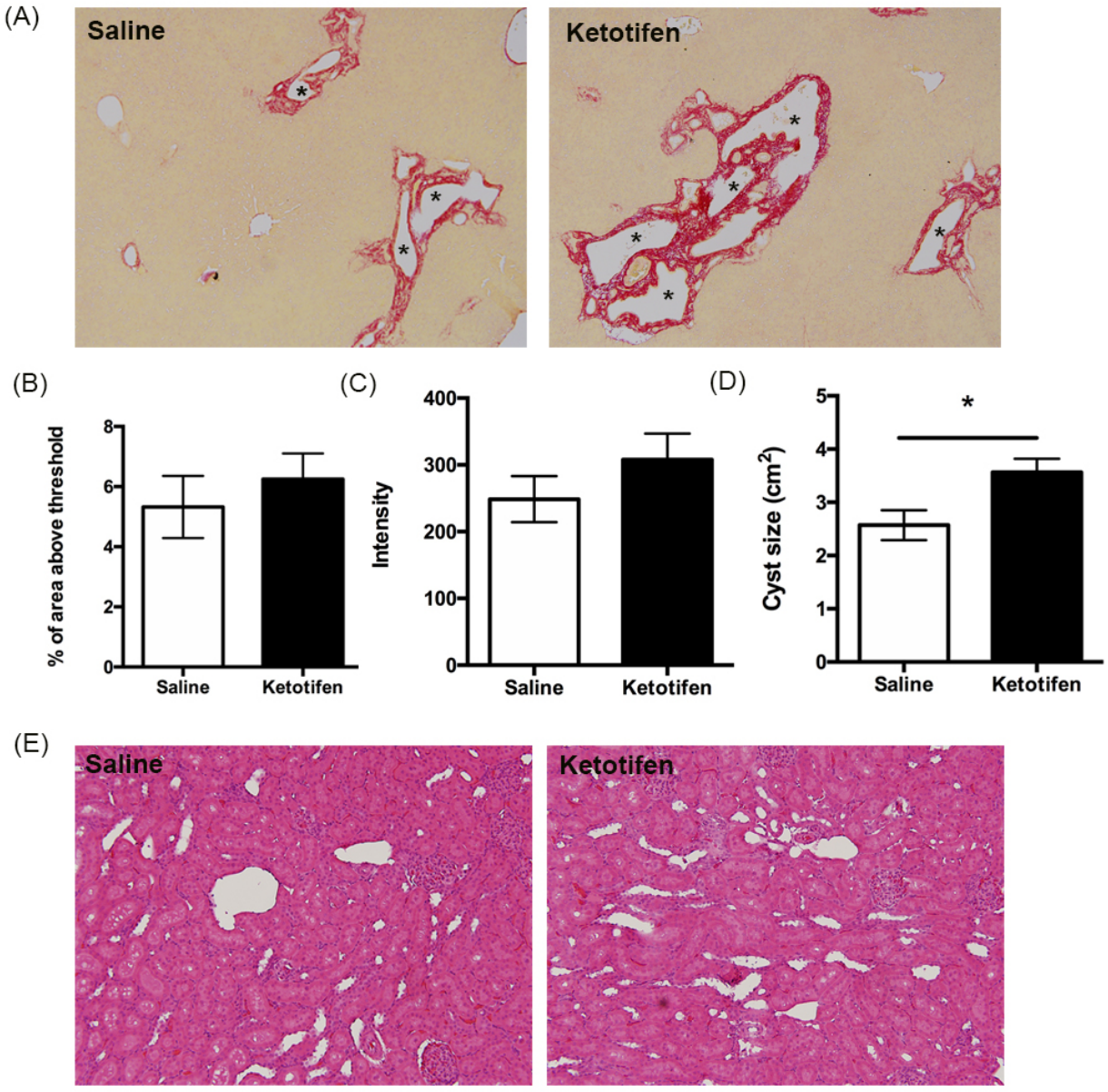

Figure 3.4.11. Evaluation of liver cysts and fibrosis following ketotifen treatment in PCK rats. (A) Representative images of Sirius red-stained liver sections from saline- and ketotifen-treated PCK rats. Images were taken at 100X magnification. Asterisks (*) indicate cysts. (B-C) Quantification of Sirius red staining by calculating percentage of Sirius red-positive area (B) and measuring intensity (C) in saline- and ketotifen-treated PCK rats. (D) Average cyst size after saline or ketotifen treatment. (E) Representative images of hematoxylin and eosin (H&E) stained kidney sections from saline and ketotifen treated PCK rats. Image was taken at 200X magnification. N=7-8 rats per group. *, $P<0.05$ between groups.

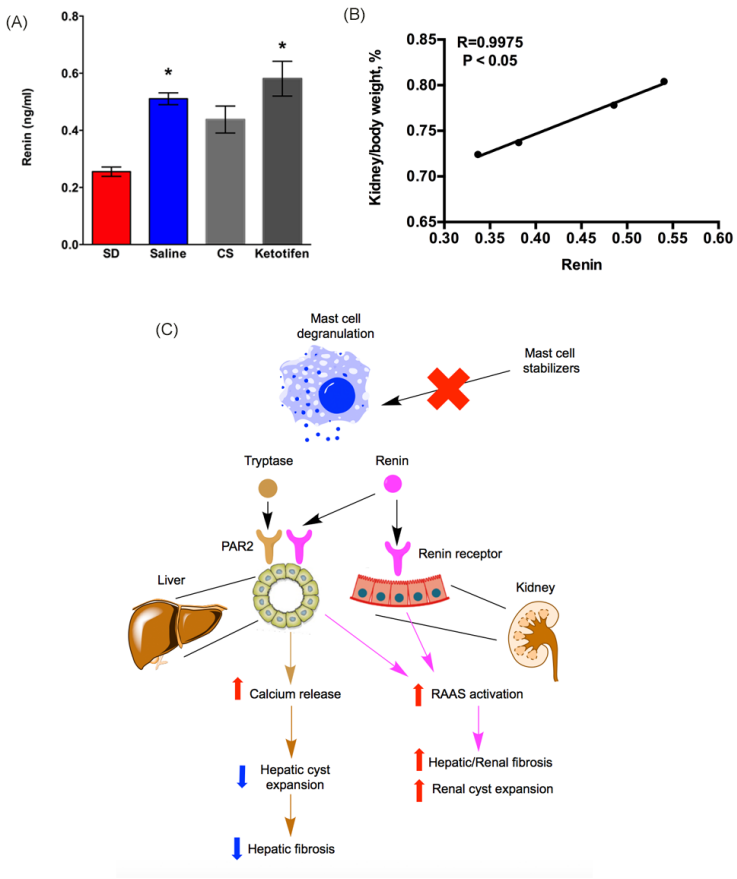

Figure 3.4.12. Evaluation of the relationship between renin and kidney cyst growth. (A) Serum level of renin in SD rats, saline-treated PCK rats, cromolyn sodium (CS) -treated PCK rats, and ketotifen-treated PCK rats. N = 4 - 13 per group. *, P<0.05 compared to SD. (B) Correlation between renin and percentage of kidney/body weight ratio in PCK rats. R = 0.9975, P < 0.05. (C) Working model: different mast cell (MC) granule components have different effects on liver vs. kidney in CHF/ARPKD. In liver samples from PCK rats, we observed an increased MC infiltration and increased expression of tryptase receptor (PAR2). Activation of PAR2 induces an increase in intracellular Ca^{2+} that prevents cyst expansion by limiting intracellular cAMP levels. Therefore, inhibition of tryptase release by mast cell stabilizing agents could prevent increases in intracellular Ca^{2+} levels, leading to a high intracellular cAMP, further exacerbating hepatic cyst expansion. Whether renin has an effect on liver cysts remains to be elucidated. In kidney, the pathogenic role for infiltrated MC is likely minimal since renal MC numbers are very low and restricted to connective tissue surrounding the kidney. However, as MC granules contain renin and the renin-angiotensin-aldosterone system promotes autosomal dominant polycystic kidney disease (Atlas 2007), inhibition of MC degranulation anywhere in the body could attenuate renin levels. Therefore, the reduction of renal cyst size we observed after stabilizing MCs could be due to a decrease in systemic renin and renin-mediated renal cyst expansion. Moreover, as renin also has pro-fibrotic effects, reduced renin levels due to MC granule stabilization could attenuate fibrogenic processes in liver or in kidney.

3.5 DISCUSSION

ARPKD is a rare genetic disease accompanied by hepatorenal cysts and pericystic fibrosis (Gunay-Aygun et al. 2010, Gunay-Aygun et al. 2013). Previously, we hypothesized that the disease is regulated by a "pathogenic triumvirate" consisting of CWEC proliferation, fibrosis, and inflammation (Jiang et al. 2016). MCs are inflammatory cells found in a number of pathologies (Bachelet et al. 2006). In this study, we investigated the role of MCs in the progression of hepatorenal cyst growth and associated fibrosis in PCK rats. Our findings provide novel evidence to support the differential function that MCs have on cholangiocyte and renal epithelial cell proliferation in an animal model of ARPKD. Our study demonstrated that: (i) MCs infiltrated the pericystic areas of PCK rat liver but did not accumulate in the cystic regions of PCK rat kidney; (ii) increased MC infiltration correlated with increased expression of MC markers in PCK rat liver, and (iii) inhibition of MC degranulation promoted hepatic cyst growth but inhibited (CS), or did not alter (ketotifen), renal cyst growth in PCK rats.

MCs function, in part, through the release of preformed mediators found in large cytoplasmic granules in a process called degranulation. Granule contents include molecules such as histamine, proteases, and proinflammatory cytokines (Borish et al. 1992). Previous studies by Kennedy *et al.* suggest that histamine is the major MC granule component that stimulates cholangiocyte proliferation in bile duct ligated rats (a model of cholestasis) (Kennedy et al. 2014). To study MC degranulation in PCK rat livers, we quantified the number of degranulated MCs in PCK rats. Our data suggested that MC degranulation peaked at PND 30, in parallel with the peak of MC infiltration. By treating PCK rats with CS, a MC stabilizer, we found MC degranulation was significantly

inhibited in line with reduced serum tryptase level. Previous studies show that CS treatment decreases cholangiocyte proliferation and increases apoptosis in animal models of cholestasis and primary sclerosing cholangitis (Kennedy et al. 2014, Jones et al. 2016). In contrast, we saw a different effect of CS in our model where CS treatment increased hepatic cyst size by increasing CWEC proliferation and decreasing CWEC apoptosis. The CS-related enhancement of hepatic cyst growth was supported by several parameters including liver to body weight ratio, cyst size, CWEC proliferation, and cell death. Consistently, inhibiting MC degranulation with ketotifen also significantly increased hepatic cyst size. We excluded the direct effect of CS on hepatic cysts by incubating isolated CWECs with CS for 48 h (Figure 9A), supporting the idea that MCs, and not CS alone, limit hepatic disease in PCK rats.

A previous study suggests that histamine from MCs stimulates cholangiocyte proliferation in a rat model of cholestasis (Kennedy et al. 2014), and inhibiting MC degranulation with CS inhibits cholangiocyte proliferation in that model. Those data suggest that histamine-histamine receptor interactions are critical for cholangiocyte proliferation. In our study, we examined the expression level of histamine receptors by real-time PCR using biliary tree samples from SD and PCK rats. We found that *Hrh1* and *Hrh2* expression in PCK rats did not differ from SD rats, and there was no systemic decrease in serum histamine level after CS treatment. This suggests that histamine may not play a pathogenic role in ARPKD. However, we observed a decrease in serum tryptase level after CS treatment, and the mRNA for its receptor, PAR2, was expressed significantly higher in PCK rats compared to SD rats. Activation of PAR2 induces a rapid intracellular Ca^{2+} influx (Moormann et al. 2006) that acts as an antagonist of cyst

expansion by repressing B-Raf, a kinase upstream of the MEK-ERK pathways and reducing cAMP levels by activating PDE1, a Ca^{2+}-dependent phosphodiesterase (Yamaguchi et al. 2004). It is plausible to speculate that reduction of tryptase by CS caused a decrease in Ca^{2+} level, which further exacerbated hepatic cyst expansion in a cAMP-depended fashion (Figure 3.4.12).

Previous studies suggest that the renin-angiotensin-aldosterone system (RAAS) is upregulated in liver and kidney from PCK rats, and its activation is associated with hepatorenal cyst expansion and fibrosis (Goto et al. 2010, Goto et al. 2010). MCs are capable of synthesizing and releasing the active form of renin. Therefore, this extra-renal renin production could further activate the RAAS (Silver et al. 2004). Consistent with previous studies, systemic renin was increased in PCK rats compared to SD rats, suggesting a role of renin in pathogenesis of ARPKD. Inhibition of MC degranulation with CS trended to reduce plasma renin levels in our study. We expected a decrease in liver fibrosis after CS treatment, but this did not happen. However, several mediators can promote fibrosis, so perhaps a reduction in renin did not attenuate fibrosis because other factors were still promoting fibrosis. For example, increased liver stiffness is a key factor driving the progression of fibrosis (Olsen et al. 2011). We observed an increase in hepatic cyst size after CS treatment which could have increased liver stiffness. Therefore, it is plausible to speculate that reduced renin levels in the context of increased liver stiffness prevented an attenuation of fibrosis after CS treatment.

MCs are associated with a variety of renal diseases. Although MCs are found infrequently in normal kidneys, their number increases in the presence of renal injury (Holdsworth et al. 2008). In PCK rat kidneys, MC number did not increase even though

they develop renal cysts and interstitial fibrosis. Therefore, we speculate that MCs may not play a pathogenic role on renal cyst growth. It is already appreciated that RAAS activation contributes to the pathophysiology of ADPKD not only through the promotion of hypertension but also by directly stimulating the growth of renal cysts (Atlas 2007). Therefore, the beneficial effect of CS treatment on renal cyst reduction could possibly due to a decrease in serum renin level (Figure 3.4.12). As we expected, although the decrease of renin in CS-treated PCK rats was moderate, we showed a strong correlation between percentage of kidney/body weight ratio and renin. In contrast, ketotifen treatment didn't affect renin level as we saw in the CS experiment. This may explain why we didn't observe renal size change after ketotifen treatment. In addition to renin, serum tryptase was not significantly suppressed in PCK rats after ketotifen treatment, despite evidence for MC granule stabilization in ketotifen-treated rats. These data suggest that the strength of the MC stabilization differed between the two compounds.

Compared to what we found in the liver, CS treatment caused a decrease in non-cystic renal epithelial cell proliferation, suggesting that MC stabilization may delay formation of renal cysts. Interestingly, we also observed a decrease in cystic renal epithelial cell death after CS treatment to PCK rats. A previous study suggests that inhibiting apoptosis in a rat model of PKD effectively inhibits cystogenesis (Tao et al. 2005). Whether a decrease in renal epithelial cell proliferation mediated by renin or other mediators or increase in cystic epithelial cell death is the driver or the outcome of cystogenesis in our study remains to be elucidated.

Finally, a previous study suggests that activation of RAAS may lead to formation of interstitial fibrosis in kidney (Cao et al. 2001). Therefore, inhibiting renin release by CS treatment may contribute to a decrease in renal fibrosis. Although kidney fibrosis is not established at this time point in PCK rats, we did observe that *Acta2* and *Col1a1*, two fibrotic genes, were reduced after CS treatment. This suggests reduced fibrogenic potential in the kidney. Further analysis is needed to determine if the decrease in fibrotic gene expression is due to a reduction in renal cyst size as discussed above for the liver, or an inhibition of RAAS activation.

In summary, we have shown that MC number is increased in liver but not kidney in PCK rats, an animal model of CHF/ARPKD. Inhibition of MC degranulation with CS had differential effects on hepatic and renal disease in the PCK rat. These data indicated a protective role of MC in hepatic pathophysiology but a pathogenic role in renal pathophysiology. Moreover, this study also suggests that mechanisms driving cholangiocyte proliferation in animal models of other biliary diseases are not directly translatable to mechanisms which drive CWEC proliferation in CHF/ARPKD. Clinically, usage of CS may be beneficial to patients who only have renal cysts but should be prescribed with caution to patients with hepatic cysts. In the case of ARPKD where patients have both hepatic and renal cysts, CS should be avoided to prevent exacerbation of hepatic disease. However, perhaps CS's reno-protective effects could be explored further and lead to kidney-targeted drug delivery approaches to achieve therapeutic benefit in that organ independent of negative impacts on hepatic cystic disease.

CHAPTER IV: THE ROLE OF YAP IN CONGENITAL HEPATIC FIBROSIS IN AUTOSOMAL RECESSIVE POLYCYSTIC KIDNEY DISEASE

This chapter is adapted from Jiang, L., L. Sun, G. Edwards, M. Manley, Jr., D. P. Wallace, S. Septer, C. Manohar, M. T. Pritchard and U. Apte (2017). "Increased YAP Activation Is Associated With Hepatic Cyst Epithelial Cell Proliferation in ARPKD/CHF." Gene Expr **17**(4): 313-326. doi: 10.3727/105221617X15034976037343 with permission from Cognizant, LLC; www.cognizantcommunications.com copyright.

4.1 ABSTRACT

Autosomal recessive polycystic kidney disease/congenital hepatic fibrosis (CHF/ARPKD) is a rare but fatal genetic disease characterized by progressive cyst development in the kidneys and liver. Liver cysts arise from aberrantly proliferative cholangiocytes accompanied by pericystic fibrosis and inflammation. Yes associated protein (YAP), the downstream effector of the Hippo signaling pathway, is implicated in human hepatic malignancies such as hepatocellular carcinoma, cholangiocarcinoma, and hepatoblastoma, but its role in hepatic cystogenesis in CHF/ARPKD is unknown. We studied the role of the YAP in hepatic cyst development using polycystic kidney (PCK) rats, an orthologous model of ARPKD, and in human CHF/ARPKD patients. The liver cyst wall epithelial cells (CWECs) in PCK rats were highly proliferative and exhibited expression of YAP. There was increased expression of YAP target genes, *Cyclin D1* and *Ctgf* (connective tissue growth factor), in PCK rat livers. Extensive expression of YAP and its target genes was also detected in human CHF/ARPKD liver samples. Finally, pharmacological inhibition of YAP activity with verteporfin and short-hairpin (sh) RNA-mediated knockdown of YAP expression in isolated liver CWECs significantly reduced their proliferation. These data indicate that increased YAP activity, possibly through dysregulation of the Hippo signaling pathway, is associated with hepatic cyst growth in CHF/ARPKD.

4.2 INTRODUCTION

Polycystic kidney disease (PKD) is heritable genetic disorder characterized by the formation and growth of fluid-filled cysts in ductal structures, including the kidneys and liver. Autosomal dominant PKD (ADPKD), the more common form of the disease (1 in 500 people affected), is caused by mutations in *PKD1* or *PKD2*, which code for polycystin-1 and polycystin-2, respectively (Ward 1994, Burn et al. 1995, Mochizuki et al. 1996). Autosomal recessive PKD (ARPKD), a rare form of disease (1 in 20,000 people affected), is caused by mutations in *PKHD1*, which encodes fibrocystin (Igarashi et al. 2002). All three proteins are localized to primary cilia on epithelial cells. However, it remains unclear how disruption of these ciliary proteins induces epithelial cyst formation (Turkbey et al. 2009, Lazaridis et al. 2015). The liver is the major extra-renal organ affected in PKD. In 60% of ADPKD and 100% of ARPKD patients, large fluid-filled cysts develop in the liver, resulting in hepatic enlargement, inflammation and fibrosis, which significantly contribute to the morbidity associated with PKD (Everson et al. 2004, Everson et al. 2008, Wen 2011).

Hepatic cytogenesis and associated complications are especially problematic in ARPKD. ARPKD patients develop hepatic cysts surrounded by extensive pericystic fibrosis during the perinatal period and suffer from congenital hepatic fibrosis (CHF) (Everson et al. 2004, Everson et al. 2008, Wen 2011). CHF/ARPKD patients exhibit significant portal hypertension secondary to pericystic fibrosis. Recent studies have characterized CHF/ARPKD as a major pediatric liver disorder with significant mortality (Turkbey et al. 2009). Aside from symptom management, the only treatment option for CHF/ARPKD patients is liver and kidney transplantation.

The hepatic cysts in PKD are made up of epithelial cells which originate from dysgenesis of biliary epithelium (Masyuk et al. 2009). One of the main aspects of CHF/ARPKD pathogenesis is the aberrant proliferation of cyst wall epithelial cells (CWECs) (Masyuk et al. 2006, Lazaridis et al. 2015). The mechanisms responsible for CWEC proliferation remain unclear. Recent studies have shown that deregulation of the Hippo signaling pathway results in increased expression and activity of its downstream effector Yes associated protein (YAP), which is involved in a number of fibro-proliferative hepatic disorders including hepatic fibrosis, hepatocellular carcinoma and cholangiocarcinoma (Camargo et al. 2007, Pan 2010, Li et al. 2012, Septer et al. 2012). When the Hippo signaling pathway is ‘on’, activation of LATS1/2 kinases directly phosphorylate YAP, which inhibits YAP nuclear translocation. When the Hippo signaling pathway is ‘off’, YAP is translocated to the nucleus and binds to different transcription factors to regulate target genes involved in cell proliferation, cell survival, and apoptosis (Di Cara et al. 2015, Yu et al. 2015). A previous study showed increased YAP activation in kidney cyst epithelial cells from ADPKD and ARPKD patients (Happe et al. 2011); however, the role of YAP in hepatic cyst development in CHF/ARPKD is not known. Our studies were undertaken to determine the role of YAP in liver CWEC proliferation with the use of human CHF/ARPKD liver tissues and animal models of CHF/ARPKD.

4.3 MATERIALS AND METHODS

Animals

Male and female polycystic kidney (PCK) rats and Sprague-Dawley (SD) rats (control strain for PCK) were purchased from Charles River and housed in an AAALAC-approved vivarium at the University of Kansas Medical Center (KUMC). *Pkhd1*$^{LSL(-)/LSL(-)}$ mice on a C57BL/N background were a kind gift from Dr. Christopher J. Ward (KUMC); wild-type mice on the same genetic background purchased from Charles River (Wilmington, MA) were used for controls. All animal studies were approved by the KUMC Institutional Animal Care and Use Committee (IACUC) and were performed in accordance with IACUC guidelines.

Tissue Harvest and Processing

Rats (n=3-4 per time point) were euthanized under isoflurane anesthesia and livers were harvested at postnatal days 0, 5, 10, 15, 20, 30 and 90. Livers were processed for obtaining paraffin sections and frozen sections, total cell extracts and RNA as described before (Septer et al. 2012, Walesky et al. 2013). Body weights and liver weights were recorded at the time of euthanasia.

Histopathological Analysis

Formalin-fixed, paraffin-embedded liver sections were used for morphological analysis and immunohistochemical staining, and frozen liver sections were used for immunofluorescence staining. Cells were cultured on coverslips to appropriate density and fixed with 4% paraformaldehyde for immunofluorescence staining. Hematoxylin and

eosin (H&E) stained sections were used to determine the number of hepatic cysts. The source and details of primary antibodies used in these studies are as follows: proliferating cell nuclear antigen (PCNA, monoclonal antibody (mAb), clone PC10, Cell Signaling Technologies, Danvers, MA), phospho-YAP (Ser127) (polyclonal antibody (pAb), cat# 4911, Cell Signaling Technologies), Cyclin D1 (mAb, clone 92G2, Cell Signaling Technologies), Ki 67 (pAb, cat# ab-15580, Abcam, Cambridge, MA), YAP (pAb, cat# 4912, Cell Signaling Technologies; cat# sc-101199, Santa Cruz Biotechnology, Santa Cruz, CA), Cytokeratin 19 (Ck19, pAb, cat# sc-33119, Santa Cruz Biotechnology), connective tissue growth factor (CTGF, pAb, cat# sc-14939, Santa Cruz Biotechnology), and β-actin (mAb, clone 13E5, Cell Signaling Technologies). Secondary antibodies for immunohistochemistry and immunofluorescence were purchased from Jackson Immunoresearch (West Grove, PA). Primary antibodies were used at a concentration of 1:100 (except PCNA, which was used at a concentration of 1:5000) and secondary antibodies were used at a concentration of 1:500. Micrographs were taken using an Olympus BX51 microscope with an Olympus DP71 camera. DP Controller software was used to acquire images at indicated magnifications (Olympus, Waltham, MA).

RNA Isolation, cDNA Synthesis and Real Time PCR

Total RNA was isolated from liver pieces and biliary trees as describe (Deshpande et al. 2016). Briefly, tissues (25-30 mg) were homogenized using an MP Biomedicals Fast Prep 24 bead homogenizer with lysing matrix D homogenization tubes (Solon, OH). Total RNA was isolated using the Qiagen RNeasy Mini Kit (Valencia, CA).

Template cDNA was obtained by reverse transcription of 4 μg total RNA using the Retroscript kit (Life Technologies/Ambion, Grand Island, NY). Real time PCR was performed with a BioRad CFX384, and results were calculated using the $2^{-\Delta\Delta Ct}$ method. The primers used in this study were as follows: rat *Ccnd1* primer, forward GCCCTAGCTGCCTACCGACT, reverse ACAGGCTTG GCAATTTTAGGC; rat *Ctgf* primer, forward GCCCTAGCTGCCTACCGACT, reverse ACAGGC TTGGCAATTTTAGGC; rat *Acta2* primer, forward AGCTCTGGTGTGTGACAATGG, reverse GGAGCATCATCACCAGCAAAG; rat *Ck7* primer, forward AGGAGATCAACCGACGCAC, reverse GTCTCGTGAAGGGTCTTGAGG; human *CTGF* primer, forward AAAAGTGCATCCGTACTCCCA, reverse CCGTCGGTACATACTCCACAG.

CHF/ARPKD Patient Liver Tissue Samples

Paraffin-embedded liver tissue blocks (n=3) and frozen liver tissues (n=5) of CHF/ARPKD patient livers were obtained from the KUMC's Liver Center Tissue Bank, PKD Biomarkers and Biomaterials Core at KUMC, the Mayo Clinic (Dr. Peter Harris) and Children's Mercy Hospital, Kansas City, MO. All studies were approved by the IRB at the associated institutions.

CWEC Isolation

CWECs from PCK rats were isolated as described by LaRusso *et al*. (Muff et al. 2006). Briefly, biliary tree was obtained by removing hepatocytes after liver perfusion with a 37^{o}C collagenase-containing solution. After cutting the biliary tree into small

pieces with sterile scissors, the tissue was further digested in 25 ml of MEM medium (Corning, Hanover Park, IL) containing 25 mM HEPES (Sigma-Aldrich), 10 mg hyaluronidase (Sigma-Aldrich), 8 mg collagenase P (Roche, Indianapolis, IN), and 6 mg DNase (Sigma-Aldrich) for 45 min in a 42^{o}C water bath. The tissue pieces were gravity sedimented, washed with cold MEM, and resuspended in DMEM/F12 media (Invitrogen, Grand Island, NY) supplemented with 1% penicillin-streptomycin (P/S, Invitrogen), 1% insulin-transferrin-selenium (ITS, Invitrogen), 10^{-7} M dexamethasone (Sigma-Aldrich), 5% fetal bovine serum (FBS, Sigma-Aldrich). The tissue pieces were subsequently placed in a 150 mm tissue culture dish and incubated for 2 h at 37^{o}C, then re-suspended in DMEM/F12 growth medium containing 5% FBS, 1% ITS, 4.11 µg/ml forskolin (Sigma-Aldrich), 393 ng/mL dexamethasone, 3.4 µg/ml 3,3', 5-triiodo-L-thyronine (Sigma-Aldrich), 1% P/S, 25 ng/ml epidermal growth factor (life Technologies, Grand Island, NY), 30 µg/ml bovine pituitary extract (Invitrogen), and poured into a tissue culture dish containing collagen gel. After 2 – 3 days of culture, cysts formed from proliferating CWECs were digested with collagenase P, trypsinized, and plated on collagen-coated plates to form cell monolayers.

Cell Proliferation Assay

Cell proliferation was measured as described by Yamaguchi *et al.* (Yamaguchi et al. 2006). Briefly, PCK CWECs were seeded in a 96-well culture plate and incubated in DMEM/F12 with 1% FBS, ITS, and P/S. After 24 h, the medium was changed to a 0.002% FBS without ITS. Cells were incubated for another 24 h before the addition of 0.1, 0.5, 2, and 5 µM verteporfin (VP, a YAP-TEAD interaction inhibitor which prevents

YAP-mediated gene transcription) with or without forskolin (a cAMP agonist). After 48 h, cell proliferation was determined based on the production of formazan from the CellTiter 96 Aqueous One Solution Cell Proliferation Assay (Promega). The amount of formazan is directly proportional to the number of living cells in the culture.

YAP knockdown in isolated CWECs

YAP knockdown experiments were conducted in primary liver CWECs isolated from PCK rats. Cells were transfected with either control shRNA (sc-108080, Santa Cruz Biotechnology) or YAP shRNA (sc-38638-V, Santa Cruz Biotechnology) for 24h. Cell proliferation rate was assessed by cell proliferation assay described above. Interference efficiency was detected by Western blotting. The ratio of YAP/β-actin was quantified with three independent Western blot results using Image J software.

Statistics

All data are represented as mean ± standard error of mean. Student's t-test was used to calculate differences between two groups. One-way ANOVA was used to compare differences in Figure 4.4.7C-D and Figure 4.4.8 A, B, and E. Two-way ANOVA was used to compare differences in Figure 4.4.5A. Post-hoc Tukey's adjustment for multiple comparisons was used after each ANOVA. In each case, $P<0.05$ was considered statistically different.

4.4 RESULTS

Extensive proliferation in PCK rat livers.

Using hematoxylin and eosin (H&E)-stained liver sections from PCK and SD rats, we evaluated liver histology from postnatal day (PND) 0 to PND 90. Hematopoietic cells (clusters of small cells with basophilic nuclei) were evident in the livers of SD rats on PND 0 and PND 5 but were absent at PND 10 (Figure 4.4.1A). This observation is consistent with the hematopoietic nature of the perinatal liver (Payushina 2012). The portal vein, hepatic artery and bile ducts (the portal triad) were readily identifiable in livers from SD rats from PND 10 onward and did not change in appearance through PND 90 (Figure 4.4.1A). Similar to SD rats, PCK rat livers contained hematopoietic cells at PND 0 and PND 5 but not PND 10 onward (Figure 4.4.1A). Bile ducts were dilated in livers from PCK rats from PND 0 onward and the number of cysts developing from dilated bile ducts increased throughout the time course, disrupting normal portal triad histological structure (Figure 4.4.1A). To determine if there was elevated proliferation of CWECs, we stained liver sections from PCK and SD rats with antibodies recognizing PCNA (Figure 4.4.1B) and Cyclin D1 (Figure 4.4.1C), markers for cell proliferation. Overall, we found more PCNA and Cyclin D1 positive cells in the liver of PCK rats compared to that in SD rats, and the PCNA/Cyclin D1 positive cells were not limited to CWECs. In order to gain a better insight into CWEC proliferation at mRNA level, we measured *Ccnd1* transcripts in biliary trees isolated from 6-month-old SD and PCK rats. Consistent with immunohistochemistry staining, *Ccnd1* mRNA was significantly up-regulated in PCK rat biliary trees (Figure 4.4.1D).

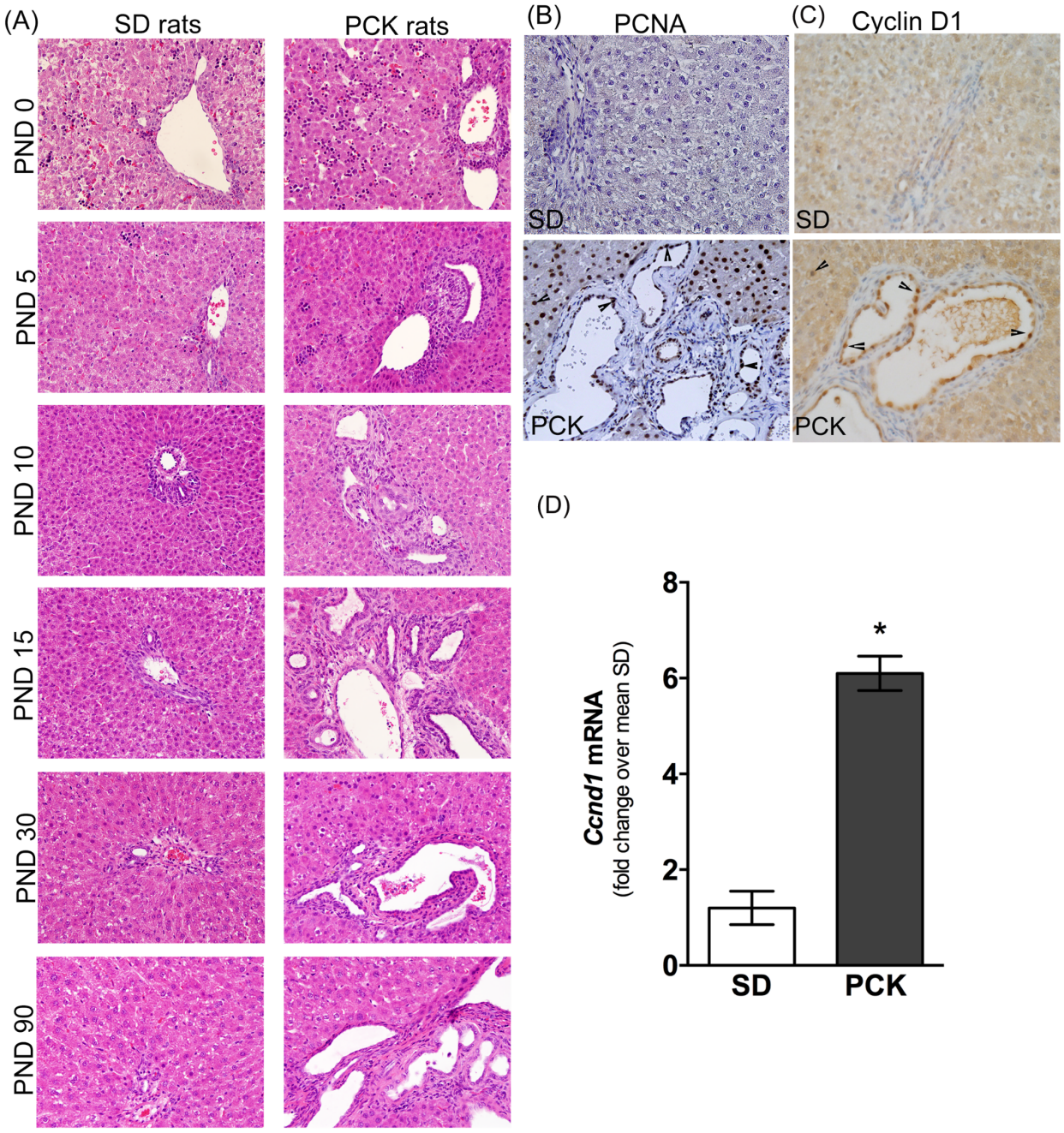

Figure 4.4.1. Cyst growth and proliferation in PCK rat livers. (A) Representative photomicrographs hematoxylin & eosin (H&E) stained livers from SD and PCK rats from postnatal day (PND) 0 to PND 90 (3 months). Immunostaining for PCNA (B) and Cyclin D1 (C) in SD and PCK rat liver sections. Images were taken at 400X. Arrowheads indicate PCNA positive cells (B) or Cyclin D1 positive cells (C). (D) *Ccnd1* transcript level in biliary trees from 6-month-old SD and PCK rats. N = 4 rats per group. *, P<0.05 between genotypes.

Increased YAP expression in CWECs from PCK rats and *Pkhd1*$^{LSL(-)/LSL(-)}$ mice.

Moderate YAP expression was observed in cholangiocytes from SD rat livers (Figure 4.4.2A). Higher YAP expression with nuclear localization was observed in the CWECs from PCK rats (Figure 4.4.2A-B). In the canonical Hippo signaling pathway, phosphorylated YAP is sequestered in the cytoplasm and targeted for degradation (Hao et al. 2008). Thus, the ratio of YAP to phospho-YAP is a surrogate marker of YAP activity. Immunohistochemistry for phospho-YAP revealed only moderate cytoplasmic staining in CWECs from PCK rat livers (Figure 4.4.2B). To further investigate the expression of YAP in another model of CHF/ARPKD, we performed YAP staining on liver samples from wild type (WT) mice and *Pkhd1*$^{LSL(-)/LSL(-)}$ mice. Similarly, liver samples from *Pkhd1*$^{LSL(-)/LSL(-)}$ mice exhibited higher YAP nuclear staining in comparison to the liver samples from wild-type mice (Figure 4.4.2C).

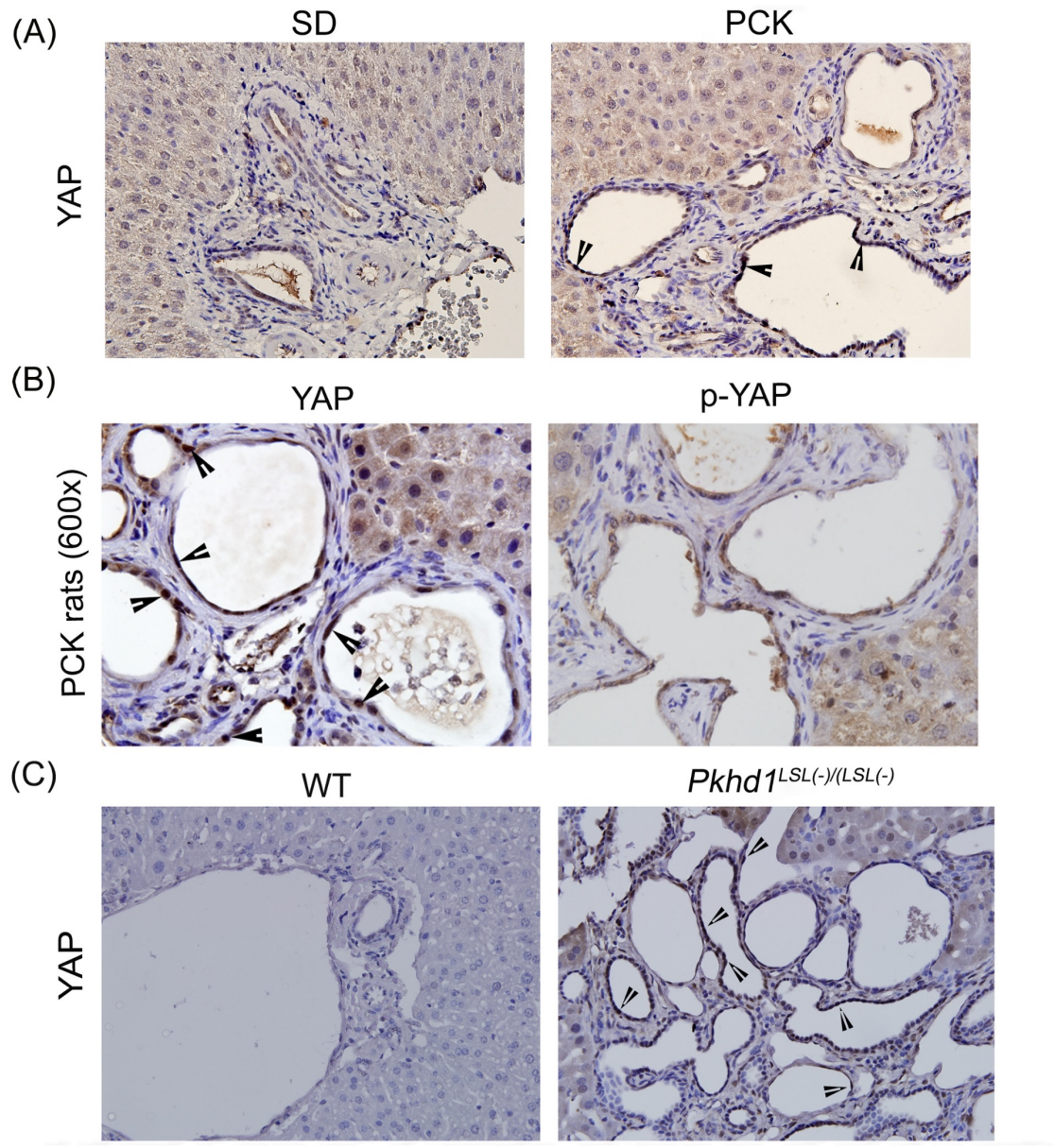

Figure 4.4.2. Increased YAP activation in PCK rat livers. (A) Representative photomicrographs (400X) of YAP immunohistochemistry in SD and PCK rat livers. (B) Representative photomicrographs (600X) of YAP and phospho-YAP immunohistochemistry in PCK rat livers. Arrowheads point to cyst wall epithelial cells (CWEC) positive for YAP. (C) Representative photomicrographs (400X) of YAP immunohistochemistry in wild-type (WT) and *Pkhd1*$^{LSL(-)/LSL(-)}$ mice.

YAP is actively expressed in proliferating PCK rat liver CWECs.

To confirm the association between YAP and CWECs, we performed co-immunofluorescence (IF) staining for Cytokeratin19 (CK19), a biliary epithelial cell marker, and YAP in PCK rat livers. Our co-IF studies showed YAP and CK19 co-localization in biliary epithelium from SD rats (Figure 4.4.3A); more co-localization of YAP and CK19 was observed in CWECs from PCK rat livers (Figure 4.4.3B). These data suggest strong association between YAP and CWECs in PCK rats. To test the role of YAP in CWEC proliferation, we performed co-IF to determine if YAP co-localizes with Ki67 (a cell proliferation marker) in CWECs. As we expected, co-localization occurs only in PCK and not in SD rats (Figure 4.4.4).

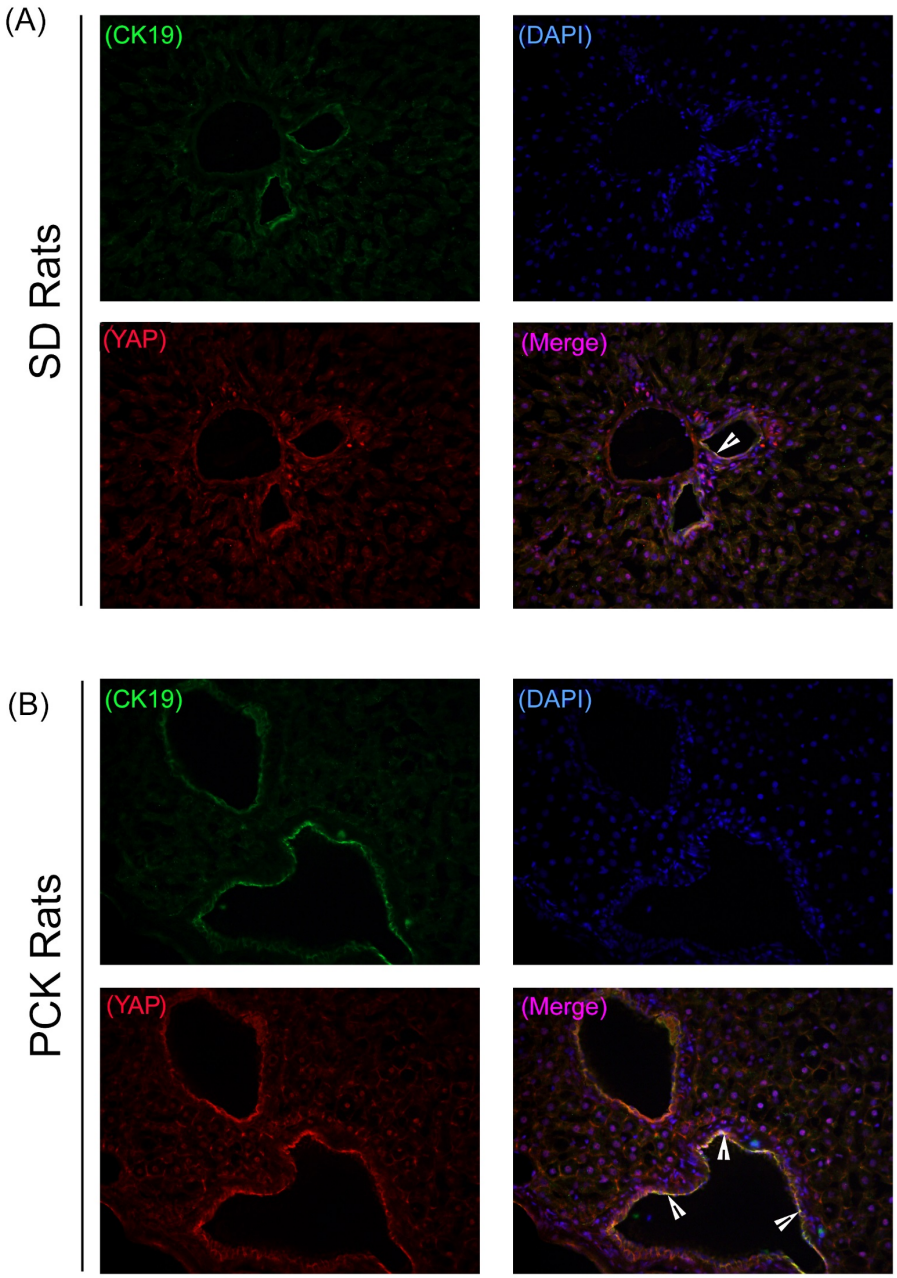

Figure 4.4.3. YAP and CK19 co-localization in CWECs. Representative photomicrographs of immunofluorescence staining of YAP (red), Cytokeratin 19 (CK19, green) and DAPI (blue) on frozen liver sections from SD rats (A) and PCK rats (B). Images were taken at 400X. Arrowheads point to co-localization of YAP and CK19.

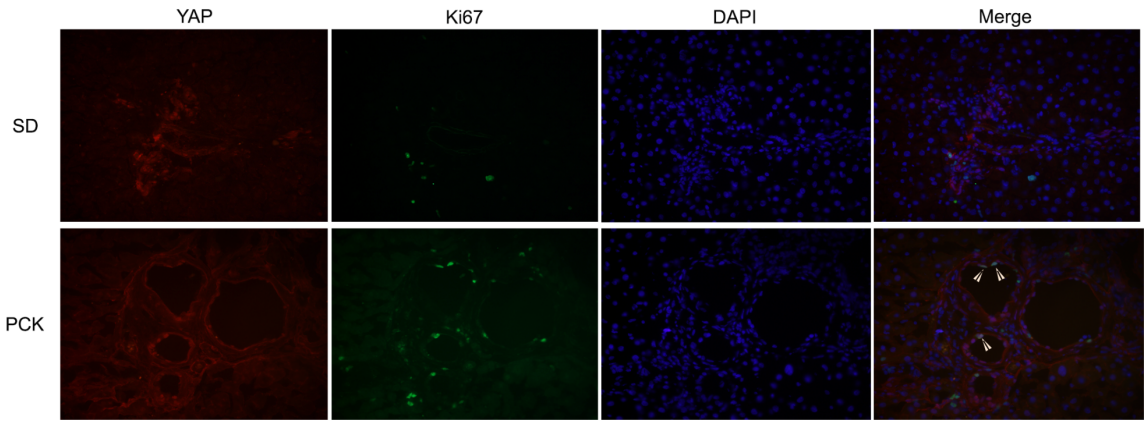

Figure 4.4.4. YAP/Ki67 co-localization is increased in PCK CWECs. Representative images of immunofluorescence staining of YAP (red), Ki67 (green), and DAPI (blue) on liver sections from SD and PCK rats are shown at 400X. Arrowheads point to co-localization of YAP, Ki67, and DAPI.

CTGF is increased in hepatic cysts in PCK rats.

YAP regulates expression of connective tissue growth factor (*Ctgf*), encoding for a matricellular protein of the CNN family (Rachfal et al. 2003, Gressner et al. 2008, Pi et al. 2008, Zhao et al. 2008, Pi et al. 2015). Real time PCR analysis showed that hepatic *Ctgf* mRNA was greater in livers from PCK rats than in SD rats beginning at PND 10 (Figure 4.4.5A). *Ctgf* transcript levels peaked at PND 20 and PND 30 in PCK rats and decreased substantially thereafter (Figure 4.4.5A). However, *Ctgf* mRNA remained 6-fold higher in the PCK rat livers compared to SD rat livers at 90 days after birth (Figure 4.4.5B). To determine *Ctgf* expression level in the absence of hepatocytes, we measured its expression in biliary trees isolated from 6-month-old SD rats and PCK rats (Figure 4.4.5C). We found *Ctgf* expression was significantly higher in PCK rat biliary trees compared to that in SD rats. Immunohistochemical analysis revealed extensive CTGF staining in CWECs from PCK rats compared to SD rats (Figure 4.4.5D). Interestingly, CTGF protein was also observed in cells within the pericystic fibrotic tissue and hepatocytes (Figure 4.4.5D). Taken together, these data suggest that increased YAP content in livers from PCK rats drives the expression of YAP target genes associated with CHF/ARPKD disease progression in PCK rats.

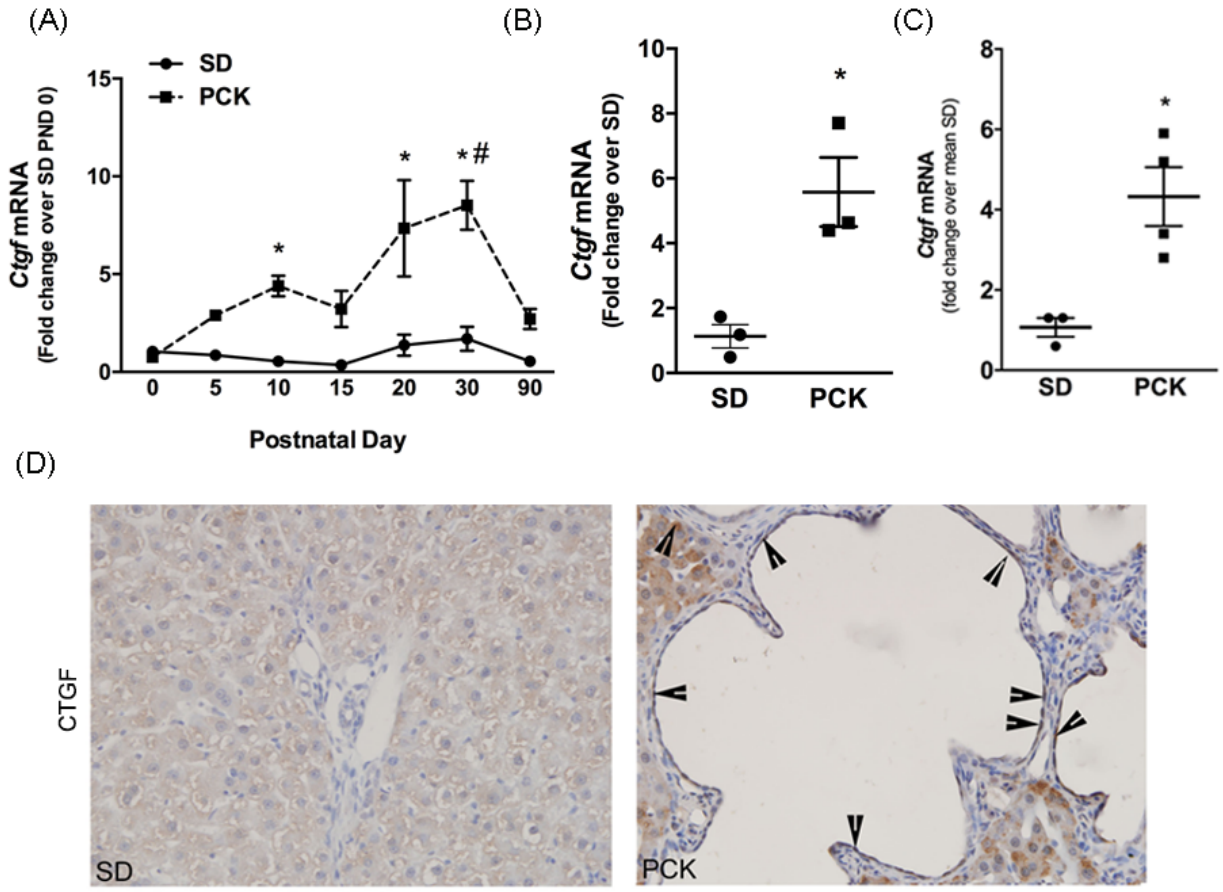

Figure 4.4.5. CTGF expression in livers from PCK rats. (A) Real time PCR was used to quantify hepatic *Ctgf* transcripts in livers from SD and PCK rats from PND 0 to PND 90. N = 3 – 4 rats per time point. (B) *Ctgf* transcript content in SD and PCK rats on PND 90. N = 3 rats in each group. In (A) and (B), filled-in circles indicate SD data while filled-in squares indicate PCK data. (C) *Ctgf* transcript content in biliary trees from 6-month-old SD and PCK rats. N = 4 rats in each group. (D) Representative CTGF immunohistochemistry from PCK rats at PND 90. Images were taken at 400X. Arrowheads indicate CTGF-positive cells. *, $P<0.05$ between genotypes at the given time point, #, $P<0.05$ compared to PND 90.

Increased YAP, PCNA and CTGF in hepatic cysts in CHF/ARPKD patient samples.

To determine YAP expression pattern in hepatic cysts in human CHF/ARPKD, we performed immunohistochemistry on paraffin-embedded liver sections from two CHF/ARPKD patients. Serial sections stained with H&E (Figure 4.4.6A), or with antibodies recognizing PCNA (Figure 4.4.6B) or YAP (Figure 4.4.6C and enlarged in Figure 4.4.6D), revealed extensive YAP expression with nuclear localization in CWECs, which also stained positive for PCNA.

We also evaluated CTGF content in patient-derived liver samples. We evaluated hepatic *CTGF* transcript levels using real time PCR in 3 normal human liver samples and 3 liver samples from patients with CHF/ARPKD. Although, there was variation in relative *CTGF* expression (Figure 4.4.6E), there was a trend towards increased *CTGF* expression in this limited number of samples. An immunohistochemical approach revealed substantial CTGF positivity in CWECs as well as in cells found in the pericystic fibrotic areas (Figure 4.4.6F and enlarged in Figure 4.4.6G). Collectively, these data suggest that, similar to findings in the PCK rat, nuclear YAP content is a prominent feature of proliferating CWECs found in CHF/ARPKD patients and is associated with hepatic CTGF content accumulation.

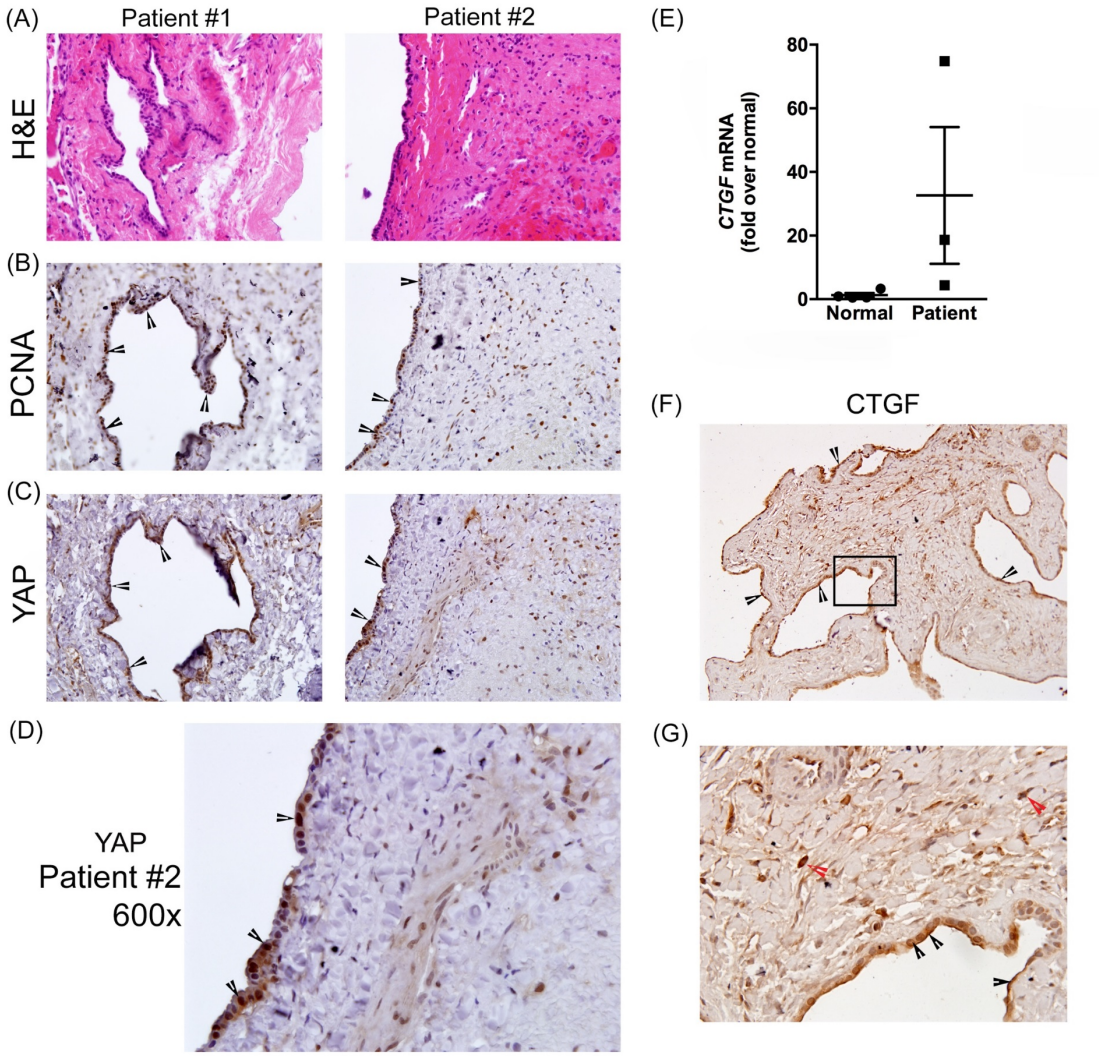

Figure 4.4.6. Characterization of YAP expression, cell proliferation, and CTGF in human CHF/ARPKD livers. Representative photomicrographs of H&E stained liver sections (A) showing hepatic cysts and surrounding pericystic tissue, and PCNA (B) and YAP (C) immunostaining in two different CHF/ARPKD patients. (D) Enlarged image (600X) of YAP immunostaining from Patient #2. (E) Real time PCR was used to measure hepatic *CTGF* transcripts in three patients. (F) CTGF immunostaining in one CHF/ARPKD patient. The black box outlines the area enlarged in (G). Black arrowheads point to CTGF positive CWECs, red arrowheads point to the CTGF positive cells in pericystic fibrotic area.

The YAP-TEAD binding disruptor, verteporfin (VP), inhibits CWEC proliferation.

YAP is not able to bind DNA directly and therefore requires interaction with *bona fide* transcription factors to regulate gene transcription. TEAD (TEA domain family member) is a transcription factor and one of the best-characterized binding partners of YAP (Vassilev et al. 2001). VP is a chemical inhibitor of the YAP-TEAD interaction and prevents YAP-mediated gene regulation(Liu-Chittenden et al. 2012). To explore the role of YAP in CWEC proliferation, we examined the ability of VP to inhibit the function of YAP in CWEC proliferation, *in vitro*. We first isolated CWECs from PCK rats and characterized them by light microscopy, co-immunofluorescence (co-IF) staining and real-time PCR. After isolation, CWECs were cultured, as a monolayer, onto collagen gel-coated plates. CWECs formed colonies of cells with a cobblestone pattern characteristic of primary epithelial cells in culture (Figure 4.4.7A). To confirm that the isolated CWECs still maintained the nuclear staining of YAP, we performed co-IF for YAP and CK19 on cultured CWECs. Consistent with co-IF staining *in vivo*, the PCK CWECs stained positive for both YAP and CK19 confirming that these primary cells were derived from cholangiocytes, and they maintain the YAP-positive feature *in vitro* (Figure 4.4.7B). This was further confirmed by real time PCR analysis for an additional cholangiocyte marker, *Ck7*. As shown in Figure 4.4.7C, CWECs were enriched for *Ck7* transcripts relative to biliary tree isolated from SD and PCK rats or relative to whole liver from SD rats. To exclude the possibility of myofibroblast contamination in our CWEC cultures, we quantified *Acta2* transcripts (α smooth muscle actin gene) in CWEC cultures by real time PCR. CWECs did not express *Acta2* while *Acta2* was found in biliary tree isolated from SD and PCK rats (Figure 4.4.7D) due to fibroblasts found in the

connective tissue surrounding the biliary tree. Interestingly, we found the *Acta2* level was significantly lower in biliary trees from PCK rats. It is possibly due to the increased proportion of CWECs in PCK rats compared to the normal cholangiocytes in SD biliary tree. *Acta2* was not detectable in livers from SD rats (Figure 4.4.7D).

Next, to determine the role of YAP in aberrant cell proliferation in PCK rats, we treated CWECs with various concentrations (0.1, 0.5, 2, and 5 μM) of VP alone or in combination with forskolin. Forskolin is a cAMP agonist that stimulates renal cystic epithelial cell proliferation in autosomal dominant polycystic kidney disease (ADPKD) through activation of the B-Raf-MEK-ERK pathway (Tesmer et al. 1997, Yamaguchi et al. 2000). VP treatment alone significantly reduced CWEC proliferation at the dose of 0.1 μM compared to the DMSO control (Figure 4.4.8A). Furthermore, VP at higher doses exhibited greater degree of inhibition on CWEC proliferation. Forskolin treatment caused a significant increase in CWEC proliferation, consistent with previous results (Francis et al. 2004). Treatment with VP blocked forskolin-mediated CWEC proliferation (Figure 4.4.8A). These data suggest that the inhibitory effect of VP on CWEC proliferation may occur downstream of a cAMP-mediated pathway. The inhibitory effect of VP on YAP-mediated gene expression was confirmed by a significant reduction of *Birc5* (survivin gene) expression (Figure 4.4.8B). The ability of VP to inhibit CWECs proliferation in our model is consistent with the observation that VP can block the proliferation in cholangiocyte and cholangiocarcinoma cell lines (Gurda et al. 2014).

YAP knockdown decreases CWEC proliferation.

As a second approach to perturb YAP-mediated gene expression, we performed a YAP knockdown experiment in isolated CWECs using short-hairpin (sh) RNA. Western blot analysis indicated a modest but significant decrease in total YAP protein in cells treated with YAP shRNA (Figure 4.4.8C and Figure 4.4.8D). Further, a cell proliferation assay indicated a significant decrease in cell proliferation after YAP shRNA treatment for 24h (Figure 4.4.8E). Taken together, these data support the hypothesis that aberrant proliferation of the CWECs is mediated, at least in part, by YAP.

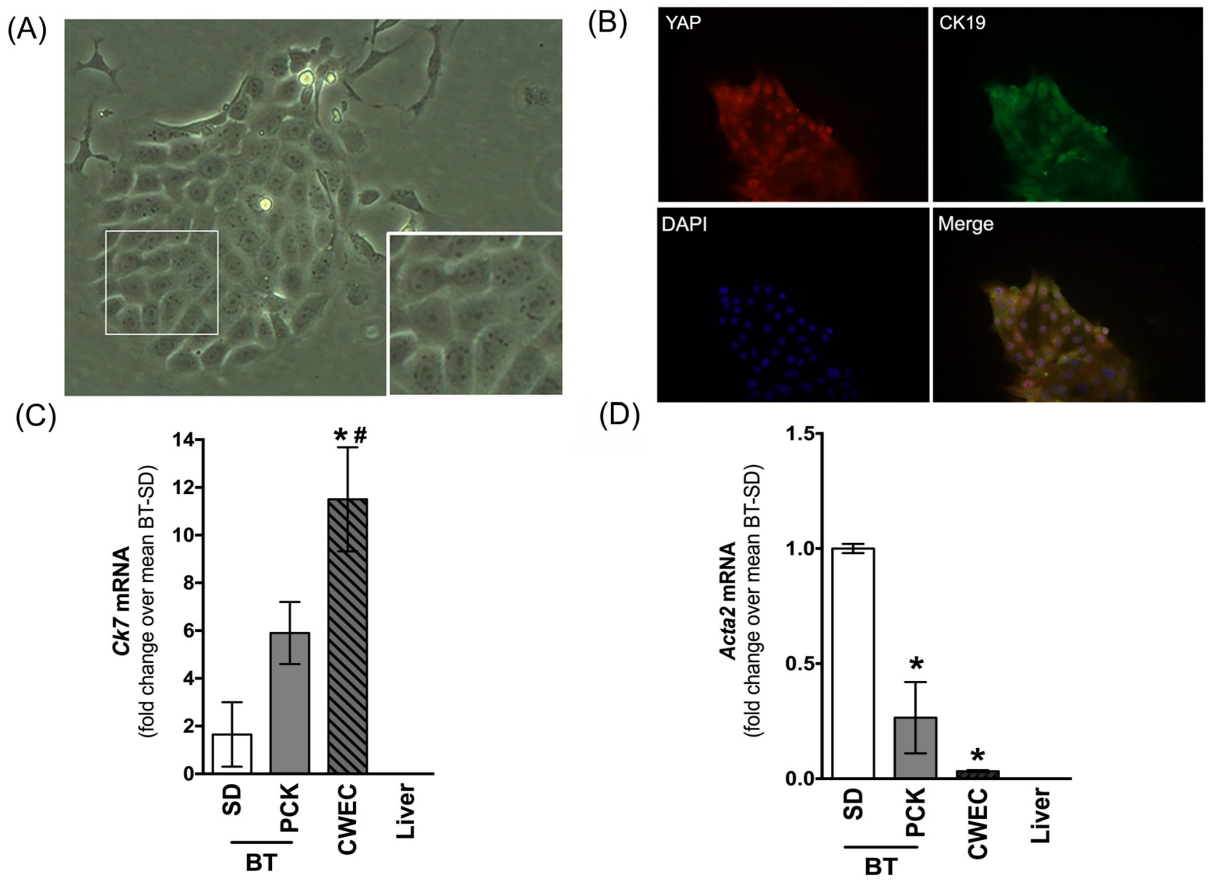

Figure 4.4.7. Characterization of CWECs isolated from PCK rats. (A) Representative phase-contrast micrograph of CWEC growing on collagen gel-coated plates as a monolayer (400X). The area demarcated by the white box in the image is enlarged in the inset in the bottom right of the same image. (B) Representative immunofluorescence image (400X) of CK19 staining in isolated CWECs. Real time PCR analysis of *Ck7* (cytokeratin 7, a cholangiocyte marker, C) and *Acta2* (αSMA, a fibroblast marker, D) from SD rat biliary tree (BT), PCK rat BT, PCK CWEC, and SD liver. * P<0.05 versus SD BT, # P<0.05 versus liver. Liver = whole liver from SD rats.

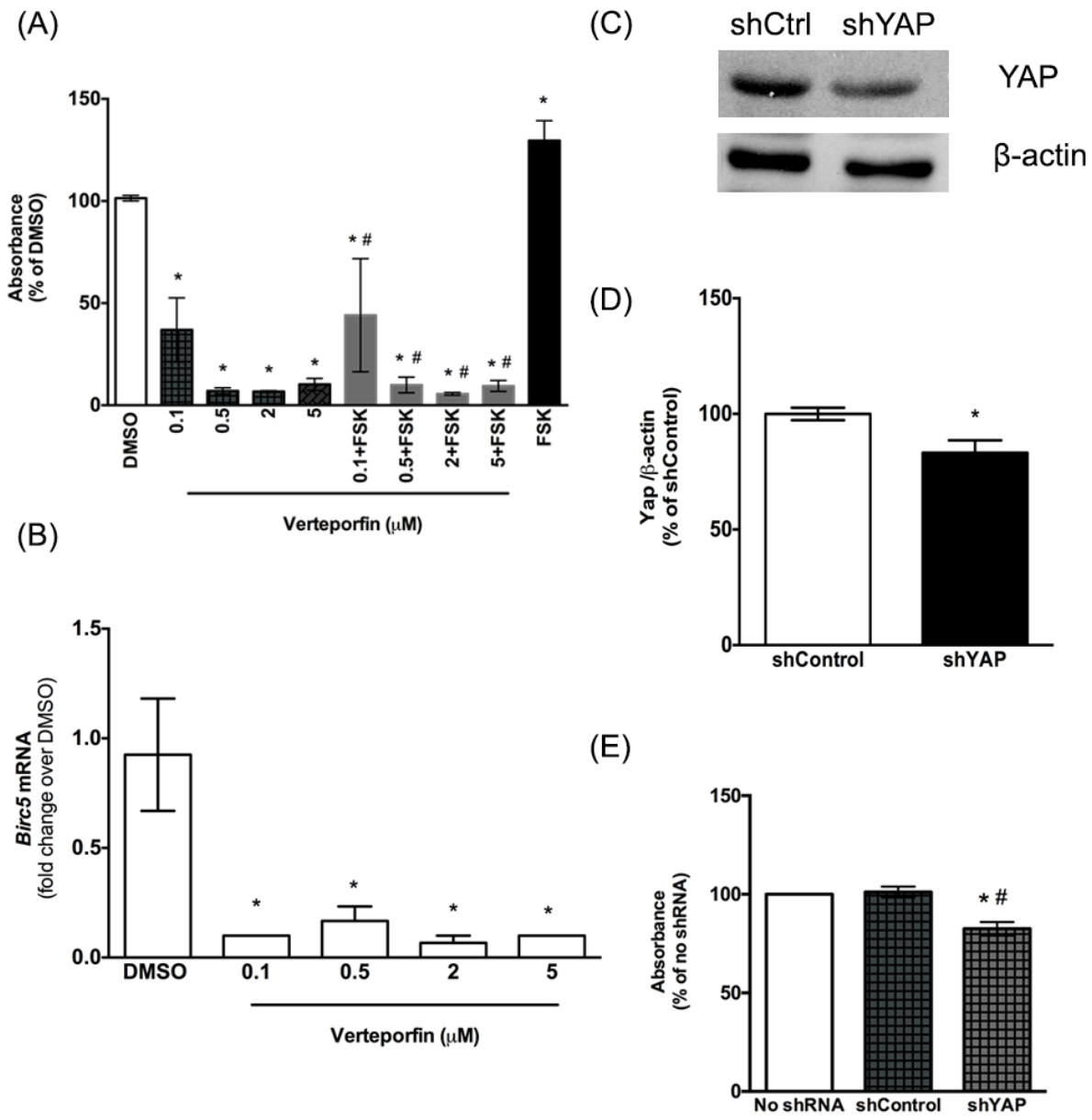

Figure 4.4.8. CWEC proliferation is reduced after inhibition of YAP activity with VP and YAP knockdown, *in vitro*. (A) Effects of different concentrations of verteporfin (VP) on cell proliferation. CWECs were treated with the indicated VP concentrations with or without forskolin (FSK). DMSO was used as control. (B) Real time PCR analysis of *Birc5* transcripts after VP treatment. *, significant decrease ($P<0.05$) relative to the DMSO; #, significant decrease ($P<0.05$) relative to FSK. (C, D) Western blotting analysis of total YAP protein after YAP shRNA-mediated knockdown. The YAP band intensity was normalized to β-actin. (E) Effect of YAP knockdown on CWEC proliferation. Each experiment was repeated three times (CWECs from 3 separate biliary trees from 3 separate rats isolated on 3 separate days). The error bars represent standard error of mean. *, significant decrease ($P<0.05$) relative to the no shRNA treatment group; #, significant decrease ($P<0.05$) relative to control shRNA.

4.5 DISCUSSION

CHF/ARPKD is a rare but devastating and progressive genetic disease that is especially debilitating in pediatric patients (Turkbey et al. 2009, Wen 2011). Hepatic complications due to rapidly developing cysts, accompanied by pericystic fibrosis, inflammation and subsequent portal hypertension, lead to significant morbidity and high perinatal mortality (Wen 2011). Thirty to forty percent of patients with this disease die in the perinatal period (Guay-Woodford 2014). Patients that survive the perinatal period require intensive treatment that can include a simultaneous liver and kidney transplant. Unfortunately, the mechanisms of hepatic cyst development remain poorly understood, which has hindered finding alternative treatment strategies. Although we previously hypothesized that a central mechanism regulating CHF/ARPKD is a 'pathogenic triumvirate' consisting of fibrogenesis, CWEC proliferation and pericystic inflammation (Jiang et al. 2016), no specific signaling pathway has been implicated to date in all three processes. We propose that one pathway which could regulate all three pathogenic processes is the Hippo signaling pathway. For example, previous studies suggest that YAP and TAZ (a related transcriptional coactivator) are key activators of fibroblasts, and they sustain fibrosis by activating fibroblasts (Liu et al. 2015). As an oncoprotein, YAP activation is found in several human cancers (Overholtzer et al. 2006, Zender et al. 2006, Zhao et al. 2007, Steinhardt et al. 2008), and it plays a key role in the Hippo pathway to control cell proliferation in response to cell contact (Zhao et al. 2007). Finally, YAP activation promotes endothelial cell proliferation and inflammatory response in atherosclerosis (Wang et al. 2016). Therefore, it is logical to predict that the

Hippo signaling pathway could be the central pathway regulating each member of the pathogenic triumvirate in CHF/ARPKD.

A major component of CHF/ARPKD, apart from progressive fibrosis and inflammation, is the rapid growth of cysts due to aberrant cell proliferation and fluid secretion. Multiple mechanisms are implicated in the regulation of CWEC proliferation including calcium and cAMP signaling, the B-Raf/MEK/ERK pathway, VEGF, Cdc25A, HDAC6 and Wnt signaling due to LRP5 mutations (Fabris et al. 2006, Gradilone et al. 2010, Spirli et al. 2010, Masyuk et al. 2012, Spirli et al. 2012, Cnossen et al. 2014, Gradilone et al. 2014). Recent studies have highlighted the role of YAP, in the regulation of normal and abnormal cell proliferation during postnatal liver growth and cancer pathogenesis (Zhou et al. 2009, Lee et al. 2010, Lu et al. 2010, Pan 2010, Song et al. 2010, Li et al. 2012, Septer et al. 2012). Interestingly, increased YAP activation is also observed in kidney cyst development in ADPKD (Happe et al. 2011). Importantly, that study demonstrated increases in renal YAP target genes, *Birc3*, *Ctgf*, *InhibA* and *Fjx1*, a planar cell polarity gene, in *Pkd1*-deleted mice and in renal tissues from ADPKD patients (Happe et al. 2011). Our results are consistent with these studies. However, our study is the first to demonstrate that hepatic CWECs have significant YAP over-expression and activation as demonstrated by increased nuclear YAP localization and increased expression of YAP target genes in animals and patients with CHF/ARPKD. Therefore, our data suggest that hepatic cystogenesis is associated with deregulation of the Hippo signaling pathway.

In this study, we used PCK rats, a variant of SD rat strain, which harbors a single splicing mutation (IVS35-2A→T) in the rat ortholog of human *PKHD1*, the gene found

mutated in human CHF/ARPKD; the PCK rat develops renal and hepatic pathology similar to human CHF/ARPKD (Katsuyama et al. 2000, Ward et al. 2002, Masyuk et al. 2004). We found increased levels of Cyclin D1 and PCNA expression in the CWECs, consistent with increased levels of cell proliferation. In addition to CWECs, Cyclin D1 and PCNA-positive cells were increased in the periportal area of PCK rat livers, suggesting that other secreted factors, possibly CTGF, promote the proliferation of hepatocytes or other interstitial cells. The mechanisms of hepatocyte proliferation and their relation to cyst enlargement are unknown. Previous studies indicated that extensive sheer stress in the liver may induce proliferative changes (Schrader et al. 2011) and it is possible that mechanical stress induced by enlarging cysts may stimulate similar changes in hepatocytes. Interestingly, a precedent for YAP/TAZ as mechanosensors capable of detecting and responding to the extracellular environment has already been established, suggesting that cystogenesis and cyst growth may regulate the Hippo signaling pathway in CHF/ARPKD (Low et al. 2014). For example, interactions between primary cilia, polycystin (defective in ADPKD), and YAP/TAZ likely occur and function as a mechanosensing system in response to alterations in extracellular matrix stiffness (Xiao et al. 2015). Therefore, it is possible that fibrocystin deficiency in CHF/ARPKD leads to YAP/TAZ activation by a mechanism involving defective primary cilia.

Our data revealed that CWECs have YAP activation in both PCK rats and in CHF/ARPKD patient livers. CWECs in rat and human livers show YAP nuclear localization and increased expression of the YAP target gene *Ctgf*. The increase in *Ctgf* was particularly interesting because of its involvement in ECM synthesis and fibrosis

(Gressner et al. 2008, Pi et al. 2015). *Ctgf* expression was also increased in pericystic cells suggesting roles for YAP and CTGF not only in CWEC proliferation but also in fibrosis associated with CHF/ARPKD. Interestingly, cross-talk between cholangiocytes and myofibroblasts have been suggested by Locatelli *et al* (Locatelli et al. 2016). By secreting chemokines (CXCL1, CXCL10, and CXCL12), cholangiocytes recruit macrophages which leads to further macrophage-mediated TGFβ1 activation, resulting in hepatic stellate cell activation and collagen accumulation (Locatelli et al. 2016).

A previous study suggests that VP is an effective inhibitor of the YAP-TEAD interaction required for YAP-mediated gene expression and exhibits few side effects (Liu-Chittenden et al. 2012). This novel VP function is independent of its current clinical application as a photosensitizer in vascular ablation procedures for treatment of some ocular diseases, including age-related macular degeneration (2001). VP-mediated blockade of the YAP-TEAD interaction does not require photoactivation as it does for its use in age-related macular degeneration yet inhibits YAP-induced liver overgrowth *in vivo and in vitro* (Liu-Chittenden et al. 2012). To test the feasibility of targeting YAP-induced CWEC proliferation as a selective means of inhibiting cyst growth in liver, we inhibited YAP-regulated target gene expression with VP, *in vitro.* We demonstrate here that VP effectively decreased CWEC proliferation in the presence and absence of forskolin. Our data indicate that the pro-proliferative effect of YAP is possibly functioned through cAMP-mediated pathway. The exact molecular mechanisms remain unknown and future work is needed to elucidate both the molecular mechanisms of YAP action and VP's efficacy in animal models of CHF/ARPKD.

In summary, our data suggest that YAP is an important contributing factor for the progression of CHF/ARPKD by promoting the proliferation of CWECs. Our study is consistent with what is currently known regarding YAP in renal cyst growth in ADPKD (Happe et al. 2011). These data have identified a new potential therapeutic target (YAP) and pharmacologic strategy (VP) to reduce disease progression in liver, and possibly the kidneys, of individuals with PKD.

CHAPTER V: PRELIMINARY CHARACTERIZATION OF THE HYALURONAN NETWORK IN CONGENITAL HEPATIC FIBROSIS IN AUTOSOMAL RECESSIVE POLYCYSTIC KIDNEY DISEASE

5.1 ABSTRACT

Autosomal recessive polycystic kidney disease (ARPKD) is a hereditary disease that primarily affects the hepatobiliary and renal systems. Congenital hepatic fibrosis (CHF) is characterized by hepatic cysts and pericystic fibrosis. Hyaluronan (HA) is a polysaccharide composed of repeating D-glucuronic acid and N-acetylglycosamine disaccharides of. HA is synthesized at the cell surface by three different hyaluronan synthases (HAS) 1, 2, and 3 and can interact with cell surface receptors such as CD44, LYVE-1, HARE, TLR2/4, and HA mediated motility receptor (HMMR) to induce a range of intracellular signals some of which promote cell proliferation, inflammation, and fibrosis. Increased serum HA level and hepatic HA content is observed in liver fibrosis caused by various conditions, such as non-alcoholic fatty liver disease, alcoholic liver diseases, hepatitis, primary biliary cirrhosis, and hepatocellular carcinoma. But the role of HA, HA degrading enzymes, HA binding proteins, and receptors (collectively the 'HA network') in CHF/ARPKD pathogenesis or progression is unknown. Based on the pathogenic roles of the HA network in other human diseases we hypothesized that HA contributes to pathogenesis of ARPKD. We observed increased HA accumulation in liver samples from polycystic kidney (PCK) rats (an animal model of ARPKD) and patients with polycystic liver disease (PLD) compared to controls. In isolated biliary tree samples, we found *Has1 and Cd44* expression were increased in PCK rats compared to Sprague Dawley (SD) rats. Further, transcripts for HA degrading enzymes hyaluronidase 1 (*Hyal1*), *Hyal2, Kiaa1199,* and transmembrane protein 2 (*Tmem2*) were decreased in PCK rat biliary trees compared to their expression in SD rats. Taken together, our data demonstrated that HA level in PCK rats is increased, and this could

be due to enhanced synthesis and possibly decreased degradation. Whether HA contributes to pathogenesis of CHF/ARPKD remains to be studied.

5.2 INTRODUCTION

Hyaluronan (HA) is a polysaccharide composed of repeating disaccharides of D-glucuronic acid and N-acetylglycosamine. It is found in the skin, joint synovium, and eye vitreous fluid. As one of the components of peri- and extra- cellular matrix, HA is synthesized on the cell surface by one of the three enzymes – HAS1, HAS2, and HAS3 (Spicer et al. 1998). HA is synthesized and released into the extracellular matrix as a high molecular weight (HMW, defined here as ≥500 kDa) polymer (Noble 2002, Ruppert et al. 2014). HMW-HA is prevalent in uninjured tissues, and it serves a variety of functions aimed at maintaining tissue homeostasis including anti-inflammatory and anti-angiogenic functions (Rooney et al. 1993, Noble 2002, Liu et al. 2008, Ruppert et al. 2014). The primary postnatal HA -synthesizing cell types are fibroblasts and endothelial cells, and in the liver, activated HSC are the primary source of HA (Vrochides et al. 1996, Spicer et al. 1998, Jiang et al. 2011, Xu et al. 2013, Neuman et al. 2016).

HA is degraded by enzymes known as hyaluronidases (Jiang et al. 2011). Hyaluronidase (HYAL) 1 and HYAL2 are the most abundant and functionally important in the body (Fraser et al. 1997, Csoka et al. 1999, Csoka et al. 2001). HYAL1 is expressed in high levels in the liver, kidney, heart and spleen, and located primarily in lysosomes within the cell (Csoka et al. 1999, McAtee et al. 2015). Activity of HYAL1 has a pH optimum in the range of 4.1-4.3 (Lokeshwar et al. 1999). HYAL2 is ubiquitously expressed (Csoka et al. 1999), and its activity at pH 3.8 is optimal (Lepperdinger et al. 1998). As more research into HA turnover is being done, new HA degrading enzymes

are being discovered including KIAA1199 and transmembrane protein 2 (TMEM2) (Yoshihara et al. 2013, Yamamoto et al. 2017). Importantly, TMEM2 is likely the long sought after extracellular HAase as its pH optimum is 7 (Yamamoto et al. 2017). In addition to these specific HAases, reactive oxygen species (ROS) also depolymerize HA (Soltes et al. 2006). Previous studies suggest that ROS mediates HA degradation by increasing HYAL2 expression and also by directly interacting with HA (Parsons et al. 2002, Monzon et al. 2010).

HA interacts with cell surface receptors such as cluster of differentiation 44 (CD44), LYVE-1, HARE, TLR2/4, and HA mediated motility receptor (HMMR) to induce a range of intracellular signals. HA and HA-mediated signaling are implicated in wound repair and in many diseases. Patients with advanced liver disease have increased HA blood levels, which have a positive correlation to disease severity (Lee et al. 2010, Lee et al. 2013, Rostami et al. 2013). Based on these observations, HA is used as a serum biomarker of liver disease (Orasan et al. 2016). Increased serum and hepatic HA level is observed in liver fibrosis caused by various conditions, such as non-alcoholic fatty liver disease (Suzuki et al. 2005), alcoholic liver diseases (Stickel et al. 2003, Gudowska et al. 2016), hepatitis C (Guechot et al. 1995, Gudowska et al. 2016), primary biliary cirrhosis (Nyberg et al. 1988), and hepatocellular carcinoma (Li et al. 2016).

Autosomal recessive polycystic kidney disease (ARPKD) is a genetic disorder caused by various mutations in *PKHD1* (Ward et al. 2003). Along with renal manifestations, affected patients also have dilated bile ductules and biliary-derived cysts, with peribiliary fibrosis, termed as congenital hepatic fibrosis (CHF, (Lazaridis et

al. 2004)). Although the clinical manifestations of CHF/ARPKD are described, the mechanisms behind disease progression remains unknown. Recently, a study using bile duct ligated-rats to mimic cholestasis suggests that biliary epithelial cells are the source of CD44, and HA-CD44 interaction promotes biliary epithelium proliferation (He et al. 2008). So far, no studies have been performed to understand the role of HA in CHF/ARPKD. Our RNA-seq analysis demonstrates that *Cd44* was significantly upregulated in PCK rats compared to SD rats from PND 15 to PND 90 (see Chapter II). Therefore, we hypothesized that HA may play a role in pathogenesis of CHF/ARPKD, and it may regulate cyst growth through interacting with CD44. In our study, we investigated the role of HA in the progression of CHF/ARPKD using polycystic kidney (PCK) rats as our animal model. Our studies indicate that HA level is increased in CHF/ARPKD, and HA accumulation is possibly due to an imbalance between HA synthesis and degradation.

5.3 MATERIALS AND METHODS

Animals and Human Tissue Collection

Polycystic kidney (PCK, an orthologous model of human ARPKD) rats and normal Sprague-Dawley (SD) and were obtained from Charles River Laboratories (Kingston, NY). *Pkhd1*$^{LSL(-)/LSL(-)}$ mice (a mouse model of human ARPKD) were a kind gift from Dr. Christopher J. Ward (KUMC). Animal treatment was approved by and performed in accordance with the Institutional Animal Care and Use Committee (IACUC) at University of Kansas Medical Center (KUMC).

For all animals, liver, and plasma were collected for further analysis as previously described (Deshpande et al. 2016). Biliary trees from untreated SD and PCK rats were also collected for RNA isolation as described previously (Jiang et al. 2017).

Paraffin-embedded liver sections from patients with polycystic liver disease (PLD) were obtained from the KUMC's Liver Center Tissue Bank. Definition of PLD was made based on clinical diagnoses for each patient in the absence of genotype data. All studies were approved by the IRB at KUMC.

RNA isolation, cDNA synthesis and real-time PCR

Total RNA was isolated from and reverse transcribed into complementary DNA (cDNA) as described before (Deshpande et al. 2016). SYBR green (Universal Super Mix, BioRad, Hercules, CA) was used for real-time PCR. Results were calculated using $2^{-\Delta\Delta Ct}$ method. The data were expressed as fold change over controls. 18S was used as the housekeeping gene and did not differ between genotypes. Primers utilized in this study are found in Table 5.3.1.

Hyaluronan Binding Protein (HABP) Staining

Formalin-fixed tissue was cut into 5.0 μM sections before use. Tissue was deparaffinized in Safe Clear II and rehydrated in a series of graded ethanols and PBS. Endogenous avidin and biotin was blocked (Avidin/Biotin Blocking kit, Vector) for one hour. Sections were incubated with normal goat serum at a concentration of 1:67 in PBS for 20 minutes followed by an hour incubation with 1mg/mL hyaluronidase (Sigma) in 0.9% normal saline for negative controls or 0.9% normal saline. After a brief rinse in

PBS, biotinylated-HABP (Calbiochem) at 1:100 in diluted normal goat serum (at a concentration of 1:67 in PBS) was applied at room temperature for one hour. To amplify the signal, an Avidin/Biotin complex applied for 30 minutes. A second amplification step using Tyramide Signal Amplification Plus Fluorescein Evaluation Kit (PerkinElmer Life Science, Boston, MA) diluted 1:400 was followed by nuclear staining using DAPI. Three to five non-overlapping 100X images were taken for each section using an Olympus BX51 microscope with an Olympus BH2RFLT3 burner and Olympus DP71 camera operated by DP Controller software (Olympus, Waltham, MA). Each image was taken using the same exposure and ImageJ was used to quantify the area and intensity of positive staining above a threshold that remained constant for all images.

Sirius Red Staining

Sirius red staining on liver tissues was performed as previously described (McCracken et al. 2016). All images were taken at 100X magnification. Five non-overlapping images were acquired per liver section. One liver section per mouse/rat in each experimental group was photographed. ImageJ was used to quantify the area of positive staining and intensity.

Statistics

All data are represented as mean ± standard error of mean. Student's t-test or one-way ANOVA was used to determine statistical differences. Post-hoc pairwise comparisons with multiple testing adjustments were completed using Tukey's method. The comparisons having p-value of less than 0.05 were considered statistically significant.

5.4 RESULTS

Hyaluronan production is increased in PKD.

We first evaluated HA level by using HA binding protein (HABP) staining on liver tissues. As HA is non-immunogenic, we utilized biotinylated HABP that can specifically bind to HA and be detected using fluorophore. Using this method, we detected an increased HA level in both human PLD patients and in PCK rats compared to their respective control (Figure 5.4.1A). To determine which cell population was the major source of HA, we isolated total RNA from whole liver, hepatic biliary tree, hepatocytes (HC), and nonparenchymal cells (NPC). The purity of isolated biliary trees was determined by real-time PCR on *Ck7* (a cholangiocyte marker). As illustrated in Figure 5.4.1B, *Ck7* mRNA expressed by PCK rat biliary trees was significantly higher than other cell populations from PCK and SD rats. *Has1* and *CD44* mRNA expression by PCK rat biliary trees were also significantly higher than other populations (Figure 5.4.1C-D). *Has2* and *Has3* mRNAs were not significantly higher in PCK rat compared to that in SD biliary trees (data not shown).

To investigate how HA level changes as the disease develops, we further evaluated HA level by HABP staining using liver sections from SD and PCK rats. We selected various time points from PND 10 to PND 90 (Figure 5.4.2). Our data show that HA was detected at PND 10 and PND 20 in both SD and PCK rats. At PND 30 and PND 90, HA level appeared to decrease in both genotypes but remained higher in PCK rats (Figure 5.4.2).

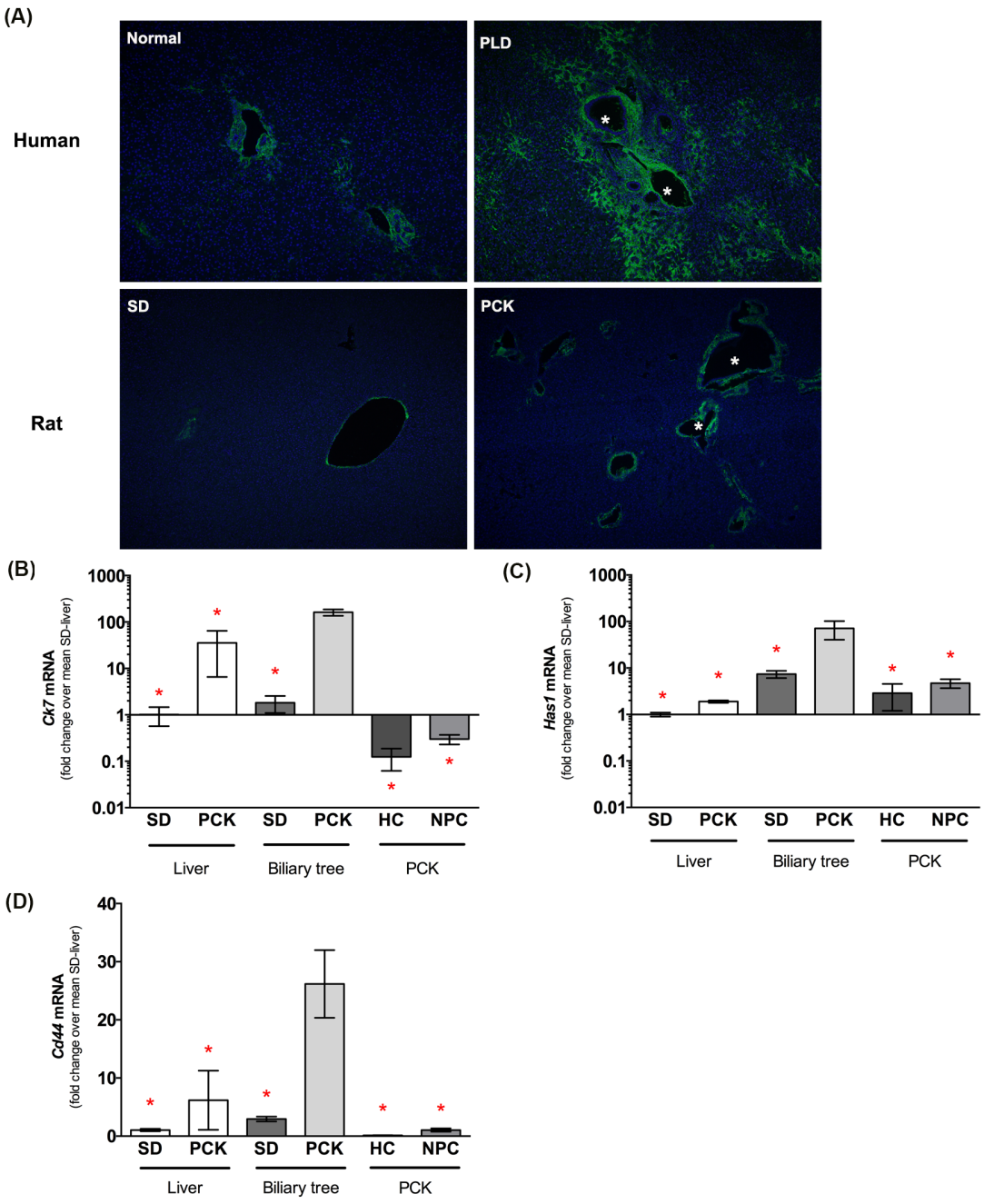

Figure 5.4.1. Hyaluronan production is increased in polycystic liver disease (PLD). (A) Representative images of biotin-conjugated hyaluronan (HA) binding protein (HABP) staining on liver sections from human (a normal and a PLD patient) and rats (a Sprague-Dawley rat and a PCK rat). The green signal is HABP and DAPI (blue) was used to visualize nuclei. (B-D) Real-time PCR was used to quantify *Ck7*, *Has1*, and *Cd44* transcripts in whole liver, biliary tree, hepatocytes (HC), and nonparenchymal cells (NPC) from SD or PCK rats. * represents $p<0.05$ comparing each group to PCK biliary trees. N = 4.

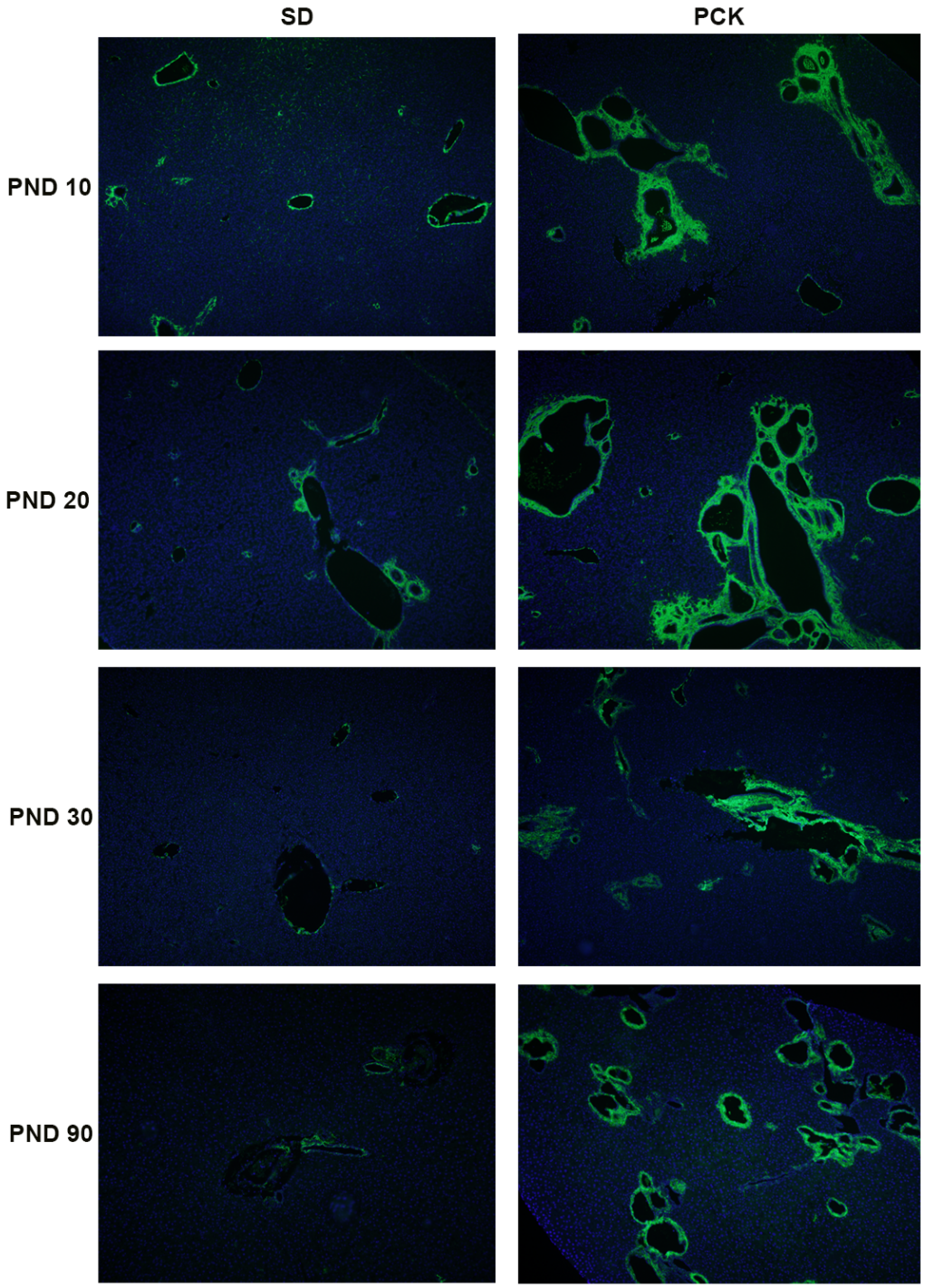

Figure 5.4.2. Hepatic HA accumulation in SD and PCK rats. Representative images of HABP staining used to localize hepatic HA accumulation in SD and PCK rats at PND 10, 20, 30, and 90. The green signal is HABP and DAPI (blue) was used to visualize nuclei**.**

Hyaluronidase expression is decreased in PCK rats.

Increased HA accumulation in livers from PLD patients and PCK rats could be due to increased HA synthesis, reduced degradation, or both. Therefore, we next measured expression of 4 hyaluronidases in isolated biliary trees (which contain biliary epithelium, and associated liver non-parenchymal cells including myofibroblasts). Our data showed that *Hyal1* and *Hyal2* expression were significantly suppressed in biliary tree samples from PCK rats compared to their levels in SD rats (Figure 5.4.3A-B). *Tmem2*, a newly identified cell surface hyaluronidase (Yamamoto et al. 2017), was also significantly lower in PCK rats (Figure 5.4.3C). *Kiaa1199* transcripts trended lower in PCK rats yet did not reach significance (Figure 5.4.3D). Our data suggest that HA degradation may be reduced in PCK rats, which could contribute to hepatic HA accumulation in CHF/ARPKD.

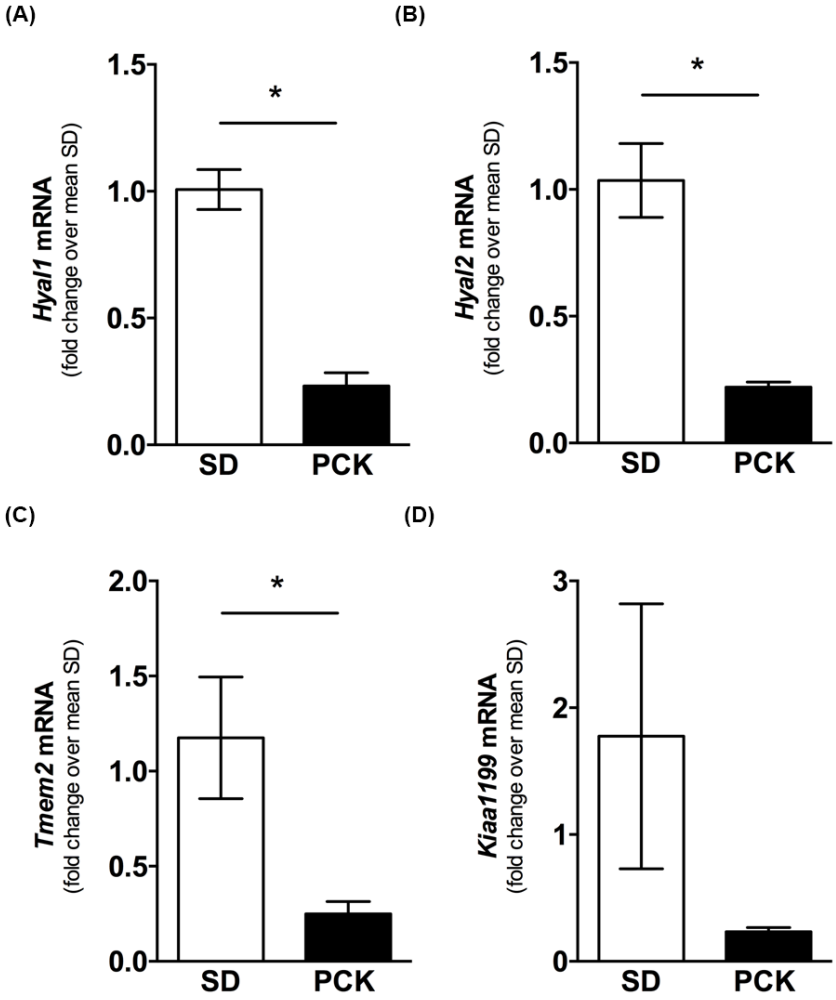

Figure 5.4.3. Hyaluronidase transcripts in biliary trees from SD and PCK rats. (A). *Hyal1*, (B). *Hyal2*, (C). *Tmem2,* and (D*) Kiaa1199* transcripts in both genotypes. * represents $p<0.05$ when comparing PCK to SD. N = 4 per genotype.

5.5 DISCUSSION

HA is a major component of ECM in liver fibrosis, and patients with advanced liver disease have increased HA blood levels, which have a positive correlation to disease severity (Lee et al. 2010, Lee et al. 2013, Rostami et al. 2013). Serum HA level is increased in various conditions with liver fibrosis, such as non-alcoholic fatty liver disease (Suzuki et al. 2005), alcoholic liver diseases (Stickel et al. 2003, Gudowska et al. 2016), hepatitis C (Guechot et al. 1995, Gudowska et al. 2016), primary biliary cirrhosis (Nyberg et al. 1988), and hepatocellular carcinoma (Li et al. 2016) and therefore, HA is used as a biomarker indicative of liver disease severity. So far, no research has examined if serum or hepatic HA increases in CHF/ARPKD. Moreover, no studies have examined if HA plays a pathogenic or protective role in CHF/ARPKD or other liver diseases. In our study, we showed that HA accumulation was increased in liver samples from PCK rats and PLD patients. Transcript levels of HA degrading enzymes was reduced in PCK rat biliary trees compared to the SD control.

Considering what we found in PCK rats and human PLD patients and what is known about HA in liver diseases, we hypothesize that HA contributes to the pathogenesis of CHF/ARPKD. As HA is synthesized by one of three enzymes (HAS1, 2, or 3), our first focus was to investigate if HA synthase expression was increased in PCK rats. Our data showed that *Has1* expression was increased greatly in biliary trees from PCK rats compared to SD rats. *Has2* and *Has3* expression level were trending to increase in PCK rats (data now shown), but the increase in *Has2* and *Has3* expression was not significantly different from SD rats. These data suggest that increased

expression of *Has1* may contribute to increased synthesis of HA and accumulation in CHF/ARPKD. Our study is the first to suggest there is an association between HA levels and CHF/ARPKD.

CD44 is a HA receptor whose biological function in inflammation and tumor cells have been investigated comprehensively (Aruffo et al. 1990, Teder et al. 2002, Misra et al. 2015). CD44 has many isoforms. These are created through alternative splicing of the mRNA and differential glycosylation of the protein. CD44 is responsible for pro-inflammatory activities, including cell–cell and cell–matrix interactions (Naor et al. 1997, Naor et al. 2002, Ponta et al. 2003, Misra et al. 2011). HA-CD44 interaction can activate receptor tyrosine kinases (RTKs), and further increased cell survival in several cancer cell lines. (Misra et al. 2006). HA-CD44 is also proposed to be crucial in regulating lung fibrosis. The ability of activated myofibroblasts to invade basal membrane is partially regulated through HA-CD44 interactions and upregulation of HAS1 in the context of increased expression of MMPs and inhibitors of MMPs (Li et al. 2011). Similarly, Midgley *et al*. showed that HAS2-dependent production of HA facilitates transforming growth factor-β (TGF-β)-dependent fibroblast differentiation through promoting CD44 interaction with EGFR within membrane-bound lipid rafts. Upon interaction, MAPK/ERK and CaMKII are activated, leading to fibroblast differentiation (Midgley et al. 2013).

CD44 is also implicated in PKD. Recent data suggest that cAMP induces renal epithelial cell proliferation and promotes cyst growth by activating Ras-dependent PKA/B-Raf/MAPK pathways in CWECs from ARPKD patients (Yamaguchi et al. 2006). Interestingly, CD44 variants containing variable exon 6 (v6) have been shown to be

important for Ras/MAPK activation, and Ras activation might in turn stimulate CD44 splicing as a positive feedback loop (Cheng et al. 2006). In addition, an increased level of epidermal growth factor receptor (EGF) is found in renal cyst fluid, which is consistent with an overexpression of EGF receptor (EGFR) mRNA and protein in renal epithelia in cpk mice (Horikoshi et al. 1991). The administration of EGFR tyrosine kinase inhibitor does not protect PCK rats from developing renal cysts, possibly due to an increased level of cAMP after treatment (Torres et al. 2004). Therefore, we propose that CD44 is playing a role in cystogenesis and fibrogenesis through binding to HA in CHF/ARPKD. In our study, we observed an increased expression of *Cd44* in biliary trees from PCK rats compared to SD rats. Since CD44 deficient rats are not commercially available, we would like to determine if CD44 is upregulated in mouse models of ARPKD. If so, we plan to generate CD44 flox/flox mice to selectively knock out CD44 in the biliary epithelial cells in *Pkhd1* mutant mice to determine if the loss of CD44 alters the course of disease.

To inhibit HA production, one approach is to create *Has* deficient mice/rats. *Has2-/-* mice are embryonically lethal due to severe defects in cardiac development (Siiskonen et al. 2015). Considering the fact that *Has1* transcripts were greatly increased in PCK rats, it is plausible to hypothesize that *Has1* may contribute disease progression more than other Has enzymes. *HAS1* expression is transcriptionally regulated by TGF-β in synoviocytes (Oguchi et al. 2004, Stuhlmeier et al. 2004) and by the pro-inflammatory cytokine interleukin-1β (IL-1β) in fibroblasts (Yamada et al. 2004, Uchiyama et al. 2005, van Zeijl et al. 2010). Multiple studies suggest that Has1 is not essential for embryogenesis, and *Has1* deficient mice are viable and fertile (Kobayashi

et al. 2010). Has1 is known as a mediator of inflammation in multiple disease, such as atherosclerosis (Marzoll et al. 2009), rheumatoid arthritis (Tanimoto et al. 2001), and asthma (Cheng et al. 2011). Further, increased expression of *HAS1* is associated with many cancers, including ovarian cancer (Yabushita et al. 2004, Yamada et al. 2004), colon cancer (Yamada et al. 2004), and multiple myeloma (Adamia et al. 2005). In order to investigate the role of Has1 on CHF/ARPKD, further studies are needed to block Has1 function by using antibodies, shRNA, siRNA, or other inhibitors s or by creating *Has1*$^{-/-}$ CHF/ARPKD mice/rats.

In summary, these data indicate that HA level is increased in CHF/ARPKD, and this is accompanied by increased expression of *Has* enzymes and *Cd44* in isolated biliary trees, and decreased expression of HA degrading enzymes. This suggests that increased HA synthesis in the absence of degradation may be responsible for HA accumulation in PCK rats. Future work will test the direct effects of the HA network in CHF/ARPKD pathogenesis and progression.

CHAPTER VI: DISCUSSION, CONCLUSIONS, AND FUTURE DIRECTIONS.

6.1 DISCUSSION

Autosomal recessive polycystic kidney disease (ARPKD) is a pediatric, ciliary disorder. Approximately 30% affected infants die shortly after birth from respiratory insufficiency (Zerres et al. 1998). Congenital hepatic fibrosis (CHF), which accompanies ARPKD, is a cholangiopathy characterized by biliary ductal plate malformation, which leads to progressive hepatic cyst formation and portal fibrosis (Turkbey et al. 2009). Previous studies have proposed different mechanisms of cyst growth. Along with cyst formation, the mechanisms of cyst expansion are proposed to be the result of: (1) cholangiocyte hyperproliferation, (2) cell-matrix interactions, and (3) fluid secretion (Gradilone et al. 2010). In Chapter I, we proposed a 'pathogenic triumvirate' in CHF/ARPKD which includes three factors, cyst growth, fibrosis, and inflammation. Our study aims to identify new pathways and central mediators that contribute to the pathogenesis by regulating the three components, and develop pharmacological agents to target those mediators to manage disease progression. Using RNA-seq analysis accompanied by previous studies in cholangiopathies (such as cholestasis), we identified three potential regulators of CHF/ARPKD: mast cells, yes-associated protein (YAP), and hyaluronan (HA). In this dissertation, we tested our hypothesis that the 'Pathogenic Triumvirate' consisting of proliferation, inflammation, and fibrosis driven by interrelated signaling contributes to CHF/ARPKD pathogenesis of CHF/ARPKD.

6.1.1 The role of mast cell in CHF/ARPKD

Mast cells (MC) are innate immune cells that exhibit pro-inflammatory, pro-fibrotic (Overed-Sayer et al. 2013), and growth-promoting activities in rodent models of

cholangiopathies (Hargrove et al. 2016, Hargrove et al. 2017). Although our RNA-seq analysis didn't detect any change in MC-related genes in PCK rats when compared to SD rats, a previous study shows that MCs surrounded by chymase, a MC granule component, were observed in the kidneys from end-stage ADPKD patients (McPherson et al. 2004). Moreover, MCs were also found at fibrotic portal tract area in liver samples from CHF/ARPKD (Ozaki et al. 2005). Our work using PCK rats demonstrated that MC infiltration increased in liver samples from PCK rats compared to Sprague Dawley (SD) rats. We provided evidence that MCs were also observed in liver samples from PKD patients. We proposed that tryptase was the major granule component that drives disease progression based on the observations that: (1) we detected increased expressions of tryptase and its receptor protease-activated receptor 2 (PAR2) in isolated biliary trees from PCK rats compared to SD rats and (2) serum tryptase level was significantly higher in PCK rats compared to SD rats. In humans, serum tryptase has become a widely used biomarker in systemic anaphylaxis (Caughey 2006), mastocytosis (Sperr et al. 2002), and chronic kidney disease (Sirvent et al. 2010). More importantly, tryptase exhibits proliferative action on fibroblasts upon binding to its receptor PAR2, which provides insights into the signaling pathway related to the interaction between tryptase and fibroblasts that may lead to new therapeutic approaches in human fibrotic disorders (Frungieri et al. 2002).

Contrary to our hypothesis, inhibiting MC degranulation with cromolyn sodium (CS, 50mg/kg) or ketotifen (1mg/kg) caused severe cyst growth in livers from PCK rats compared to rats given saline (control group). We excluded the off-target effects of CS by treating isolated CWECs with CS. Our data suggest that tryptase may function as a

protective mediator in hepatic cyst development in CHF/ARPKD. In future experiments, we can test our hypothesis by selectively inhibiting tryptase using pharmacological strategies. A previous study suggests that inhibiting tryptase activity with a widely accepted tryptase inhibitor APC366 inhibits hepatic stellate cell (HSC) proliferation and collagen synthesis in a rat model of hepatic fibrosis induced by bile duct ligation (BDL) (Lu et al. 2014). Therefore, if tryptase is protective in CHF/ARPKD, we speculate that treating PCK rats with APC366 would exacerbate disease progression.

There is substantial evidence showing that chymase has pro-collagenase activity, as it induces the activation of pro- matrix metalloproteinase (MMP2 and pro-MMP9, *in vivo* (Tchougounova et al. 2005). Chymase exhibits protective effects on renal tubulointerstitial fibrosis through decreasing inflammatory cell infiltrate and degrading interstitial deposits of fibronectin (Beghdadi et al. 2013). Consistently, the absence of MCs strikingly exacerbates hyperhomocysteinemia-induced adverse cardiac remodeling and diastolic dysfunction, indicating a potential protective role for MCs in cardiac injury (Joseph et al. 2005). On the other hand, chymase aggravates bleomycin-induced pulmonary fibrosis by digesting latent transforming growth factor-β1 (TGF-β1) to its active form. The chymase inhibitor SUN C8077 reduces collagen accumulation in the lung by blocking TGF-β1 activation and collagen synthesis in this model (Tomimori et al. 2003). It is possible that different MC granule components may have different roles in CHF/ARPKD, which depends on type of organ and the type of disease. The effects of MCs on disease progression may also depend on factors such as the kinetics of fibrosis development and the organ affected.

In trying to understand which MC granule component may be protective in CHF/ARPKD, one next step could be to treat isolated hepatic CWECs with individual MC granule components and measure cell proliferation change. Furthermore, it is likely that deficiency of *PKHD1* expression in CHF/ARPKD causes a differential response to MCs. It would be plausible to test the response to MC granule components in normal cholangiocytes from SD rats. In addition to observing an exacerbated effect on hepatic cyst growth after CS treatment, we noticed that renal cyst size was decreased by CS. Our study reveals that there might be an organ specific effects of MCs that may in part be determined by the disease stage and the pathological environment. To further investigate the effects of MCs on renal cyst growth, treating isolated renal cystic epithelial cells with isolated MC granules, and comparing the response to that of normal renal epithelial cells will provide evidence for our hypothesis. In particular, we would like to test the effect of renin, one of the MC granule components, on renal epithelial cell proliferation. Previous studies suggest that renin-angiotensin system (RAS) is upregulated in liver and kidney samples from PCK rats (Goto et al. 2010, Goto et al. 2010). In ADPKD, RAS activation contributes the progression of disease not only through promoting hypertension, but also by stimulating renal cyst growth (Torres et al. 2012). In order to achieve therapeutic effects on both liver and kidneys, it is imperative to target the specific MC granule component that has similar effects on both organs instead of inhibiting MC degranulation.

6.1.2 The role of YAP in CHF/ARPKD

Our work revealed that YAP was activated in liver samples from PCK rats and PKD patients, and that preventing YAP function with Verteporfin can inhibit hepatic cyst wall epithelial cell (CWEC) proliferation. Verteporfin is a YAP-TEAD interaction inhibitor, and it leads to cytoplasmic YAP sequestration through increasing the levels of 14-3-3σ, a YAP chaperon protein. By increasing 14-3-3σ level, Verteporfin prevents YAP translocation from nucleus to cytoplasm. (Wang et al. 2016). Interestingly, p53 is required for 14-3-3σ to effectively retain YAP in the cytoplasm and target it for degradation by the proteasome (Wang et al. 2016). *In vivo*, Verteporfin exhibited a significant inhibitory effect on tumor growth in a mouse model of ovarian cancer (Feng et al. 2016). Similarly, Verteporfin can suppress hepatomegaly/tumorigenesis resulting from YAP overexpression (Liu-Chittenden et al. 2012). In our study, we injected PCK rats and *Pkhd1*$^{LSL/LSL}$ mice with Verteporfin (90 mg/kg) three times per week for two weeks to investigate the *in vivo* efficacy of Verteporfin, but we did not observe any beneficial impact on hepatic cyst growth or fibrosis (data not shown). We also noticed that Verteporfin was not fully absorbed by animals suggesting solubility issues prevented the expected therapeutic effect. Verteporfin was initially dissolved in DMSO, and diluted to desired concentration. Thus, we propose to dissolve Verteporfin in a different solvent or a different percentage of DMSO to achieve better solubility and therapeutic efficacy.

In this study, we provided evidence that YAP is a critical mediator of CHF/ARPKD, and it drives disease progression by regulating downstream target gene expression (*CTGF, CCND1,*). In addition to pharmacologically inhibiting YAP activity,

we also genetically deleted YAP in CWECs from PCK rat livers using YAP-targeting shRNA. Although we only achieved 50% reduction in YAP, we demonstrated an inhibition of CWEC proliferation. Consistently, epigenetic regulation of YAP by microRNA-375 also suppresses YAP protein in primary hepatocellular carcinoma cell lines (Liu et al. 2010). Thus, miR-375 could be used with YAP shRNA in our animal models to increase YAP inhibition, and further attenuate CHF/ARPKD progression. Furthermore, we would like to investigate upstream regulators of YAP, such as large tumor suppressor homolog 1/2 (Lats1/2) and Mammalian sterile 20-like kinase 1/2 (Mst1/2), in PCK rats and in ARPKD patients. A previous study shows that Lats1/2 phosphorylates YAP and results in YAP inactivation via Ser-127 phosphorylation-mediated spatial regulation and Ser-381 phosphorylation-mediated temporal regulation (Zhao et al. 2010). More importantly, Lats1/2 kinases regulate the development of liver progenitor cell differentiation and maturation in hepatocytes and biliary epithelial cells through regulating activation of YAP/ TAZ (transcriptional coactivator with a PDZ-binding domain, (Yi et al. 2016). Thus, it is plausible to hypothesize that Lats1/2 activity is reduced in CHF/ARPKD. Deletion of Lats1/2 in CHF/ARPKD should abolish the phosphorylation effect of YAP/TAZ, leading to hyperactivation of YAP and detrimental effects on disease progression.

6.1.3 Is there a role for hyaluronan dysregulation in CHF/ARPKD?

CD44-HA interactions could drive each component of the ‘pathogenic triumvirate’. For example, in a rat model of cholestasis, biliary epithelial cells (BEC) are the major source of CD44, and HA treatment stimulates BEC proliferation (He et al.

2008). Therefore, we hypothesize that HA-CD44 interaction may stimulate CHF/ARPKD progression through regulating CWEC proliferation. Additionally, CD44-HA interactions can exacerbate inflammation. For example, expressed on the majority of immune cells, CD44 contributes a variety of inflammatory diseases including inflammatory bowel disease (Wittig et al. 1999), collagen- and proteoglycan-induced arthritis (Zeidler et al. 1995), and inflammatory colitis (Wittig et al. 2000). Therefore, it is reasonable to hypothesize that HA-CD44 interaction drives inflammation in CHF/ARPKD. Finally, HA-CD44 drives fibrosis. CD44 promotes lung fibrosis by interacting with HA and, as a consequence, upregulates HAS2, an HA synthase. HA-CD44 interaction and upregulation of HAS2 promote fibroblast invasion and lung fibrosis. Consistently, blocking CD44 with a neutralizing antibody reduces lung fibrosis in mice *in vivo* (Li et al. 2011).

Using our data regarding *Cd44* transcripts in livers from PCK rats and published literature as a solid foundation, we sought to further characterize on the HA network (HA and associated biosynthetic/degrading enzymes, receptors, and binding proteins) in CHF/ARPKD. We found that hepatic HA content was increased in PCK rats. Consistently, transcript analysis for hyaluronan synthases and hyaluronan degrading enzymes suggests that HA synthesis is increased and HA degradation is suppressed in PCK rats. Previous studies suggest that inhibiting HA synthesis can inhibit diseases. For example, a chow diet containing 5% 4-Methylumbelliferone (4-MU) effectively inhibits serum HA level at day 7 and prevents disease in a mouse model of experimental autoimmune encephalomyelitis (EAE) and autoimmune diabetes (Kuipers et al. 2016). More importantly, 4-MU treatment suppresses HSC activation and liver

fibrosis in a rat model of cholestasis (Sawada et al. 2016). *In vivo*, oral dosage of 4-MU is rapidly metabolized by conjugating to either a glucuronic acid to form 4-MU glucuronide (4-MUG) or a sulphate, forming 4-MU sulphate (4-MUS) within 24h (Kuipers et al. 2016). Interestingly, oral but not i.p. dosage of 4-MU inhibits HA synthesis and shows therapeutic effects in autoimmune diseases in mice, suggesting uptake of 4-MU through the gut contributes to its therapeutic efficacy (Kuipers et al. 2016). The direct connection between the gut and the liver provides strong rationale for the therapeutic efficacy of 4-MU in models of liver disease such as the study by Kuipers et al. (Kuipers et al. 2016). Together, these data suggest that HA-CD44 interaction can be pathogenic in the progression of CHF/ARPKD, and inhibition of HA synthesis with 4-MU may have beneficial effects.

In future studies, we plan to inhibit HA synthesis, and we also propose to interrupt HA-CD44 interaction by using a CD44-neutralizingantibody. Previously published work suggests that incubation of cultured fibroblasts with anti-CD44 monoclonal antibodies induces fibroblast apoptosis within fibrin matrices (Henke et al. 1996). We observed increased *Cd44* expression in isolated biliary trees from PCK rats compared to SD rats. Considering that biliary trees are composed of CWECs and attached myofibroblasts, we speculate that both of them may express *Cd44*. If so, blocking CD44 function may show beneficial effects by inducing fibroblast apoptosis, and inhibiting CWEC proliferation. By targeting two components of the ‘pathogenic triumvirate’, we expect that blocking CD44 activity can have beneficial effects on CHF/ARPKD. Alternatively, we can breed CD44-deficient mice with mouse models of CHF/ARPKD, and test how does this affect the pathogenesis of the disease.

6.1.4 RNA-seq analysis identified several potential mediators in CHF/ARPKD

Our RNA-seq analysis showed that members of STAT family were activated in PCK rats, such as STAT1, STAT3, STAT4, and STAT5B. STATs are proteins that can regulate gene transcription after activated by phosphorylation on tyrosine (Darnell et al. 1994). Recent work has revealed that polycystin 1 can regulate the transcription factor STAT3, and that STAT3 is aberrantly activated by tyrosine-phosphorylation in the kidneys of ADPKD patients and PKD mouse models (Talbot et al. 2011, Weimbs et al. 2013). The membrane anchored PC-1 activates STAT3 in JAK2-dependent manner, but the cleaved tail of PC-1 can only coactivate STAT3 in a mechanism requiring STAT phosphorylation by cytokines or growth factors (Talbot et al. 2011). Inhibition STAT3 activation with curcumin reduced proliferation index, cystic index, and kidney weight/body weight ratios in a mouse model of ADPKD. In addition, renal failure was significantly postponed in the study (Leonhard et al. 2011). In PCK rats, STAT3 was predicted to be activated at PND 30 and PND 90 by our RNA-seq analysis. Therefore, we propose to inhibit STAT3 or its upstream regulator JAK2 in PCK rats from PND 30, which also coincides with the rapid increase of hepatic cysts. In addition to curcumin, S3I-201 has been synthesized as a selective STAT3 inhibitor to treat tumors. It preferentially inhibits STAT3 DNA-binding activity and diminishes STAT3 tyrosine phosphorylation (Siddiquee et al. 2007). During skin tumor development, STAT3 functions as an anti-apoptotic molecule during tumor initiation, and it functions as a regulator of cell proliferation and survival during tumor promotion (Chan et al. 2004). SAR317461, a JAK2 specific inhibitor, inhibits STAT3 phosphorylation and has substantial activity against stem cells from glioblastoma multiforme (Mukthavaram et al. 2015). We speculate that inhibiting STAT3 activity in PCK

rats should exhibit therapeutic effects by decreasing hepato-/renal- CWEC proliferation and by increasing CWEC apoptosis.

Investigate the role of HNF4α in CHF/ARPKD

Hepatocyte-nuclear-factor 4-alpha (HNF4α) is a nuclear receptor that is associated with transcriptional regulation of hepatocyte genes involved in lipid metabolism, gluconeogenesis, bile acid synthesis, conjugation and transport (Hayhurst et al. 2001, Rhee et al. 2003, Inoue et al. 2004). HNF4α is important for morphological and functional differentiation of hepatocytes (Hang et al. 2017), and is the dominant regulator of the epithelial phenotype for normal liver architecture (Parviz et al. 2003). Our IPA analysis suggested that HNF4α was inhibited in PCK rats at PND 30 and PND 90. Inhibition of HNF4α is likely to cause impairment in hepatocyte development and function. Full body knockout of HNF4α is embryonic lethal, and the liver-specific albumin promoter-driven Cre recombinase knockout mice display severe hepatic metabolic disruption and death at 6–8 weeks of age (Chen et al. 1994, Hayhurst et al. 2001). The role of HNF4α has not been investigated in ARPKD so far. Interestingly, mice double mutants for Pkd1 and HNF4α had a worsened phenotype, suggesting that HNF4α may play a role in cystogenesis (Menezes et al. 2012). The role of HNF4α in ARPKD can be tested by activating HNF4α in PCK rats or mouse models of ARPKD either genetically or pharmacologically. *In vitro,* overexpressing HNF4α in isolated hepatic CWECs with doxycycline (Dox)-inducible HNF4α using lentiviral vectors should have inhibitory effect on CWEC proliferation.

Study the role of TGF-β1 in CHF/ARPKD

Transforming growth factor-β1 (TGF-β1) is a pro-fibrotic cytokine that exerts its effects by activating downstream SMAD signaling (Wrana et al. 1994). TGF-β1 plays pathogenic roles in fibrosis by three possible mechanisms: (1) TGF-β1 promotes production of ECM through SMAD3- dependent- and independent- mechanisms (Samarakoon et al. 2012); (2) TGF-β1 inhibits ECM degradation by inhibiting MMPs but inducing TIMPs (tissue inhibitor of metalloproteinase) (Kwak et al. 2006); (3) TGF-β1 plays a critical role in transdifferentiation toward myofibroblast from different cell types (Wu et al. 2013). SMAD7 is an inhibitory effector of TGF-β/SMAD signaling. Our RNA-seq analysis suggests that SMAD7 was inhibited in PCK rats at PND 30 and PND 90. We found that TGF-β level was significantly increased in biliary tree samples from PCK rats compared to SD rats (data not shown). Therefore, we propose that TGFβ/SMAD signaling can be a therapeutic target in CHF/ARPKD. TGF-β inhibitors have been tested in preclinical and clinical trials. In the future, studies using different TGF-β inhibitors could be tested in PCK rats.

6.2 CONCLUSIONS

The studies outlined in this dissertation provide insight into novel mechanisms in progression of CHF/ARPKD. So far, the treatment options for CHF/ARPKD are limited. Our work revealed that the disease is regulated by the 'pathogenic triumvirate' including cyst growth, fibrosis, and inflammation. Our studies identified several mediators, such as YAP, mast cells, and HA that may regulate the 'pathogenic triumvirate', some of which were surprising and worthy of further study. We also analyzed the disease at

transcriptional level by performing RNA-seq analysis. We uncovered several potential mediators such as STATs, HNF4α, and TGF-β/SMAD signaling that can be tested in future studies (Figure 6.2.1).

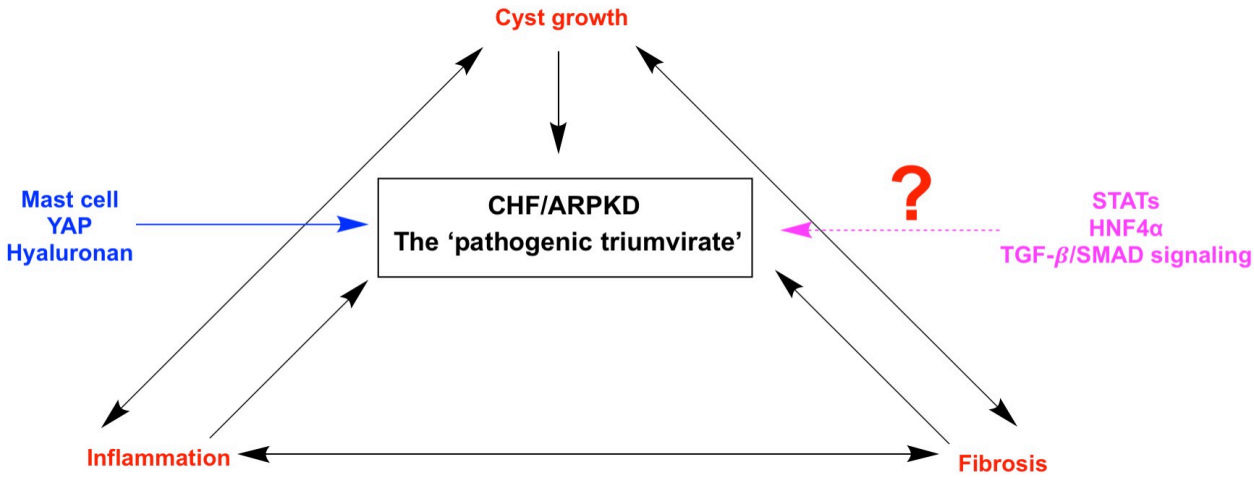

Figure 6.2.1. Current working model describing the role of the 'pathogenic triumvirate' and its mediators in CHF/ARPKD. We proposed that there is a 'pathogenic triumvirate' in CHF/ARPKD that is composed of cyst growth, inflammation, and fibrosis. In this dissertation, we described the role of mast cells, YAP, and hyaluronan in CHF/ARPKD pathogenesis. We also proposed several other mediators including STATs, HNF4α, and TGF-β/SMAD signaling for future studies.

REFERENCES

Adamia, S., T. Reiman, M. Crainie, M. J. Mant, A. R. Belch and L. M. Pilarski (2005). "Intronic splicing of hyaluronan synthase 1 (HAS1): a biologically relevant indicator of poor outcome in multiple myeloma." Blood **105**(12): 4836-4844.

Amin, K. (2012). "The role of mast cells in allergic inflammation." Respir Med **106**(1): 9-14.

Anders, S., P. T. Pyl and W. Huber (2015). "HTSeq-a Python framework to work with high-throughput sequencing data." Bioinformatics **31**(2): 166-169.

Armbrust, T., D. Batusic, B. Ringe and G. Ramadori (1997). "Mast cells distribution in human liver disease and experimental rat liver fibrosis. Indications for mast cell participation in development of liver fibrosis." Journal of Hepatology **26**(5): 1042-1054.

Aruffo, A., I. Stamenkovic, M. Melnick, C. Underhill and B. Seed (1990). "CD44 is the principal cell surface receptor for hyaluronate." Cell **61**: 1303-1313.

Atlas, S. A. (2007). "The renin-angiotensin aldosterone system: pathophysiological role and pharmacologic inhibition." J Manag Care Pharm **13**(8 Suppl B): 9-20.

Avner, E. D., F. E. Studnicki, M. C. Young, W. E. Sweeney, Jr., N. P. Piesco, D. Ellis and G. H. Fettermann (1987). "Congenital murine polycystic kidney disease. I. The ontogeny of tubular cyst formation." Pediatr Nephrol **1**(4): 587-596.

Avni, F. E., G. Guissard, M. Hall, F. Janssen, V. DeMaertelaer and F. Rypens (2002). "Hereditary polycystic in children: changing through childhood kidney diseases sonographic patterns." Pediatric Radiology **32**(3): 169-174.

Bachelet, I., F. Levi-Schaffer and Y. A. Mekori (2006). "Mast cells: not only in allergy." Immunol Allergy Clin North Am **26**(3): 407-425.

Bachem, M. G., U. Riess, R. Melchior, K. M. Sell and A. M. Gressner (1989). "Transforming growth factors (TGF alpha and TGF beta 1) stimulate chondroitin sulfate and hyaluronate synthesis in cultured rat liver fat storing cells." Febs Letters **257**(1): 134-137.

Bakeberg, J. L., R. Tammachote, J. R. Woollard, M. C. Hogan, H. F. Tuan, M. Li, J. M. van Deursen, Y. Wu, B. Q. Huang, V. E. Torres, P. C. Harris and C. J. Ward (2011). "Epitope-tagged Pkhd1 tracks the processing, secretion, and localization of fibrocystin." J Am Soc Nephrol **22**(12): 2266-2277.

Banales Jú, M., T. V. Masyuk, S. A. Gradilone, A. I. Masyuk, J. F. Medina and N. F. LaRusso (2009). "The cAMP Effectors Epac and PKA are Involved in the Hepatic Cystogenesis of an Animal Model of ARPKD." Hepatology **49**(1): 160-174.

Beghdadi, W., L. C. Madjene, J. Claver, G. Pejler, L. Beaudoin, A. Lehuen, E. Daugas and U. Blank (2013). "Mast cell chymase protects against renal fibrosis in murine unilateral ureteral obstruction." Kidney Int **84**(2): 317-326.

Bergmann, C. (2015). "ARPKD and early manifestations of ADPKD: the original polycystic kidney disease and phenocopies." Pediatric Nephrology **30**(1): 15-30.

Bergmann, C., J. Senderek, B. Sedlacek, I. Pegiazoglou, P. Puglia, T. Eggermann, S. Rudnik-Schoneborn, L. Furu, L. F. Onuchic, M. De Baca, G. G. Germino, L. Guay-Woodford, S. Somlo, M. Moser, R. Buttner and K. Zerres (2003). "Spectrum of mutations in the gene for autosomal recessive polycystic kidney disease (ARPKD/PKHD1)." J Am Soc Nephrol **14**(1): 76-89.

Bergmann, C., J. Senderek, E. Windelen, F. Kupper, I. Middeldorf, F. Schneider, C. Dornia, S. Rudnik-Schoneborn, M. Konrad, C. P. Schmitt, T. Seeman, T. J. Neuhaus, U. Vester, J. Kirfel, R. Buttner, K. Zerres and Apn (2005). "Clinical consequences of PKHD1 mutations in 164 patients with autosomal-recessive polycystic kidney disease (ARPKD)." Kidney Int **67**(3): 829-848.

Bernstein, J., M. Chandra, J. Creswell, E. Kahn, N. N. Malouf, M. McVicar, A. G. Weinberg and R. E. Wybel (1987). "Renal-hepatic-pancreatic dysplasia: a syndrome reconsidered." Am J Med Genet **26**(2): 391-403.

Blazer-Yost, B. L., J. Haydon, T. Eggleston-Gulyas, J. H. Chen, X. Wang, V. Gattone and V. E. Torres (2010). "Pioglitazone Attenuates Cystic Burden in the PCK Rodent Model of Polycystic Kidney Disease." PPAR Res **2010**: 274376.

Blyth, H. and B. G. Ockenden (1971). "Polycystic disease of kidney and liver presenting in childhood." Journal of Medical Genetics **8**(3): 257-284.

Blyth, H. and B. G. Ockenden (1971). "Polycystic Disease of Kidneys and Liver Presenting in Childhood." Journal of Medical Genetics **8**(3): 257-284.

Boesiger, J., M. Tsai, M. Maurer, M. Yamaguchi, L. F. Brown, K. P. Claffey, H. F. Dvorak and S. J. Galli (1998). "Mast cells can secrete vascular permeability factor/ vascular endothelial cell growth factor and exhibit enhanced release after immunoglobulin E-dependent upregulation of fc epsilon receptor I expression." J Exp Med **188**(6): 1135-1145.

Borish, L. and B. Z. Joseph (1992). "Inflammation and the allergic response." Med Clin North Am **76**(4): 765-787.

Borkham-Kamphorst, E., C. Schaffrath, E. Van de Leur, U. Haas, L. Tihaa, S. K. Meurer, Y. A. Nevzorova, C. Liedtke and R. Weiskirchen (2014). "The anti-fibrotic effects of CCN1/CYR61 in primary portal myofibroblasts are mediated through induction of reactive oxygen species resulting in cellular senescence, apoptosis and attenuated

TGF-β signaling." Biochimica et Biophysica Acta (BBA) - Molecular Cell Research **1843**(5): 902-914.

Burn, T. C., T. D. Connors, W. R. Dackowski, L. R. Petry, T. J. van Raay, J. M. Millholland, M. Venet, G. Miller, R. M. Hakim, G. M. Landes, K. W. Kilnger, F. Qian, L. F. Onuchic, T. Watnick, G. G. Germino and N. A. Doggett (1995). "Analysis of the genomic sequence for the autosomal dominant polycystic kidney disease (PKD1) gene predicts the presence of a leucine-rich repeatThe AMERICAN PKD1 Consortium (APKD1 Consortium)." Human Molecular Genetics **4**(4): 575-582.

Calvet, J. P. and J. J. Grantham (2001). "The genetics and physiology of polycystic kidney disease." Semin Nephrol **21**(2): 107-123.

Camargo, F. D., S. Gokhale, J. B. Johnnidis, D. Fu, G. W. Bell, R. Jaenisch and T. R. Brummelkamp (2007). "YAP1 increases organ size and expands undifferentiated progenitor cells." Curr Biol **17**(23): 2054-2060.

Cao, Z. and M. E. Cooper (2001). "Role of angiotensin II in tubulointerstitial injury." Semin Nephrol **21**(6): 554-562.

Caughey, G. H. (2006). "Tryptase genetics and anaphylaxis." J Allergy Clin Immunol **117**(6): 1411-1414.

Chan, K. S., S. Sano, K. Kiguchi, J. Anders, N. Komazawa, J. Takeda and J. DiGiovanni (2004). "Disruption of Stat3 reveals a critical role in both the initiation and the promotion stages of epithelial carcinogenesis." Journal of Clinical Investigation **114**(5): 720-728.

Chen, W. S., K. Manova, D. C. Weinstein, S. A. Duncan, A. S. Plump, V. R. Prezioso, R. F. Bachvarova and J. E. Darnell, Jr. (1994). "Disruption of the HNF-4 gene, expressed in visceral endoderm, leads to cell death in embryonic ectoderm and impaired gastrulation of mouse embryos." Genes Dev **8**(20): 2466-2477.

Cheng, C., M. B. Yaffe and P. A. Sharp (2006). "A positive feedback loop couples Ras activation and CD44 alternative splicing." Genes Dev **20**(13): 1715-1720.

Cheng, G., S. Swaidani, M. Sharma, M. E. Lauer, V. C. Hascall and M. A. Aronica (2011). "Hyaluronan deposition and correlation with inflammation in a murine ovalbumin model of asthma." Matrix Biol **30**(2): 126-134.

Cnossen, W. R., R. H. te Morsche, A. Hoischen, C. Gilissen, M. Chrispijn, H. Venselaar, S. Mehdi, C. Bergmann, J. A. Veltman and J. P. Drenth (2014). "Whole-exome sequencing reveals LRP5 mutations and canonical Wnt signaling associated with hepatic cystogenesis." Proc Natl Acad Sci U S A **111**(14): 5343-5348.

Csoka, A. B., G. I. Frost and R. Stern (2001). "The six hyaluronidase-like genes in the human and mouse genomes." Matrix Biol **20**(8): 499-508.

Csoka, A. B., S. W. Scherer and R. Stern (1999). "Expression analysis of six paralogous human hyaluronidase genes clustered on chromosomes 3p21 and 7q31." Genomics **60**(3): 356-361.

Darnell, J. E., Jr., I. M. Kerr and G. R. Stark (1994). "Jak-STAT pathways and transcriptional activation in response to IFNs and other extracellular signaling proteins." Science **264**(5164): 1415-1421.

Dell, K. M. (2011). "The spectrum of polycystic kidney disease in children." Adv Chronic Kidney Dis **18**(5): 339-347.

Deshpande, K. T., S. Liu, J. M. McCracken, L. Jiang, T. E. Gaw, L. N. Kaydo, Z. C. Richard, M. F. O'Neil and M. T. Pritchard (2016). "Moderate (2%, v/v) Ethanol Feeding Alters Hepatic Wound Healing after Acute Carbon Tetrachloride Exposure in Mice." Biomolecules **6**(1): 5.

Desmet, V. J. (1992). "What is congenital hepatic fibrosis?" Histopathology **20**(6): 465-477.

Di Cara, F., T. M. Maile, B. D. Parsons, A. Magico, S. Basu, N. Tapon and K. King-Jones (2015). "The Hippo pathway promotes cell survival in response to chemical stress." Cell Death Differ **22**(9): 1526-1539.

Dobin, A., C. A. Davis, F. Schlesinger, J. Drenkow, C. Zaleski, S. Jha, P. Batut, M. Chaisson and T. R. Gingeras (2013). "STAR: ultrafast universal RNA-seq aligner." Bioinformatics **29**(1): 15-21.

Dooley, S., J. Hamzavi, K. Breitkopf, E. Wiercinska, H. M. Said, J. Lorenzen, P. Ten Dijke and A. M. Gressner (2003). "Smad7 prevents activation of hepatic stellate cells and liver fibrosis in rats." Gastroenterology **125**(1): 178-191.

Dranoff, J. A. and R. G. Wells (2010). "Portal fibroblasts: Underappreciated mediators of biliary fibrosis." Hepatology **51**(4): 1438-1444.

Engstrom-Laurent, A., N. Feltelius, R. Hallgren and A. Wasteson (1985). "Raised serum hyaluronate levels in scleroderma: an effect of growth factor induced activation of connective tissue cells?" Ann Rheum Dis **44**(9): 614-620.

Everson, G. T., M. Emmett, W. R. Brown, P. Redmond and D. Thickman (1990). "Functional similarities of hepatic cystic and biliary epithelium: studies of fluid constituents and in vivo secretion in response to secretin." Hepatology **11**(4): 557-565.

Everson, G. T., S. M. Helmke and B. Doctor (2008). "Advances in management of polycystic liver disease." Expert Rev Gastroenterol Hepatol **2**(4): 563-576.

Everson, G. T., M. R. Taylor and R. B. Doctor (2004). "Polycystic disease of the liver." Hepatology **40**(4): 774-782.

Fabris, L., M. Cadamuro, R. Fiorotto, T. Roskams, C. Spirli, S. Melero, A. Sonzogni, R. E. Joplin, L. Okolicsanyi and M. Strazzabosco (2006). "Effects of angiogenic factor overexpression by human and rodent cholangiocytes in polycystic liver diseases." Hepatology **43**(5): 1001-1012.

Farrell, D. J., J. E. Hines, A. F. Walls, P. J. Kelly, M. K. Bennett and A. D. Burt (1995). "Intrahepatic mast cells in chronic liver diseases." Hepatology **22**(4 Pt 1): 1175-1181.

Feng, J., J. Gou, J. Jia, T. Yi, T. Cui and Z. Li (2016). "Verteporfin, a suppressor of YAP–TEAD complex, presents promising antitumor properties on ovarian cancer." OncoTargets and therapy **9**: 5371-5381.

Flores, J., R. Arnon, R. A. Morotti, L. Guay-Woodford, S. Emre and B. L. Shneider (2008). "Rapid evolution of congenital hepatic fibrosis after liver transplantation for acute liver failure: the potential role of extrahepatic factors." Liver Transpl **14**(5): 660-664.

Francis, H., S. Glaser, Y. Ueno, G. Lesage, L. Marucci, A. Benedetti, S. Taffetani, M. Marzioni, D. Alvaro, J. Venter, R. Reichenbach, G. Fava, J. L. Phinizy and G. Alpini (2004). "cAMP stimulates the secretory and proliferative capacity of the rat intrahepatic biliary epithelium through changes in the PKA/Src/MEK/ERK1/2 pathway." J Hepatol **41**(4): 528-537.

Francis, H. and C. J. Meininger (2010). "A review of mast cells and liver disease: What have we learned?" Dig Liver Dis **42**(8): 529-536.

Frangogiannis, N. G., L. H. Michael and M. L. Entman (2000). "Myofibroblasts in reperfused myocardial infarcts express the embryonic form of smooth muscle myosin heavy chain (SMemb)." Cardiovasc Res **48**(1): 89-100.

Fraser, J. R., T. C. Laurent and U. B. Laurent (1997). "Hyaluronan: its nature, distribution, functions and turnover." J Intern Med **242**(1): 27-33.

Friedman, S. L. (2003). "Liver fibrosis -- from bench to bedside." J Hepatol **38 Suppl 1**: S38-53.

Frungieri, M. B., S. Weidinger, V. Meineke, F. M. Köhn and A. Mayerhofer (2002). "Proliferative action of mast-cell tryptase is mediated by PAR2, COX2, prostaglandins, and PPARγ: Possible relevance to human fibrotic disorders." Proceedings of the National Academy of Sciences **99**(23): 15072.

Gabele, E., D. A. Brenner and R. A. Rippe (2003). "Liver fibrosis: signals leading to the amplification of the fibrogenic hepatic stellate cell." Front Biosci **8**: d69-77.

Gallagher, A. R., E. L. Esquivel, T. S. Briere, X. Tian, M. Mitobe, L. F. Menezes, G. S. Markowitz, D. Jain, L. F. Onuchic and S. Somlo (2008). "Biliary and pancreatic

dysgenesis in mice harboring a mutation in Pkhd1." American Journal of Pathology **172**(2): 417-429.

Gattone, V. H., 2nd, J. P. Calvet, B. D. Cowley, Jr., A. P. Evan, T. S. Shaver, K. Helmstadter and J. J. Grantham (1988). "Autosomal recessive polycystic kidney disease in a murine model. A gross and microscopic description." Lab Invest **59**(2): 231-238.

Gattone, V. H., 2nd, X. Wang, P. C. Harris and V. E. Torres (2003). "Inhibition of renal cystic disease development and progression by a vasopressin V2 receptor antagonist." Nat Med **9**(10): 1323-1326.

Gore-Hyer, E., D. Shegogue, M. Markiewicz, S. Lo, D. Hazen-Martin, E. L. Greene, G. Grotendorst and M. Trojanowska (2002). "TGF-beta and CTGF have overlapping and distinct fibrogenic effects on human renal cells." Am J Physiol Renal Physiol **283**(4): F707-716.

Goto, M., N. Hoxha, R. Osman and K. M. Dell (2010). "The renin-angiotensin system and hypertension in autosomal recessive polycystic kidney disease." Pediatr Nephrol **25**(12): 2449-2457.

Goto, M., N. Hoxha, R. Osman, J. Wen, R. G. Wells and K. M. Dell (2010). "Renin-angiotensin system activation in congenital hepatic fibrosis in the PCK rat model of

autosomal recessive polycystic kidney disease." J Pediatr Gastroenterol Nutr **50**(6): 639-644.

Gradilone, S. A., S. Habringer, T. V. Masyuk, B. N. Howard, A. I. Masyuk and N. F. Larusso (2014). "HDAC6 is overexpressed in cystic cholangiocytes and its inhibition reduces cystogenesis." Am J Pathol **184**(3): 600-608.

Gradilone, S. A., T. V. Masyuk, B. Q. Huang, J. M. Banales, G. L. Lehmann, B. N. Radtke, A. Stroope, A. I. Masyuk, P. L. Splinter and N. F. LaRusso (2010). "Activation of Trpv4 reduces the hyperproliferative phenotype of cystic cholangiocytes from an animal model of ARPKD." Gastroenterology **139**(1): 304-314.e302.

Graham, P. C. and G. B. Lindop (1988). "The anatomy of the renin-secreting cell in adult polycystic kidney disease." Kidney Int **33**(6): 1084-1090.

Gressner, O. A. and A. M. Gressner (2008). "Connective tissue growth factor: a fibrogenic master switch in fibrotic liver diseases." Liver Int **28**(8): 1065-1079.

Grotendorst, G. R., H. Rahmanie and M. R. Duncan (2004). "Combinatorial signaling pathways determine fibroblast proliferation and myofibroblast differentiation." FASEB J **18**(3): 469-479.

Group, V. I. P. T. S. (2001). "Verteporfin therapy of subfoveal choroidal neovascularization in age-related macular degeneration: two-year results of a randomized clinical trial including lesions with occult with no classic choroidal neovascularization--verteporfin in photodynamic therapy report 2." Am J Ophthalmol **131**(5): 541-560.

Guay-Woodford, L. M. (2014). "Autosomal recessive polycystic kidney disease: the prototype of the hepato-renal fibrocystic diseases." J Pediatr Genet **3**(2): 89-101.

Guay-Woodford, L. M. and R. A. Desmond (2003). "Autosomal recessive polycystic kidney disease: The clinical experience in North America." Pediatrics **111**(5): 1072-1080.

Gudowska, M., E. Gruszewska, A. Panasiuk, B. Cylwik, R. Flisiak, M. Swiderska, M. Szmitkowski and L. Chrostek (2016). "Hyaluronic acid concentration in liver diseases." Clin Exp Med **16**(4): 523-528.

Guechot, J., A. Loria, L. Serfaty, P. Giral, J. Giboudeau and R. Poupon (1995). "Serum Hyaluronan as a Marker of Liver Fibrosis in Chronic Viral Hepatitis-C - Effect of Alpha-Interferon Therapy." Journal of Hepatology **22**(1): 22-26.

Gunay-Aygun, M., E. D. Avner, R. L. Bacallao, P. L. Choyke, J. T. Flynn, G. G. Germino, L. Guay-Woodford, P. Harris, T. Heller, J. Ingelfinger, F. Kaskel, R. Kleta, N.

F. LaRusso, P. Mohan, G. J. Pazour, B. L. Shneider, V. E. Torres, P. Wilson, C. Zak, J. Zhou and W. A. Gahl (2006). "Autosomal recessive polycystic kidney disease and congenital hepatic fibrosis: summary statement of a first National Institutes of Health/Office of Rare Diseases conference." J Pediatr **149**(2): 159-164.

Gunay-Aygun, M., E. Font-Montgomery, L. Lukose, M. Tuchman Gerstein, K. Piwnica-Worms, P. Choyke, K. T. Daryanani, B. Turkbey, R. Fischer, I. Bernardini, M. Sincan, X. Zhao, N. G. Sandler, A. Roque, D. C. Douek, J. Graf, M. Huizing, J. C. Bryant, P. Mohan, W. A. Gahl and T. Heller (2013). "Characteristics of congenital hepatic fibrosis in a large cohort of patients with autosomal recessive polycystic kidney disease." Gastroenterology **144**(1): 112-121.

Gunay-Aygun, M., E. Font-Montgomery, L. Lukose, M. Tuchman, J. Graf, J. C. Bryant, R. Kleta, A. Garcia, H. Edwards, K. Piwnica-Worms, D. Adams, I. Bernardini, R. E. Fischer, D. Krasnewich, N. Oden, A. Ling, Z. Quezado, C. Zak, K. T. Daryanani, B. Turkbey, P. Choyke, L. M. Guay-Woodford and W. A. Gahl (2010). "Correlation of kidney function, volume and imaging findings, and PKHD1 mutations in 73 patients with autosomal recessive polycystic kidney disease." Clin J Am Soc Nephrol **5**(6): 972-984.

Gurda, G. T., Q. Zhu, H. Bai, C. A. Devadason, D. Pan, K. B. Schwarz and R. A. Anders (2014). "The utility of Yes-associated protein (YAP) expression in the diagnosis of persistent neonatal cholestatic liver disease." Hum Pathol **45**(5): 1057-1064.

Hamzavi, J., S. Ehnert, P. Godoy, L. Ciuclan, H. Weng, P. R. Mertens, R. Heuchel and S. Dooley (2008). "Disruption of the Smad7 gene enhances CCI4-dependent liver damage and fibrogenesis in mice." J Cell Mol Med **12**(5B): 2130-2144.

Hang, H. L., X. Y. Liu, H. T. Wang, N. Xu, J. M. Bian, J. J. Zhang, L. Xia and Q. Xia (2017). "Hepatocyte nuclear factor 4A improves hepatic differentiation of immortalized adult human hepatocytes and improves liver function and survival." Exp Cell Res **360**(2): 81-93.

Hao, Y., A. Chun, K. Cheung, B. Rashidi and X. Yang (2008). "Tumor suppressor LATS1 is a negative regulator of oncogene YAP." J Biol Chem **283**(9): 5496-5509.

Happe, H., A. M. van der Wal, W. N. Leonhard, S. J. Kunnen, M. H. Breuning, E. de Heer and D. J. Peters (2011). "Altered Hippo signalling in polycystic kidney disease." J Pathol **224**(1): 133-142.

Hargrove, L., A. Graf-Eaton, L. Kennedy, J. Demieville, J. Owens, K. Hodges, B. Ladd and H. Francis (2016). "Isolation and characterization of hepatic mast cells from cholestatic rats." Lab Invest **96**(11): 1198-1210.

Hargrove, L., L. Kennedy, J. Demieville, H. Jones, F. Meng, S. DeMorrow, W. Karstens, T. Madeka, J. Greene, Jr. and H. Francis (2017). "Bile duct ligation-induced biliary hyperplasia, hepatic injury, and fibrosis are reduced in mast cell-deficient Kit(W-sh) mice." Hepatology **65**(6): 1991-2004.

Harris, P. C. and S. Rossetti (2004). "Molecular genetics of autosomal recessive polycystic kidney disease." Mol Genet Metab **81**(2): 75-85.

Harris, P. C. and V. E. Torres (2014). "Genetic mechanisms and signaling pathways in autosomal dominant polycystic kidney disease." J Clin Invest **124**(6): 2315-2324.

Hayhurst, G. P., Y. H. Lee, G. Lambert, J. M. Ward and F. J. Gonzalez (2001). "Hepatocyte nuclear factor 4alpha (nuclear receptor 2A1) is essential for maintenance of hepatic gene expression and lipid homeostasis." Mol Cell Biol **21**(4): 1393-1403.

He, Y., G. D. Wu, T. Sadahiro, S. I. Noh, H. Wang, D. Talavera, H. Wang, J. M. Vierling and A. S. Klein (2008). "Interaction of CD44 and hyaluronic acid enhances biliary epithelial proliferation in cholestatic livers." Am J Physiol Gastrointest Liver Physiol **295**(2): G305-312.

Hei, Z. Q., X. L. Gan, G. J. Luo, S. R. Li and J. Cai (2007). "Pretreatment of cromolyn sodium prior to reperfusion attenuates early reperfusion injury after the small intestine ischemia in rats." World J Gastroenterol **13**(38): 5139-5146.

Henke, C., P. Bitterman, U. Roongta, D. Ingbar and V. Polunovsky (1996). "Induction of fibroblast apoptosis by anti-CD44 antibody: implications for the treatment of fibroproliferative lung disease." Am J Pathol **149**(5): 1639-1650.

Herzig, D. J. and E. J. Kusner (1975). "Effect of cromolyn sodium and deuterium oxide on anaphylactic histamine release from rat peritoneal mast cells in vitro." J Pharmacol Exp Ther **194**(2): 457-462.

Holditch, S. J., C. A. Schreiber, P. C. Harris, N. F. LaRusso, M. Ramirez-Alvarado, A. Cataliotti, V. E. Torres and Y. Ikeda (2017). "B-type natriuretic peptide overexpression ameliorates hepatorenal fibrocystic disease in a rat model of polycystic kidney disease." Kidney Int **92**(3): 657-668.

Holdsworth, S. R. and S. A. Summers (2008). "Role of mast cells in progressive renal diseases." J Am Soc Nephrol **19**(12): 2254-2261.

Horikoshi, S., S. Kubota, G. R. Martin, Y. Yamada and P. E. Klotman (1991). "Epidermal growth factor (EGF) expression in the congenital polycystic mouse kidney." Kidney Int **39**(1): 57-62.

Hou, X. Y., M. Mrug, B. K. Yoder, E. J. Lefkowitz, G. Kremmidiotis, P. D'Eustachio, D. R. Beier and L. M. Guay-Woodford (2002). "Cystin, a novel cilia-associated protein, is disrupted in the cpk mouse model of polycystic kidney disease." Journal of Clinical Investigation **109**(4): 533-540.

Huang, G. and D. R. Brigstock (2012). "Regulation of hepatic stellate cells by connective tissue growth factor." Front Biosci (Landmark Ed) **17**: 2495-2507.

Huangfu, D., A. Liu, A. S. Rakeman, N. S. Murcia, L. Niswander and K. V. Anderson (2003). "Hedgehog signalling in the mouse requires intraflagellar transport proteins." Nature **426**(6962): 83-87.

Igarashi, P. and S. Somlo (2002). "Genetics and pathogenesis of polycystic kidney disease." J Am Soc Nephrol **13**(9): 2384-2398.

Inoue, Y., A. M. Yu, J. Inoue and F. J. Gonzalez (2004). "Hepatocyte nuclear factor 4alpha is a central regulator of bile acid conjugation." J Biol Chem **279**(4): 2480-2489.

Ishii, M., M. Iwai, Y. Harada, T. Morikawa, T. Okanoue, T. Kishikawa, Y. Tsuchihashi, K. Hanai and N. Arizono (2005). "A role of mast cells for hepatic fibrosis in primary sclerosing cholangitis." Hepatol Res **31**(3): 127-131.

Jhandier, M. N., E. A. Kruglov, E. G. Lavoie, J. Sevigny and J. A. Dranoff (2005). "Portal fibroblasts regulate the proliferation of bile duct epithelia via expression of NTPDase2." J Biol Chem **280**(24): 22986-22992.

Jiang, D., J. Liang and P. W. Noble (2011). "Hyaluronan as an immune regulator in human diseases." Physiol Rev **91**(1): 221-264.

Jiang, L., P. P. Fang, J. L. Weemhoff, U. Apte and M. T. Pritchard (2016). "Evidence for a "pathogenic triumvirate" in congenital hepatic fibrosis in autosomal recessive polycystic kidney disease." Biomed Research International **2016**: 10.

Jiang, L., L. Sun, G. Edwards, M. Manley, Jr., D. P. Wallace, S. Septer, C. Manohar, M. T. Pritchard and U. Apte (2017). "Increased YAP Activation Is Associated With Hepatic Cyst Epithelial Cell Proliferation in ARPKD/CHF." Gene Expr **17**(4): 313-326.

Jones, H., L. Hargrove, L. Kennedy, F. Y. Meng, A. Graf-Eaton, J. Owens, G. Alpini, C. Johnson, F. Bernuzzi, J. Demieville, S. DeMorrow, P. Invernizzi and H. Francis (2016). "Inhibition of Mast Cell-Secreted Histamine Decreases Biliary Proliferation and Fibrosis in Primary Sclerosing Cholangitis Mdr2(-/-) Mice." Hepatology **64**(4): 1202-1216.

Joseph, J., R. H. Kennedy, S. Devi, J. Wang, L. Joseph and M. Hauer-Jensen (2005). "Protective role of mast cells in homocysteine-induced cardiac remodeling." Am J Physiol Heart Circ Physiol **288**(5): H2541-2545.

Kadosh, D. and K. Struhl (1997). "Repression by Ume6 involves recruitment of a complex containing Sin3 corepressor and Rpd3 histone deacetylase to target promoters." Cell **89**(3): 365-371.

Kaspareit-Rittinghausen, J., K. Rapp, F. Deerberg, A. Wcislo and C. Messow (1989). "Hereditary polycystic kidney disease associated with osteorenal syndrome in rats." Vet Pathol **26**(3): 195-201.

Katsuyama, M., T. Masuyama, I. Komura, T. Hibino and H. Takahashi (2000). "Characterization of a novel polycystic kidney rat model with accompanying polycystic liver." Exp Anim **49**(1): 51-55.

Kennedy, L. L., L. A. Hargrove, A. B. Graf, T. C. Francis, K. M. Hodges, Q. P. Nguyen, Y. Ueno, J. F. Greene, F. Meng, V. D. Huynh and H. L. Francis (2014). "Inhibition of mast cell-derived histamine secretion by cromolyn sodium treatment decreases biliary hyperplasia in cholestatic rodents." Lab Invest **94**(12): 1406-1418.

Kern, S., L. B. Zimmerhackl, F. Hildebrandt, B. Ermisch-Omran and M. Uhl (2000). "Appearance of autosomal recessive polycystic kidney disease in magnetic resonance imaging and RARE-MR-urography." Pediatric Radiology **30**(3): 156-160.

Kinet, J. P. (1999). "The high-affinity IgE receptor (Fc epsilon RI): from physiology to pathology." Annu Rev Immunol **17**: 931-972.

Kobayashi, N., S. Miyoshi, T. Mikami, H. Koyama, M. Kitazawa, M. Takeoka, K. Sano, J. Amano, Z. Isogai, S. Niida, K. Oguri, M. Okayama, J. A. McDonald, K. Kimata, S. Taniguchi and N. Itano (2010). "Hyaluronan deficiency in tumor stroma impairs macrophage trafficking and tumor neovascularization." Cancer Res **70**(18): 7073-7083.

Kondo, S., S. Kagami, H. Kido, F. Strutz, G. A. Muller and Y. Kuroda (2001). "Role of mast cell tryptase in renal interstitial fibrosis." J Am Soc Nephrol **12**(8): 1668-1676.

Kruger-Krasagakes, S., A. Moller, G. Kolde, U. Lippert, M. Weber and B. M. Henz (1996). "Production of interleukin-6 by human mast cells and basophilic cells." J Invest Dermatol **106**(1): 75-79.

Kruglov, E. A., R. A. Nathanson, T. Nguyen and J. A. Dranoff (2006). "Secretion of MCP-1/CCL2 by bile duct epithelia induces myofibroblastic transdifferentiation of portal fibroblasts." Am J Physiol Gastrointest Liver Physiol **290**(4): G765-771.

Kuipers, H. F., N. Nagy, S. M. Ruppert, V. G. Sunkari, P. L. Marshall, J. A. Gebe, H. D. Ishak, S. G. Keswani, J. Bollyky, A. R. Frymoyer, T. N. Wight, L. Steinman and P. L. Bollyky (2016). "The pharmacokinetics and dosing of oral 4-methylumbelliferone for inhibition of hyaluronan synthesis in mice." Clin Exp Immunol **185**(3): 372-381.

Kwak, H. J., M. J. Park, H. Cho, C. M. Park, S. I. Moon, H. C. Lee, I. C. Park, M. S. Kim, C. H. Rhee and S. I. Hong (2006). "Transforming growth factor-beta1 induces tissue inhibitor of metalloproteinase-1 expression via activation of extracellular signal-regulated kinase and Sp1 in human fibrosarcoma cells." Mol Cancer Res **4**(3): 209-220.

Lager, D. J., Q. Qian, R. J. Bengal, M. Ishibashi and V. E. Torres (2001). "The pck rat: A new model that resembles human autosomal dominant polycystic kidney and liver disease." Kidney Int **59**(1): 126-136.

Lazaridis, K. N. and N. F. LaRusso (2015). "The Cholangiopathies." Mayo Clin Proc.

Lazaridis, K. N., M. Strazzabosco and N. F. Larusso (2004). "The cholangiopathies: disorders of biliary epithelia." Gastroenterology **127**(5): 1565-1577.

Leclere, M., M. Desnoyers, G. Beauchamp and J. P. Lavoie (2006). "Comparison of four staining methods for detection of mast cells in equine bronchoalveolar lavage fluid." J Vet Intern Med **20**(2): 377-381.

Lee, C. H., B. Shah, E. K. Moioli and J. J. Mao (2015). "CTGF directs fibroblast differentiation from human mesenchymal stem/stromal cells and defines connective tissue healing in a rodent injury model." The Journal of Clinical Investigation **125**(10): 3992-3992.

Lee, C. K., A. R. Perez-Atayde, P. D. Mitchell, R. Raza, N. H. Afdhal and M. M. Jonas (2013). "Serum biomarkers and transient elastography as predictors of advanced liver fibrosis in a United States cohort: the Boston children's hospital experience." J Pediatr **163**(4): 1058-1064 e1052.

Lee, H. H., Y. S. Seo, S. H. Um, N. H. Won, H. Yoo, E. S. Jung, Y. D. Kwon, S. Park, B. Keum, Y. S. Kim, H. J. Yim, Y. T. Jeen, H. J. Chun, C. D. Kim and H. S. Ryu (2010). "Usefulness of non-invasive markers for predicting significant fibrosis in patients with chronic liver disease." J Korean Med Sci **25**(1): 67-74.

Lee, K. P., J. H. Lee, T. S. Kim, T. H. Kim, H. D. Park, J. S. Byun, M. C. Kim, W. I. Jeong, D. F. Calvisi, J. M. Kim and D. S. Lim (2010). "The Hippo-Salvador pathway restrains hepatic oval cell proliferation, liver size, and liver tumorigenesis." Proc Natl Acad Sci U S A **107**(18): 8248-8253.

Leonhard, W. N., A. van der Wal, Z. Novalic, S. J. Kunnen, R. T. Gansevoort, M. H. Breuning, E. de Heer and D. J. Peters (2011). "Curcumin inhibits cystogenesis by simultaneous interference of multiple signaling pathways: in vivo evidence from a Pkd1-deletion model." Am J Physiol Renal Physiol **300**(5): F1193-1202.

Lepperdinger, G., B. Strobl and G. Kreil (1998). "HYAL2, a human gene expressed in many cells, encodes a lysosomal hyaluronidase with a novel type of specificity." J Biol Chem **273**(35): 22466-22470.

Levesque, H., B. Delpech, X. Le Loet and P. Deshayes (1988). "Serum hyaluronate in rheumatoid arthritis: study by affino-immunoenzymatic assay." Br J Rheumatol **27**(6): 445-449.

Li, G., Q. Xie, Y. Shi, D. Li, M. Zhang, S. Jiang, H. Zhou, H. Lu and Y. Jin (2006). "Inhibition of connective tissue growth factor by siRNA prevents liver fibrosis in rats." J Gene Med **8**(7): 889-900.

Li, H., A. Wolfe, S. Septer, G. Edwards, X. Zhong, A. B. Abdulkarim, S. Ranganathan and U. Apte (2012). "Deregulation of Hippo kinase signalling in human hepatic malignancies." Liver Int **32**(1): 38-47.

Li, J. H., Y. C. Wang, C. D. Qin, R. R. Yao, R. Zhang, Y. Wang, X. Y. Xie, L. Zhang, Y. H. Wang and Z. G. Ren (2016). "Over expression of hyaluronan promotes progression of HCC via CD44-mediated pyruvate kinase M2 nuclear translocation." Am J Cancer Res **6**(2): 509-521.

Li, S. S., L. Z. Huang, Y. Y. Sun, Y. J. Bai, F. Yang, W. Z. Yu, F. T. Li, Q. Zhang, B. Wang, J. G. Geng and X. X. Li (2015). "Slit2 Promotes Angiogenic Activity Via the Robo1-VEGFR2-ERK1/2 Pathway in Both In Vivo and In Vitro Studies." Investigative Ophthalmology & Visual Science **56**(9): 5210-5217.

Li, X., B. S. Magenheimer, S. Xia, T. Johnson, D. P. Wallace, J. P. Calvet and R. Li (2008). "A tumor necrosis factor-alpha-mediated pathway promoting autosomal dominant polycystic kidney disease." Nat Med **14**(8): 863-868.

Li, Y., D. Jiang, J. Liang, E. B. Meltzer, A. Gray, R. Miura, L. Wogensen, Y. Yamaguchi and P. W. Noble (2011). "Severe lung fibrosis requires an invasive fibroblast phenotype regulated by hyaluronan and CD44." J Exp Med **208**(7): 1459-1471.

Li, Y., D. Jiang, J. Liang, E. B. Meltzer, A. Gray, R. Miura, L. Wogensen, Y. Yamaguchi and P. W. Noble (2011). "Severe lung fibrosis requires an invasive fibroblast phenotype regulated by hyaluronan and CD44." J Exp Med **208**(7): 1459-1471.

Li, Z., J. A. Dranoff, E. P. Chan, M. Uemura, J. Sevigny and R. G. Wells (2007). "Transforming growth factor-beta and substrate stiffness regulate portal fibroblast activation in culture." Hepatology **46**(4): 1246-1256.

Lipson, K. E., C. Wong, Y. Teng and S. Spong (2012). "CTGF is a central mediator of tissue remodeling and fibrosis and its inhibition can reverse the process of fibrosis." Fibrogenesis Tissue Repair **5**(Suppl 1): S24.

Liu, A. M., R. T. Poon and J. M. Luk (2010). "MicroRNA-375 targets Hippo-signaling effector YAP in liver cancer and inhibits tumor properties." Biochem Biophys Res Commun **394**(3): 623-627.

Liu, F., D. Lagares, K. M. Choi, L. Stopfer, A. Marinkovic, V. Vrbanac, C. K. Probst, S. E. Hiemer, T. H. Sisson, J. C. Horowitz, I. O. Rosas, L. E. Fredenburgh, C. Feghali-Bostwick, X. Varelas, A. M. Tager and D. J. Tschumperlin (2015). "Mechanosignaling through YAP and TAZ drives fibroblast activation and fibrosis." American Journal of Physiology-Lung Cellular and Molecular Physiology **308**(4): L344-L357.

Liu, Y. Y., C. H. Lee, R. Dedaj, H. Zhao, H. Mrabat, A. Sheidlin, O. Syrkina, P. M. Huang, H. G. Garg, C. A. Hales and D. A. Quinn (2008). "High-molecular-weight hyaluronan--a possible new treatment for sepsis-induced lung injury: a preclinical study in mechanically ventilated rats." Crit Care **12**(4): R102.

Liu-Chittenden, Y., B. Huang, J. S. Shim, Q. Chen, S. J. Lee, R. A. Anders, J. O. Liu and D. Pan (2012). "Genetic and pharmacological disruption of the TEAD-YAP complex suppresses the oncogenic activity of YAP." Genes Dev **26**(12): 1300-1305.

Locatelli, L., M. Cadamuro, C. Spirli, R. Fiorotto, S. Lecchi, C. M. Morell, Y. Popov, R. Scirpo, M. De Matteis, M. Amenduni, A. Pietrobattista, G. Torre, D. Schuppan, L. Fabris and M. Strazzabosco (2016). "Macrophage recruitment by fibrocystin-defective biliary epithelial cells promotes portal fibrosis in congenital hepatic fibrosis." Hepatology **63**(3): 965-982.

Lokeshwar, V. B., M. J. Young, G. Goudarzi, N. Iida, A. I. Yudin, G. N. Cherr and M. G. Selzer (1999). "Identification of bladder tumor-derived hyaluronidase: its similarity to HYAL1." Cancer Res **59**(17): 4464-4470.

Low, B. C., C. Q. Pan, G. V. Shivashankar, A. Bershadsky, M. Sudol and M. Sheetz (2014). "YAP/TAZ as mechanosensors and mechanotransducers in regulating organ size and tumor growth." Febs Letters **588**(16): 2663-2670.

Lu, J., B. A. Chen, S. L. Li and Q. Sun (2014). "Tryptase inhibitor APC 366 prevents hepatic fibrosis by inhibiting collagen synthesis induced by tryptase/protease-activated receptor 2 interactions in hepatic stellate cells." International Immunopharmacology **20**(2): 352-357.

Lu, L., Y. Li, S. M. Kim, W. Bossuyt, P. Liu, Q. Qiu, Y. D. Wang, G. Halder, M. J. Finegold, J. S. Lee and R. L. Johnson (2010). "Hippo signaling is a potent in vivo growth and tumor suppressor pathway in the mammalian liver." Proceedings of the National Academy of Sciences of the United States of America **107**(4): 1437-1442.

Marioni, J. C., C. E. Mason, S. M. Mane, M. Stephens and Y. Gilad (2008). "RNA-seq: an assessment of technical reproducibility and comparison with gene expression arrays." Genome Res **18**(9): 1509-1517.

Marra, F., R. DeFranco, C. Grappone, S. Milani, S. Pastacaldi, M. Pinzani, R. G. Romanelli, G. Laffi and P. Gentilini (1998). "Increased expression of monocyte chemotactic protein-1 during active hepatic fibrogenesis: correlation with monocyte infiltration." Am J Pathol **152**(2): 423-430.

Marzoll, A., N. Nagy, L. Wordehoff, G. Dai, S. Fries, V. Lindner, T. Grosser and J. W. Fischer (2009). "Cyclooxygenase inhibitors repress vascular hyaluronan-synthesis in murine atherosclerosis and neointimal thickening." J Cell Mol Med **13**(9B): 3713-3719.

Masyuk, A. I., T. V. Masyuk and N. F. LaRusso (2008). "Cholangiocyte primary cilia in liver health and disease." Developmental Dynamics **237**(8): 2007-2012.

Masyuk, A. I., T. V. Masyuk, P. L. Splinter, B. Q. Huang, A. J. Stroope and N. F. LaRusso (2006). "Cholangiocyte cilia detect changes in luminal fluid flow and transmit them into intracellular Ca2+ and cAMP signaling." Gastroenterology **131**(3): 911-920.

Masyuk, T. and N. LaRusso (2006). "Polycystic liver disease: New insights into disease pathogenesis." Hepatology **43**(5): 906-908.

Masyuk, T., A. Masyuk and N. LaRusso (2009). "Cholangiociliopathies: genetics, molecular mechanisms and potential therapies." Curr Opin Gastroenterol **25**(3): 265-271.

Masyuk, T. V., B. Q. Huang, A. I. Masyuk, E. L. Ritman, V. E. Torres, X. F. Wang, P. C. Harris and N. F. LaRusso (2004). "Biliary dysgenesis in the PCK rat, an orthologous model of autosomal recessive polycystic kidney disease." American Journal of Pathology **165**(5): 1719-1730.

Masyuk, T. V., A. I. Masyuk and N. F. La Russo (2015). "Therapeutic Targets In Polycystic Liver Disease." Curr Drug Targets **18**(8): 950-957.

Masyuk, T. V., A. I. Masyuk, V. E. Torres, P. C. Harris and N. F. Larusso (2007). "Octreotide inhibits hepatic cystogenesis in a rodent model of polycystic liver disease by reducing cholangiocyte adenosine 3',5'-cyclic monophosphate." Gastroenterology **132**(3): 1104-1116.

Masyuk, T. V., B. N. Radtke, A. J. Stroope, J. M. Banales, A. I. Masyuk, S. A. Gradilone, G. B. Gajdos, N. Chandok, J. L. Bakeberg, C. J. Ward, E. L. Ritman, H. Kiyokawa and N. F. LaRusso (2012). "Inhibition of Cdc25A suppresses hepato-renal cystogenesis in rodent models of polycystic kidney and liver disease." Gastroenterology **142**(3): 622-633.

Matsuoka, M. and H. Tsukamoto (1990). "Stimulation of hepatic lipocyte collagen production by Kupffer cell-derived transforming growth factor beta: implication for a pathogenetic role in alcoholic liver fibrogenesis." Hepatology **11**(4): 599-605.

McAtee, C. O., A. R. Berkebile, C. G. Elowsky, T. Fangman, J. J. Barycki, J. K. Wahl, 3rd, O. Khalimonchuk, N. Naslavsky, S. Caplan and M. A. Simpson (2015). "Hyaluronidase Hyal1 Increases Tumor Cell Proliferation and Motility through Accelerated Vesicle Trafficking." J Biol Chem **290**(21): 13144-13156.

McCarthy, D. J., Y. Chen and G. K. Smyth (2012). "Differential expression analysis of multifactor RNA-Seq experiments with respect to biological variation." Nucleic Acids Res **40**(10): 4288-4297.

McCracken, J. M., L. Jiang, K. T. Deshpande, M. F. O'Neil and M. T. Pritchard (2016). "Differential effects of hyaluronan synthase 3 deficiency after acute vs chronic liver injury in mice." Fibrogenesis Tissue Repair **9**: 4.

McPherson, E. A., Z. Luo, R. A. Brown, L. S. LeBard, C. C. Corless, R. C. Speth and S. P. Bagby (2004). "Chymase-like angiotensin II-generating activity in end-stage human autosomal dominant polycystic kidney disease." J Am Soc Nephrol **15**(2): 493-500.

Medina, J., L. Caveda, P. Sanz-Cameno, A. G. Arroyo, S. Martin-Vilchez, P. L. Majano, L. Garcia-Buey, F. Sanchez-Madrid and R. Moreno-Otero (2003). "Hepatocyte growth factor activates endothelial proangiogenic mechanisms relevant in chronic hepatitis C-associated neoangiogenesis." J Hepatol **38**(5): 660-667.

Menezes, L. F., Y. Cai, Y. Nagasawa, A. M. Silva, M. L. Watkins, A. M. Da Silva, S. Somlo, L. M. Guay-Woodford, G. G. Germino and L. F. Onuchic (2004). "Polyductin, the PKHD1 gene product, comprises isoforms expressed in plasma membrane, primary cilium, and cytoplasm." Kidney Int **66**(4): 1345-1355.

Menezes, L. F., F. Zhou, A. D. Patterson, K. B. Piontek, K. W. Krausz, F. J. Gonzalez and G. G. Germino (2012). "Network Analysis of a Pkd1-Mouse Model of Autosomal Dominant Polycystic Kidney Disease Identifies HNF4α as a Disease Modifier." PLOS Genetics **8**(11): e1003053.

Metcalfe, D. D., D. Baram and Y. A. Mekori (1997). "Mast cells." Physiol Rev **77**(4): 1033-1079.

Midgley, A. C., M. Rogers, M. B. Hallett, A. Clayton, T. Bowen, A. O. Phillips and R. Steadman (2013). "Transforming growth factor-beta1 (TGF-beta1)-stimulated fibroblast to myofibroblast differentiation is mediated by hyaluronan (HA)-facilitated epidermal growth factor receptor (EGFR) and CD44 co-localization in lipid rafts." J Biol Chem **288**(21): 14824-14838.

Misra, S., V. C. Hascall, R. R. Markwald and S. Ghatak (2015). "Interactions between hyaluronan and its receptors (CD44, RHAMM) regulate the activities of inflammation and cancer." Frontiers in Immunology **6**.

Misra, S., P. Heldin, V. C. Hascall, N. K. Karamanos, S. S. Skandalis, R. R. Markwald and S. Ghatak (2011). "Hyaluronan-CD44 interactions as potential targets for cancer therapy." Febs Journal **278**(9): 1429-1443.

Misra, S., B. P. Toole and S. Ghatak (2006). "Hyaluronan constitutively regulates activation of multiple receptor tyrosine kinases in epithelial and carcinoma cells." Journal of Biological Chemistry **281**(46): 34936-34941.

Mochizuki, T., G. Q. Wu, T. Hayashi, S. L. Xenophontos, B. Veldhuisen, J. J. Saris, D. M. Reynolds, Y. Q. Cai, P. A. Gabow, A. Pierides, W. J. Kimberling, M. H. Breuning, C.

C. Deltas, D. J. M. Peters and S. Somlo (1996). "PKD2, a gene for polycystic kidney disease that encodes an integral membrane protein." Science **272**(5266): 1339-1342.

Monzon, M. E., N. Fregien, N. Schmid, N. S. Falcon, M. Campos, S. M. Casalino-Matsuda and R. M. Forteza (2010). "Reactive oxygen species and hyaluronidase 2 regulate airway epithelial hyaluronan fragmentation." J Biol Chem **285**(34): 26126-26134.

Moormann, C., M. Artuc, E. Pohl, G. Varga, J. Buddenkotte, N. Vergnolle, R. Brehler, B. M. Henz, S. W. Schneider, T. A. Luger and M. Steinhoff (2006). "Functional characterization and expression analysis of the proteinase-activated receptor-2 in human cutaneous mast cells." J Invest Dermatol **126**(4): 746-755.

Mortazavi, A., B. A. Williams, K. McCue, L. Schaeffer and B. Wold (2008). "Mapping and quantifying mammalian transcriptomes by RNA-Seq." Nature Methods **5**: 621.

Moser, M., S. Matthiesen, J. Kirfel, H. Schorle, C. Bergmann, J. Senderek, S. Rudnik-Schoneborn, K. Zerres and R. Buettner (2005). "A mouse model for cystic biliary dysgenesis in autosomal recessive polycystic kidney disease (ARPKD)." Hepatology **41**(5): 1113-1121.

Mrug, M., J. Zhou, Y. Woo, X. Cui, A. J. Szalai, J. Novak, G. A. Churchill and L. M. Guay-Woodford (2008). "Overexpression of innate immune response genes in a model of recessive polycystic kidney disease." Kidney Int **73**(1): 63-76.

Muff, M. A., T. V. Masyuk, A. J. Stroope, B. Q. Huang, P. L. Splinter, S. O. Lee and N. F. Larusso (2006). "Development and characterization of a cholangiocyte cell line from the PCK rat, an animal model of Autosomal Recessive Polycystic Kidney Disease." Lab Invest **86**(9): 940-950.

Mukthavaram, R., X. Ouyang, R. Saklecha, P. Jiang, N. Nomura, S. C. Pingle, F. Guo, M. Makale and S. Kesari (2015). "Effect of the JAK2/STAT3 inhibitor SAR317461 on human glioblastoma tumorspheres." J Transl Med **13**: 269.

Murphy, F. R., R. Issa, X. Y. Zhou, S. Ratnarajah, H. Nagase, M. J. P. Arthur, C. Benyon and J. P. Iredale (2002). "Inhibition of apoptosis of activated hepatic stellate cells by tissue inhibitor of metalloproteinase-1 is mediated via effects on matrix metalloproteinase inhibition - Implications for reversibility of liver fibrosis." Journal of Biological Chemistry **277**(13): 11069-11076.

Murphy, S. and H. W. Kelly (1987). "Cromolyn Sodium - a Review of Mechanisms and Clinical Use in Asthma." Drug Intelligence & Clinical Pharmacy **21**(1): 22-35.

Nadasdy, T., Z. Laszik, G. Lajoie, K. E. Blick, D. E. Wheeler and F. G. Silva (1995). "Proliferative activity of cyst epithelium in human renal cystic diseases." J Am Soc Nephrol **5**(7): 1462-1468.

Nagao, S., M. Kugita, D. Yoshihara and T. Yamaguchi (2012). "Animal Models for Human Polycystic Kidney Disease." Experimental Animals **61**(5): 477-488.

Nakano, T., C. Y. Lai, S. Goto, L. W. Hsu, S. Kawamoto, K. Ono, K. D. Chen, C. C. Lin, K. W. Chiu, C. C. Wang, Y. F. Cheng and C. L. Chen (2012). "Immunological and regenerative aspects of hepatic mast cells in liver allograft rejection and tolerance." PLoS One **7**(5): e37202.

Nakanuma, Y., K. Harada, Y. Sato and H. Ikeda (2010). "Recent progress in the etiopathogenesis of pediatric biliary disease, particularly Caroli's disease with congenital hepatic fibrosis and biliary atresia." Histol Histopathol **25**(2): 223-235.

Naor, D., S. Nedvetzki, I. Golan, L. Melnik and Y. Faitelson (2002). "CD44 in cancer." Crit Rev Clin Lab Sci **39**(6): 527-579.

Naor, D., R. V. Sionov and D. Ish-Shalom (1997). "CD44: structure, function, and association with the malignant process." Adv Cancer Res **71**: 241-319.

Neuman, M. G., L. B. Cohen and R. M. Nanau (2016). "Hyaluronic acid as a non-invasive biomarker of liver fibrosis." Clin Biochem **49**(3): 302-315.

Ni, Y., J. M. Li, M. K. Liu, T. T. Zhang, D. P. Wang, W. H. Zhou, L. Z. Hu and W. L. Lv (2017). "Pathological process of liver sinusoidal endothelial cells in liver diseases." World J Gastroenterol **23**(43): 7666-7677.

Nichols, M. T., E. Gidey, T. Matzakos, R. Dahl, G. Stiegmann, R. J. Shah, J. J. Grantham, J. G. Fitz and R. B. Doctor (2004). "Secretion of cytokines and growth factors into autosomal dominant polycystic kidney disease liver cyst fluid." Hepatology **40**(4): 836-846.

Noble, P. W. (2002). "Hyaluronan and its catabolic products in tissue injury and repair." Matrix Biol **21**(1): 25-29.

Nowak, K. L., H. Farmer, M. A. Cadnapaphornchai, B. Gitomer and M. Chonchol (2017). "Vascular dysfunction in children and young adults with autosomal dominant polycystic kidney disease." Nephrol Dial Transplant **32**(2): 342-347.

Nyberg, A., A. Engstrom-Laurent and L. Loof (1988). "Serum hyaluronate in primary biliary cirrhosis--a biochemical marker for progressive liver damage." Hepatology **8**(1): 142-146.

Oguchi, T. and N. Ishiguro (2004). "Differential stimulation of three forms of hyaluronan synthase by TGF-beta, IL-1beta, and TNF-alpha." Connect Tissue Res **45**(4-5): 197-205.

Olsan, E. E., S. Mukherjee, B. Wulkersdorfer, J. M. Shillingford, A. J. Giovannone, G. Todorov, X. Song, Y. Pei and T. Weimbs (2011). "Signal transducer and activator of transcription-6 (STAT6) inhibition suppresses renal cyst growth in polycystic kidney disease." Proc Natl Acad Sci U S A **108**(44): 18067-18072.

Olsen, A. L., S. A. Bloomer, E. P. Chan, M. D. Gaca, P. C. Georges, B. Sackey, M. Uemura, P. A. Janmey and R. G. Wells (2011). "Hepatic stellate cells require a stiff environment for myofibroblastic differentiation." Am J Physiol Gastrointest Liver Physiol **301**(1): G110-118.

Onuchic, L. F., L. Furu, Y. Nagasawa, X. Y. Hou, T. Eggermann, Z. Y. Ren, C. Bergmann, J. Senderek, E. Esquivel, R. Zeltner, S. Rudnik-Schoneborn, M. Mrug, W. Sweeney, E. D. Avner, K. Zerres, L. M. Guay-Woodford, S. Somlo and G. G. Germino (2002). "PKHD1, the polycystic kidney and hepatic disease 1 gene, encodes a novel large protein containing multiple immunoglobulin-like plexin-transcription-factor domains and parallel beta-helix 1 repeats." American Journal of Human Genetics **70**(5): 1305-1317.

Orasan, O. H., G. Ciulei, A. Cozma, M. Sava and D. L. Dumitrascu (2016). "Hyaluronic acid as a biomarker of fibrosis in chronic liver diseases of different etiologies." Clujul Med **89**(1): 24-31.

Osathanondh, V. and E. L. Potter (1964). "PATHOGENESIS OF POLYCYSTIC KIDNEYS. TYPE 1 DUE TO HYPERPLASIA OF INTERSTITIAL PORTIONS OF COLLECTING TUBULES." Arch Pathol **77**: 466-473.

Ostrowski, N. L., W. S. Young, 3rd, M. A. Knepper and S. J. Lolait (1993). "Expression of vasopressin V1a and V2 receptor messenger ribonucleic acid in the liver and kidney of embryonic, developing, and adult rats." Endocrinology **133**(4): 1849-1859.

Overed-Sayer, C., L. Rapley, T. Mustelin and D. L. Clarke (2013). "Are mast cells instrumental for fibrotic diseases?" Front Pharmacol **4**: 174.

Overholtzer, M., J. Zhang, G. A. Smolen, B. Muir, W. Li, D. C. Sgroi, C. X. Deng, J. S. Brugge and D. A. Haber (2006). "Transforming properties of YAP, a candidate oncogene on the chromosome 11q22 amplicon." Proc Natl Acad Sci U S A **103**(33): 12405-12410.

Ozaki, S., Y. Sato, M. Yasoshima, K. Harada and Y. Nakanuma (2005). "Diffuse expression of heparan sulfate proteoglycan and connective tissue growth factor in

fibrous septa with many mast cells relate to unresolving hepatic fibrosis of congenital hepatic fibrosis." Liver Int **25**(4): 817-828.

Pan, D. (2010). "The hippo signaling pathway in development and cancer." Dev Cell **19**(4): 491-505.

Paradis, V., D. Dargere, F. Bonvoust, M. Vidaud, P. Segarini and P. Bedossa (2002). "Effects and regulation of connective tissue growth factor on hepatic stellate cells." Lab Invest **82**(6): 767-774.

Paradis, V., D. Dargere, M. Vidaud, A. C. De Gouville, S. Huet, V. Martinez, J. M. Gauthier, N. Ba, R. Sobesky, V. Ratziu and P. Bedossa (1999). "Expression of connective tissue growth factor in experimental rat and human liver fibrosis." Hepatology **30**(4): 968-976.

Parsons, B. J., S. Al-Assaf, S. Navaratnam and G. O. Phillips (2002). "Comparision of the reactivity of different reactive oxidative species (ROS) towards hyaluronan." Hyaluronan, Woodhead Publishing**:** 141-150.

Parsons, C. J., M. Takashima and R. A. Rippe (2007). "Molecular mechanisms of hepatic fibrogenesis." Journal of Gastroenterology and Hepatology **22**: S79-S84.

Parviz, F., C. Matullo, W. D. Garrison, L. Savatski, J. W. Adamson, G. Ning, K. H. Kaestner, J. M. Rossi, K. S. Zaret and S. A. Duncan (2003). "Hepatocyte nuclear factor 4alpha controls the development of a hepatic epithelium and liver morphogenesis." Nat Genet **34**(3): 292-296.

Patterson, M., J. C. Gonzalez-Vitale and C. J. Fagan (1982). "Polycystic liver disease: a study of cyst fluid constituents." Hepatology **2**(4): 475-478.

Payushina, O. V. (2012). "Hematopoietic Microenvironment in the Fetal Liver: Roles of Different Cell Populations." ISRN Cell Biology **2012**: 7.

Perugorria, M. J., T. V. Masyuk, J. J. Marin, M. Marzioni, L. Bujanda, N. F. LaRusso and J. M. Banales (2014). "Polycystic liver diseases: advanced insights into the molecular mechanisms." Nature Reviews Gastroenterology & Hepatology **11**(12): 750-761.

Pi, L., X. Ding, M. Jorgensen, J. J. Pan, S. H. Oh, D. Pintilie, A. Brown, W. Y. Song and B. E. Petersen (2008). "Connective tissue growth factor with a novel fibronectin binding site promotes cell adhesion and migration during rat oval cell activation." Hepatology **47**(3): 996-1004.

Pi, L., P. M. Robinson, M. Jorgensen, S. H. Oh, A. R. Brown, P. H. Weinreb, T. L. Trinh, P. Yianni, C. Liu, A. Leask, S. M. Violette, E. W. Scott, G. S. Schultz and B. E. Petersen (2015). "Connective tissue growth factor and integrin alphavbeta6: a new pair of

regulators critical for ductular reaction and biliary fibrosis in mice." Hepatology **61**(2): 678-691.

Pirson, Y., D. Chauveau and V. Torres (2002). "Management of cerebral aneurysms in autosomal dominant polycystic kidney disease." J Am Soc Nephrol **13**(1): 269-276.

Polverini, P. J., P. S. Cotran, M. A. Gimbrone, Jr. and E. R. Unanue (1977). "Activated macrophages induce vascular proliferation." Nature **269**(5631): 804-806.

Ponta, H., L. Sherman and P. A. Herrlich (2003). "CD44: from adhesion molecules to signalling regulators." Nat Rev Mol Cell Biol **4**(1): 33-45.

Poy, M. N., L. Eliasson, J. Krutzfeldt, S. Kuwajima, X. Ma, P. E. Macdonald, S. Pfeffer, T. Tuschl, N. Rajewsky, P. Rorsman and M. Stoffel (2004). "A pancreatic islet-specific microRNA regulates insulin secretion." Nature **432**(7014): 226-230.

Poy, M. N., J. Hausser, M. Trajkovski, M. Braun, S. Collins, P. Rorsman, M. Zavolan and M. Stoffel (2009). "miR-375 maintains normal pancreatic alpha- and beta-cell mass." Proc Natl Acad Sci U S A **106**(14): 5813-5818.

Preminger, G. M., W. E. Koch, F. A. Fried, E. McFarland, E. D. Murphy and J. Mandell (1982). "Murine congenital polycystic kidney disease: a model for studying development of cystic disease." J Urol **127**(3): 556-560.

Pritchard, M. T. and L. E. Nagy (2010). "Hepatic fibrosis is enhanced and accompanied by robust oval cell activation after chronic carbon tetrachloride administration to Egr-1-deficient mice." Am J Pathol **176**(6): 2743-2752.

Qian, Q. (2010). "Isolated polycystic liver disease." Adv Chronic Kidney Dis **17**(2): 181-189.

Rachfal, A. W. and D. R. Brigstock (2003). "Connective tissue growth factor (CTGF/CCN2) in hepatic fibrosis." Hepatol Res **26**(1): 1-9.

Raghu, G., M. B. Scholand, J. de Andrade, L. Lancaster, Y. Mageto, J. Goldin, K. K. Brown, K. R. Flaherty, M. Wencel, J. Wanger, T. Neff, F. Valone, J. Stauffer and S. Porter (2016). "FG-3019 anti-connective tissue growth factor monoclonal antibody: results of an open-label clinical trial in idiopathic pulmonary fibrosis." European Respiratory Journal **47**(5): 1481-1491.

Reddy, G. K. and C. S. Enwemeka (1996). "A simplified method for the analysis of hydroxyproline in biological tissues." Clin Biochem **29**(3): 225-229.

Rhee, J., Y. Inoue, J. C. Yoon, P. Puigserver, M. Fan, F. J. Gonzalez and B. M. Spiegelman (2003). "Regulation of hepatic fasting response by PPARgamma coactivator-1alpha (PGC-1): requirement for hepatocyte nuclear factor 4alpha in gluconeogenesis." Proc Natl Acad Sci U S A **100**(7): 4012-4017.

Ricker, J. L., V. H. Gattone, 2nd, J. P. Calvet and C. A. Rankin (2000). "Development of autosomal recessive polycystic kidney disease in BALB/c-cpk/cpk mice." J Am Soc Nephrol **11**(10): 1837-1847.

Robinson, M. D., D. J. McCarthy and G. K. Smyth (2010). "edgeR: a Bioconductor package for differential expression analysis of digital gene expression data." Bioinformatics **26**(1): 139-140.

Rooney, P. and S. Kumar (1993). "Inverse relationship between hyaluronan and collagens in development and angiogenesis." Differentiation **54**(1): 1-9.

Rostami, S. and H. Parsian (2013). "Hyaluronic Acid: From Biochemical Characteristics to its Clinical Translation in Assessment of Liver Fibrosis." Hepat Mon **13**(12): e13787.

Rowe, I. (2013). "Defective Glucose Metabolism in Polycystic Kidney Disease Identifies A Novel Therapeutic Paradigm." **19**(4): 488-493.

Roy, S., M. J. Dillon, R. S. Trompeter and T. M. Barratt (1997). "Autosomal recessive polycystic kidney disease: long-term outcome of neonatal survivors." Pediatr Nephrol **11**(3): 302-306.

Rundlett, S. E., A. A. Carmen, N. Suka, B. M. Turner and M. Grunstein (1998). "Transcriptional repression by UME6 involves deacetylation of lysine 5 of histone H4 by RPD3." Nature **392**(6678): 831-835.

Ruppert, S. M., T. R. Hawn, A. Arrigoni, T. N. Wight and P. L. Bollyky (2014). "Tissue integrity signals communicated by high-molecular weight hyaluronan and the resolution of inflammation." Immunol Res **58**(2-3): 186-192.

Sakai, N., M. Nakamura, K. E. Lipson, T. Miyake, Y. Kamikawa, A. Sagara, Y. Shinozaki, S. Kitajima, T. Toyama, A. Hara, Y. Iwata, M. Shimizu, K. Furuichi, S. Kaneko, A. M. Tager and T. Wada (2017). "Inhibition of CTGF ameliorates peritoneal fibrosis through suppression of fibroblast and myofibroblast accumulation and angiogenesis." Sci Rep **7**(1): 5392.

Samarakoon, R., J. M. Overstreet, S. P. Higgins and P. J. Higgins (2012). "TGF-beta1 --> SMAD/p53/USF2 --> PAI-1 transcriptional axis in ureteral obstruction-induced renal fibrosis." Cell Tissue Res **347**(1): 117-128.

Savani, R. C., G. Hou, P. Liu, C. Wang, E. Simons, P. C. Grimm, R. Stern, A. H. Greenberg, H. M. DeLisser and N. Khalil (2000). "A role for hyaluronan in macrophage accumulation and collagen deposition after bleomycin-induced lung injury." Am J Respir Cell Mol Biol **23**(4): 475-484.

Sawada, N., K. Mikami, G. Igarashi, Endo，Tetsu, Sato，Ken, I. Kakizaki and S. Fukuda (2016). "Beneficial effect of 4-methylumbelliferone against bile duct ligation-induced hepatic fibrosis in rats." Hirosaki Medical Journal **66**(2/4): 143-151.

Schneider, L., C. A. Clement, S. C. Teilmann, G. J. Pazour, E. K. Hoffmann, P. Satir and S. T. Christensen (2005). "PDGFRalphaalpha signaling is regulated through the primary cilium in fibroblasts." Curr Biol **15**(20): 1861-1866.

Schrader, J., T. T. Gordon-Walker, R. L. Aucott, M. van Deemter, A. Quaas, S. Walsh, D. Benten, S. J. Forbes, R. G. Wells and J. P. Iredale (2011). "Matrix stiffness modulates proliferation, chemotherapeutic response, and dormancy in hepatocellular carcinoma cells." Hepatology **53**(4): 1192-1205.

Sedlaczek, N., J. D. Jia, M. Bauer, H. Herbst, M. Ruehl, E. G. Hahn and D. Schuppan (2001). "Proliferating bile duct epithelial cells are a major source of connective tissue growth factor in rat biliary fibrosis." Am J Pathol **158**(4): 1239-1244.

Septer, S., G. Edwards, S. Gunewardena, A. Wolfe, H. Li, J. Daniel and U. Apte (2012). "Yes-associated protein is involved in proliferation and differentiation during postnatal liver development." Am J Physiol Gastrointest Liver Physiol **302**(5): G493-503.

Shneider, B. L. and M. S. Magid (2005). "Liver disease in autosomal recessive polycystic kidney disease." Pediatr Transplant **9**(5): 634-639.

Siddiquee, K., S. Zhang, W. C. Guida, M. A. Blaskovich, B. Greedy, H. R. Lawrence, M. L. R. Yip, R. Jove, M. M. McLaughlin, N. J. Lawrence, S. M. Sebti and J. Turkson (2007). "Selective chemical probe inhibitor of Stat3, identified through structure-based

virtual screening, induces antitumor activity." Proceedings of the National Academy of Sciences of the United States of America **104**(18): 7391-7396.

Siiskonen, H., S. Oikari, S. Pasonen-Seppänen and K. Rilla (2015). "Hyaluronan Synthase 1: A Mysterious Enzyme with Unexpected Functions." Frontiers in Immunology **6**: 43.

Silver, R. B., A. C. Reid, C. J. Mackins, T. Askwith, U. Schaefer, D. Herzlinger and R. Levi (2004). "Mast cells: a unique source of renin." Proc Natl Acad Sci U S A **101**(37): 13607-13612.

Singh, S. P., S. Tao, T. A. Fields, S. Webb, R. C. Harris and R. Rao (2015). "Glycogen synthase kinase-3 inhibition attenuates fibroblast activation and development of fibrosis following renal ischemia-reperfusion in mice." Dis Model Mech **8**(8): 931-940.

Sirvent, A. E., C. Gonzalez, R. Enriquez, J. Fernandez, I. Millan, X. Barber and F. Amoros (2010). "Serum tryptase levels and markers of renal dysfunction in a population with chronic kidney disease." Journal of Nephrology **23**(3): 282-290.

Soltes, L., R. Mendichi, G. Kogan, J. Schiller, M. Stankovska and J. Arnhold (2006). "Degradative action of reactive oxygen species on hyaluronan." Biomacromolecules **7**(3): 659-668.

Song, H., K. K. Mak, L. Topol, K. Yun, J. Hu, L. Garrett, Y. Chen, O. Park, J. Chang, R. M. Simpson, C. Y. Wang, B. Gao, J. Jiang and Y. Yang (2010). "Mammalian Mst1 and Mst2 kinases play essential roles in organ size control and tumor suppression." Proc Natl Acad Sci U S A **107**(4): 1431-1436.

Sperr, W. R., J. H. Jordan, M. Fiegl, L. Escribano, C. Bellas, S. Dirnhofer, H. Semper, I. Simonitsch-Klupp, H. P. Horny and P. Valent (2002). "Serum tryptase levels in patients with mastocytosis: correlation with mast cell burden and implication for defining the category of disease." Int Arch Allergy Immunol **128**(2): 136-141.

Spicer, A. P. and J. A. McDonald (1998). "Characterization and molecular evolution of a vertebrate hyaluronan synthase gene family." J Biol Chem **273**(4): 1923-1932.

Spirli, C., C. M. Morell, L. Locatelli, S. Okolicsanyi, C. Ferrero, A. K. Kim, L. Fabris, R. Fiorotto and M. Strazzabosco (2012). "Cyclic AMP/PKA-dependent paradoxical activation of Raf/MEK/ERK signaling in polycystin-2 defective mice treated with sorafenib." Hepatology **56**(6): 2363-2374.

Spirli, C., S. Okolicsanyi, R. Fiorotto, L. Fabris, M. Cadamuro, S. Lecchi, X. Tian, S. Somlo and M. Strazzabosco (2010). "Mammalian target of rapamycin regulates vascular endothelial growth factor-dependent liver cyst growth in polycystin-2-defective mice." Hepatology **51**(5): 1778-1788.

Steinhardt, A. A., M. F. Gayyed, A. P. Klein, J. Dong, A. Maitra, D. Pan, E. A. Montgomery and R. A. Anders (2008). "Expression of Yes-associated protein in common solid tumors." Hum Pathol **39**(11): 1582-1589.

Stickel, F., G. Poeschl, D. Schuppan, C. Conradt, A. Strenge-Hesse, F. S. Fuchs, W. J. Hofmann and H. K. Seitz (2003). "Serum hyaluronate correlates with histological progression in alcoholic liver disease." Eur J Gastroenterol Hepatol **15**(9): 945-950.

Stuhlmeier, K. M. and C. Pollaschek (2004). "Differential effect of transforming growth factor beta (TGF-beta) on the genes encoding hyaluronan synthases and utilization of the p38 MAPK pathway in TGF-beta-induced hyaluronan synthase 1 activation." J Biol Chem **279**(10): 8753-8760.

Suzuki, A., P. Angulo, J. Lymp, D. Li, S. Satomura and K. Lindor (2005). "Hyaluronic acid, an accurate serum marker for severe hepatic fibrosis in patients with non-alcoholic fatty liver disease." Liver Int **25**(4): 779-786.

Swenson-Fields, K. I., C. J. Vivian, S. M. Salah, J. D. Peda, B. M. Davis, N. van Rooijen, D. P. Wallace and T. A. Fields (2013). "Macrophages promote polycystic kidney disease progression." Kidney Int **83**(5): 855-864.

Takahashi, H., J. P. Calvet, D. Dittemore-Hoover, K. Yoshida, J. J. Grantham and V. H. Gattone, 2nd (1991). "A hereditary model of slowly progressive polycystic kidney disease in the mouse." J Am Soc Nephrol **1**(7): 980-989.

Takakura, A., E. A. Nelson, N. Haque, B. D. Humphreys, K. Zandi-Nejad, D. A. Frank and J. Zhou (2011). "Pyrimethamine inhibits adult polycystic kidney disease by modulating STAT signaling pathways." Hum Mol Genet **20**(21): 4143-4154.

Talbot, J. J., J. M. Shillingford, S. Vasanth, N. Doerr, S. Mukherjee, M. T. Kinter, T. Watnick and T. Weimbs (2011). "Polycystin-1 regulates STAT activity by a dual mechanism." Proc Natl Acad Sci U S A **108**(19): 7985-7990.

Tamaki, S., T. Ueno, T. Torimura, M. Sata and K. Tanikawa (1996). "Evaluation of hyaluronic acid binding ability of hepatic sinusoidal endothelial cells in rats with liver cirrhosis." Gastroenterology **111**(4): 1049-1057.

Tanimoto, K., S. Ohno, K. Fujimoto, K. Honda, C. Ijuin, N. Tanaka, T. Doi, M. Nakahara and K. Tanne (2001). "Proinflammatory cytokines regulate the gene expression of hyaluronic acid synthetase in cultured rabbit synovial membrane cells." Connect Tissue Res **42**(3): 187-195.

Tao, S., V. Kakade, J. Woodgett, P. Pandey, E. Suderman, M. Rajagopal and R. Rao (2015). "Glycogen synthase kinase-3β promotes cyst expansion in polycystic kidney disease." Kidney Int **87**(6): 1164-1175.

Tao, Y., J. Kim, S. Faubel, J. C. Wu, S. A. Falk, R. W. Schrier and C. L. Edelstein (2005). "Caspase inhibition reduces tubular apoptosis and proliferation and slows disease progression in polycystic kidney disease." Proc Natl Acad Sci U S A **102**(19): 6954-6959.

Taunton, J., C. A. Hassig and S. L. Schreiber (1996). "A mammalian histone deacetylase related to the yeast transcriptional regulator Rpd3p." Science **272**(5260): 408-411.

Tchougounova, E., A. Lundequist, I. Fajardo, J. O. Winberg, M. Abrink and G. Pejler (2005). "A key role for mast cell chymase in the activation of pro-matrix metalloprotease-9 and pro-matrix metalloprotease-2." J Biol Chem **280**(10): 9291-9296.

Teder, P., R. W. Vandivier, D. Jiang, J. Liang, L. Cohn, E. Pure, P. M. Henson and P. W. Noble (2002). "Resolution of lung inflammation by CD44." Science **296**(5565): 155-158.

Terada, T. and Y. Matsunaga (2000). "Increased mast cells in hepatocellular carcinoma and intrahepatic cholangiocarcinoma." J Hepatol **33**(6): 961-966.

Terada, Y., S. Hanada, A. Nakao, M. Kuwahara, S. Sasaki and F. Marumo (2002). "Gene transfer of Smad7 using electroporation of adenovirus prevents renal fibrosis in post-obstructed kidney." Kidney Int **61**(1 Suppl): S94-98.

Tesmer, J. J., R. K. Sunahara, A. G. Gilman and S. R. Sprang (1997). "Crystal structure of the catalytic domains of adenylyl cyclase in a complex with Gsalpha.GTPgammaS." Science **278**(5345): 1907-1916.

Tomimori, Y., T. Muto, K. Saito, T. Tanaka, H. Maruoka, M. Sumida, H. Fukami and Y. Fukuda (2003). "Involvement of mast cell chymase in bleomycin-induced pulmonary fibrosis in mice." Eur J Pharmacol **478**(2-3): 179-185.

Torres, V. E. (2007). "Treatment of Polycystic Liver Disease: One Size Does Not Fit All." American Journal of Kidney Diseases **49**(6): 725-728.

Torres, V. E. (2008). "Vasopressin antagonists in polycystic kidney disease." Semin Nephrol **28**(3): 306-317.

Torres, V. E., A. B. Chapman, O. Devuyst, R. T. Gansevoort, J. J. Grantham, E. Higashihara, R. D. Perrone, H. B. Krasa, J. Ouyang, F. S. Czerwiec and T. T. Investigators (2012). "Tolvaptan in patients with autosomal dominant polycystic kidney disease." N Engl J Med **367**(25): 2407-2418.

Torres, V. E., A. B. Chapman, R. D. Perrone, K. T. Bae, K. Z. Abebe, J. E. Bost, D. C. Miskulin, T. I. Steinman, W. E. Braun, F. T. Winklhofer, M. C. Hogan, F. R. Oskoui, C. Kelleher, A. Masoumi, J. Glockner, N. J. Halin, D. R. Martin, E. Remer, N. Patel, I. Pedrosa, L. H. Wetzel, P. A. Thompson, J. P. Miller, C. M. Meyers, R. W. Schrier and H. P. S. Group (2012). "Analysis of baseline parameters in the HALT polycystic kidney disease trials." Kidney Int **81**(6): 577-585.

Torres, V. E., K. A. Donovan, G. Scicli, K. E. Holley, S. N. Thibodeau, O. A. Carretero, T. Inagami, J. A. McAteer and C. M. Johnson (1992). "Synthesis of renin by tubulocystic epithelium in autosomal-dominant polycystic kidney disease." Kidney Int **42**(2): 364-373.

Torres, V. E., P. C. Harris and Y. Pirson (2007). "Autosomal dominant polycystic kidney disease." Lancet **369**(9569): 1287-1301.

Torres, V. E., W. E. Sweeney, Jr., X. Wang, Q. Qian, P. C. Harris, P. Frost and E. D. Avner (2004). "Epidermal growth factor receptor tyrosine kinase inhibition is not protective in PCK rats." Kidney Int **66**(5): 1766-1773.

Tracy, T. F., Jr., P. Dillon, E. S. Fox, K. Minnick and C. Vogler (1996). "The inflammatory response in pediatric biliary disease: macrophage phenotype and distribution." J Pediatr Surg **31**(1): 121-125; discussion 125-126.

Trapnell, C., A. Roberts, L. Goff, G. Pertea, D. Kim, D. R. Kelley, H. Pimentel, S. L. Salzberg, J. L. Rinn and L. Pachter (2012). "Differential gene and transcript expression analysis of RNA-seq experiments with TopHat and Cufflinks." Nat Protoc **7**(3): 562-578.

Trapnell, C., B. A. Williams, G. Pertea, A. Mortazavi, G. Kwan, M. J. van Baren, S. L. Salzberg, B. J. Wold and L. Pachter (2010). "Transcript assembly and quantification by RNA-Seq reveals unannotated transcripts and isoform switching during cell differentiation." Nat Biotechnol **28**(5): 511-515.

Turkbey, B., I. Ocak, K. Daryanani, E. Font-Montgomery, L. Lukose, J. Bryant, M. Tuchman, P. Mohan, T. Heller, W. A. Gahl, P. L. Choyke and M. Gunay-Aygun (2009). "Autosomal recessive polycystic kidney disease and congenital hepatic fibrosis (ARPKD/CHF)." Pediatric Radiology **39**(2): 100-111.

Uchiyama, T., T. Sakuta and T. Kanayama (2005). "Regulation of hyaluronan synthases in mouse uterine cervix." Biochem Biophys Res Commun **327**(3): 927-932.

Urb, M. and D. C. Sheppard (2012). "The role of mast cells in the defence against pathogens." PLoS Pathog **8**(4): e1002619.

Urbich, C., L. Rossig, D. Kaluza, M. Potente, J. N. Boeckel, A. Knau, F. Diehl, J. G. Geng, W. K. Hofmann, A. M. Zeiher and S. Dimmeler (2009). "HDAC5 is a repressor of angiogenesis and determines the angiogenic gene expression pattern of endothelial cells." Blood **113**(22): 5669-5679.

van Zeijl, C. J., E. Fliers, C. J. van Koppen, O. V. Surovtseva, M. E. de Gooyer, M. P. Mourits, W. M. Wiersinga, A. M. Miltenburg and A. Boelen (2010). "Effects of thyrotropin and thyrotropin-receptor-stimulating Graves' disease immunoglobulin G on cyclic adenosine monophosphate and hyaluronan production in nondifferentiated orbital fibroblasts of Graves' ophthalmopathy patients." Thyroid **20**(5): 535-544.

Vareesangthip, K., P. Tong, R. Wilkinson and T. H. Thomas (1997). "Insulin resistance in adult polycystic kidney disease." Kidney Int **52**(2): 503-508.

Vassilev, A., K. J. Kaneko, H. Shu, Y. Zhao and M. L. DePamphilis (2001). "TEAD/TEF transcription factors utilize the activation domain of YAP65, a Src/Yes-associated protein localized in the cytoplasm." Genes Dev **15**(10): 1229-1241.

Veizis, E. I., C. R. Carlin and C. U. Cotton (2004). "Decreased amiloride-sensitive Na+ absorption in collecting duct principal cells isolated from BPK ARPKD mice." Am J Physiol Renal Physiol **286**(2): F244-254.

Vickers, A. E. M., M. Saulnier, E. Cruz, M. T. Merema, K. Rose, P. Bentley and P. Olinga (2004). "Organ Slice Viability Extended for Pathway Characterization: An in Vitro Model to Investigate Fibrosis." Toxicological Sciences **82**(2): 534-544.

Vogler, C., S. Homan, A. Pung, C. Thorpe, J. Barker, E. H. Birkenmeier and P. Upadhya (1999). "Clinical and pathologic findings in two new allelic murine models of polycystic kidney disease." J Am Soc Nephrol **10**(12): 2534-2539.

Vrochides, D., V. Papanikolaou, H. Pertoft, A. A. Antoniades and P. Heldin (1996). "Biosynthesis and degradation of hyaluronan by nonparenchymal liver cells during liver regeneration." Hepatology **23**(6): 1650-1655.

Walesky, C. and U. Apte (2015). "Role of hepatocyte nuclear factor 4alpha (HNF4alpha) in cell proliferation and cancer." Gene Expr **16**(3): 101-108.

Walesky, C., G. Edwards, P. Borude, S. Gunewardena, M. O'Neil, B. Yoo and U. Apte (2013). "Hepatocyte nuclear factor 4 alpha deletion promotes diethylnitrosamine-induced hepatocellular carcinoma in rodents." Hepatology **57**(6): 2480-2490.

Wang, C., X. Zhu, W. Feng, Y. Yu, K. Jeong, W. Guo, Y. Lu and G. B. Mills (2016). "Verteporfin inhibits YAP function through up-regulating 14-3-3σ sequestering YAP in the cytoplasm." American Journal of Cancer Research **6**(1): 27-37.

Wang, K. C., Y. T. Yeh, P. Nguyen, E. Limqueco, J. Lopez, S. Thorossian, K. L. Guan, Y. J. Li and S. Chien (2016). "Flow-dependent YAP/TAZ activities regulate endothelial phenotypes and atherosclerosis." Proc Natl Acad Sci U S A **113**(41): 11525-11530.

Wang, X., V. Gattone, 2nd, P. C. Harris and V. E. Torres (2005). "Effectiveness of vasopressin V2 receptor antagonists OPC-31260 and OPC-41061 on polycystic kidney disease development in the PCK rat." J Am Soc Nephrol **16**(4): 846-851.

Ward, C. J. (1994). "The Polycystic Kidney-Disease-1 Gene Encodes a 14 Kb Transcript and Lies within a Duplicated Region on Chromosome-16 (Vol 77, Pg 881, 1994)." Cell **78**(4): 725-725.

Ward, C. J., M. C. Hogan, S. Rossetti, D. Walker, T. Sneddon, X. Wang, V. Kubly, J. M. Cunningham, R. Bacallao, M. Ishibashi, D. S. Milliner, V. E. Torres and P. C. Harris (2002). "The gene mutated in autosomal recessive polycystic kidney disease encodes a large, receptor-like protein." Nat Genet **30**(3): 259-269.

Ward, C. J., D. Yuan, T. V. Masyuk, X. Wang, R. Punyashthiti, S. Whelan, R. Bacallao, R. Torra, N. F. LaRusso, V. E. Torres and P. C. Harris (2003). "Cellular and subcellular localization of the ARPKD protein; fibrocystin is expressed on primary cilia." Hum Mol Genet **12**(20): 2703-2710.

Weimbs, T. and J. J. Talbot (2013). "STAT3 Signaling in Polycystic Kidney Disease." Drug Discov Today Dis Mech **10**(3-4): e113-e118.

Wen, J. (2011). "Congenital hepatic fibrosis in autosomal recessive polycystic kidney disease." Clin Transl Sci **4**(6): 460-465.

Williams, S. S., P. Cobo-Stark, L. R. James, S. Somlo and P. Igarashi (2008). "Kidney cysts, pancreatic cysts, and biliary disease in a mouse model of autosomal recessive polycystic kidney disease." Pediatr Nephrol **23**(5): 733-741.

Wills, E. S., R. Roepman and J. P. Drenth (2014). "Polycystic liver disease: ductal plate malformation and the primary cilium." Trends Mol Med **20**(5): 261-270.

Wilson , P. D. (2004). "Polycystic Kidney Disease." New England Journal of Medicine **350**(2): 151-164.

Wittig, B., S. Seiter, D. S. Schmidt, M. Zuber, M. Neurath and M. Zoller (1999). "CD44 variant isoforms on blood leukocytes in chronic inflammatory bowel disease and other systemic autoimmune diseases." Lab Invest **79**(6): 747-759.

Wittig, B. M., B. Johansson, M. Zoller, C. Schwarzler and U. Gunthert (2000). "Abrogation of experimental colitis correlates with increased apoptosis in mice deficient for CD44 variant exon 7 (CD44v7)." J Exp Med **191**(12): 2053-2064.

Woollard, J. R., R. Punyashtiti, S. Richardson, T. V. Masyuk, S. Whelan, B. Q. Huang, D. J. Lager, J. vanDeursen, V. E. Torres, V. H. Gattone, N. F. LaRusso, P. C. Harris and C. J. Ward (2007). "A mouse model of autosomal recessive polycystic kidney disease with biliary duct and proximal tubule dilatation." Kidney Int **72**(3): 328-336.

Wrana, J. L., L. Attisano, R. Wieser, F. Ventura and J. Massague (1994). "Mechanism of activation of the TGF-beta receptor." Nature **370**(6488): 341-347.

Wu, C. F., W. C. Chiang, C. F. Lai, F. C. Chang, Y. T. Chen, Y. H. Chou, T. H. Wu, G. R. Linn, H. Ling, K. D. Wu, T. J. Tsai, Y. M. Chen, J. S. Duffield and S. L. Lin (2013). "Transforming growth factor beta-1 stimulates profibrotic epithelial signaling to activate pericyte-myofibroblast transition in obstructive kidney fibrosis." Am J Pathol **182**(1): 118-131.

Xiao, Z. and L. D. Quarles (2015). "Physiological mechanisms and therapeutic potential of bone mechanosensing." Rev Endocr Metab Disord **16**(2): 115-129.

Xu, R., F. Lin, J. He, L. Jin, J. Y. Zhang, J. Fu, H. Liu, S. Wang, Z. Zhang and F. S. Wang (2013). "Complement 5a stimulates hepatic stellate cells in vitro, and is increased in the plasma of patients with chronic hepatitis B." Immunology **138**(3): 228-234.

Yabushita, H., M. Noguchi, T. Kishida, K. Fusano, Y. Noguchi, N. Itano, K. Kimata and M. Noguchi (2004). "Hyaluronan synthase expression in ovarian cancer." Oncol Rep **12**(4): 739-743.

Yamada, Y., N. Itano, K. Hata, M. Ueda and K. Kimata (2004). "Differential regulation by IL-1beta and EGF of expression of three different hyaluronan synthases in oral mucosal

epithelial cells and fibroblasts and dermal fibroblasts: quantitative analysis using real-time RT-PCR." J Invest Dermatol **122**(3): 631-639.

Yamada, Y., N. Itano, H. Narimatsu, T. Kudo, K. Morozumi, S. Hirohashi, A. Ochiai, M. Ueda and K. Kimata (2004). "Elevated transcript level of hyaluronan synthase1 gene correlates with poor prognosis of human colon cancer." Clin Exp Metastasis **21**(1): 57-63.

Yamaguchi, T., S. J. Hempson, G. A. Reif, A. M. Hedge and D. P. Wallace (2006). "Calcium restores a normal proliferation phenotype in human polycystic kidney disease epithelial cells." J Am Soc Nephrol **17**(1): 178-187.

Yamaguchi, T., J. C. Pelling, N. T. Ramaswamy, J. W. Eppler, D. P. Wallace, S. Nagao, L. A. Rome, L. P. Sullivan and J. J. Grantham (2000). "cAMP stimulates the in vitro proliferation of renal cyst epithelial cells by activating the extracellular signal-regulated kinase pathway." Kidney Int **57**(4): 1460-1471.

Yamaguchi, T., D. P. Wallace, B. S. Magenheimer, S. J. Hempson, J. J. Grantham and J. P. Calvet (2004). "Calcium restriction allows cAMP activation of the B-Raf/ERK pathway, switching cells to a cAMP-dependent growth-stimulated phenotype." J Biol Chem **279**(39): 40419-40430.

Yamamoto, H., Y. Tobisawa, T. Inubushi, F. Irie, C. Ohyama and Y. Yamaguchi (2017). "A mammalian homolog of the zebrafish transmembrane protein 2 (TMEM2) is the long-sought-after cell-surface hyaluronidase." J Biol Chem **292**(18): 7304-7313.

Yi, J., L. Lu, K. Yanger, W. Q. Wang, B. H. Sohn, B. Z. Stanger, M. Zhang, J. F. Martin, J. A. Ajani, J. J. Chen, J. S. Lee, S. M. Song and R. L. Johnson (2016). "Large tumor suppressor homologs 1 and 2 regulate mouse liver progenitor cell proliferation and maturation through antagonism of the coactivators YAP and TAZ." Hepatology **64**(5): 1757-1772.

Yoshihara, D., M. Kugita, M. Sasaki, S. Horie, K. Nakanishi, T. Abe, H. M. Aukema, T. Yamaguchi and S. Nagao (2013). "Telmisartan ameliorates fibrocystic liver disease in an orthologous rat model of human autosomal recessive polycystic kidney disease." PLoS One **8**(12): e81480.

Yu, F. X., B. Zhao and K. L. Guan (2015). "Hippo Pathway in Organ Size Control, Tissue Homeostasis, and Cancer." Cell **163**(4): 811-828.

Zeidler, A., R. Brauer, K. Thoss, J. Bahnsen, V. Heinrichs, D. Jablonski-Westrich, M. Wroblewski, S. Rebstock and A. Hamann (1995). "Therapeutic effects of antibodies against adhesion molecules in murine collagen type II-induced arthritis." Autoimmunity **21**(4): 245-252.

Zeier, M., P. Fehrenbach, S. Geberth, K. Mohring, R. Waldherr and E. Ritz (1992). "Renal histology in polycystic kidney disease with incipient and advanced renal failure." Kidney Int **42**(5): 1259-1265.

Zender, L., M. S. Spector, W. Xue, P. Flemming, C. Cordon-Cardo, J. Silke, S. T. Fan, J. M. Luk, M. Wigler, G. J. Hannon, D. Mu, R. Lucito, S. Powers and S. W. Lowe (2006). "Identification and validation of oncogenes in liver cancer using an integrative oncogenomic approach." Cell **125**(7): 1253-1267.

Zerres, K., S. Rudnik-Schoneborn, C. Steinkamm, J. Becker and G. Mucher (1998). "Autosomal recessive polycystic kidney disease." J Mol Med (Berl) **76**(5): 303-309.

Zhao, B., L. Li, K. Tumaneng, C.-Y. Wang and K.-L. Guan (2010). "A coordinated phosphorylation by Lats and CK1 regulates YAP stability through SCF(β-TRCP)." Genes & Development **24**(1): 72-85.

Zhao, B., X. Wei, W. Li, R. S. Udan, Q. Yang, J. Kim, J. Xie, T. Ikenoue, J. Yu, L. Li, P. Zheng, K. Ye, A. Chinnaiyan, G. Halder, Z. C. Lai and K. L. Guan (2007). "Inactivation of YAP oncoprotein by the Hippo pathway is involved in cell contact inhibition and tissue growth control." Genes Dev **21**(21): 2747-2761.

Zhao, B., X. Ye, J. Yu, L. Li, W. Li, S. Li, J. Yu, J. D. Lin, C. Y. Wang, A. M. Chinnaiyan, Z. C. Lai and K. L. Guan (2008). "TEAD mediates YAP-dependent gene induction and growth control." Genes Dev **22**(14): 1962-1971.

Zhao, S., W. P. Fung-Leung, A. Bittner, K. Ngo and X. Liu (2014). "Comparison of RNA-Seq and microarray in transcriptome profiling of activated T cells." PLoS One **9**(1): e78644.

Zhou, D. W., C. Conrad, F. Xia, J. S. Park, B. Payer, Y. Yin, G. Y. Lauwers, W. Thasler, J. T. Lee, J. Avruch and N. Bardeesy (2009). "Mst1 and Mst2 Maintain Hepatocyte Quiescence and Suppress Hepatocellular Carcinoma Development through Inactivation of the Yap1 Oncogene." Cancer Cell **16**(5): 425-438.

Zoja, C., D. Corna, M. Locatelli, D. Rottoli, A. Pezzotta, M. Morigi, C. Zanchi, S. Buelli, A. Guglielmotti, N. Perico, A. Remuzzi and G. Remuzzi (2015). "Effects of MCP-1 inhibition by bindarit therapy in a rat model of polycystic kidney disease." Nephron **129**(1): 52-61.